AD-A280 286

COPY 1

ARL 125
PART I

SUPERSONIC CASCADE STUDIES

PART I — PASSAGE STUDIES

DTIC
ELECTE
MAY 25 1994
S B D

ANDREW A. FEJER
GEORGE L. HEATH

THE UNIVERSITY OF TOLEDO
TOLEDO, OHIO

DISTRIBUTION STATEMENT A
Approved for public release;
Distribution Unlimited

DECEMBER 1961

AERONAUTICAL RESEARCH LABORATORY
OFFICE OF AEROSPACE RESEARCH
UNITED STATES AIR FORCE

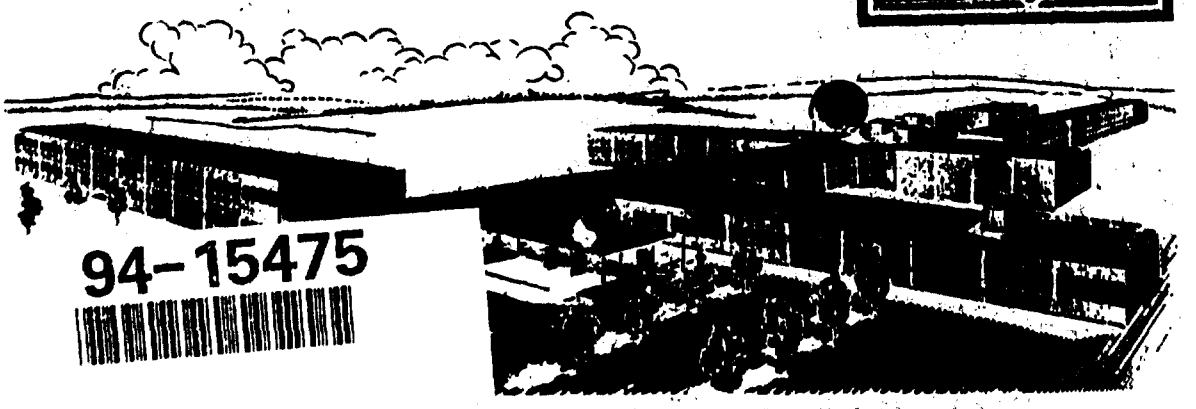

94-15475

LIBRARY COPY
FEB 27 1962

94 5 23 050

NOTICES

When Government drawings, specifications, or other data are used for any purpose other than in connection with a definitely related Government procurement operation, the United States Government thereby incurs no responsibility nor any obligation whatsoever; and the fact that the Government may have formulated, furnished, or in any way supplied the said drawings, specifications, or other data, is not to be regarded by implication or otherwise as in any manner licensing the holder or any other person or corporation, or conveying any rights or permission to manufacture, use, or sell any patented invention that may in any way be related thereto.

Qualified requesters may obtain copies of this report from the Armed Services Technical Information Agency, (ASTIA), Arlington Hall Station, Arlington 12, Virginia.

This report has been released to the Office of Technical Services, U. S. Department of Commerce, Washington 25, D. C. for sale to the general public.

Copies of ARL Technical Reports and Technical Notes should not be returned to Aeronautical Research Laboratory unless return is required by security considerations, contractual obligations, or notices on a specific document.

The University of Toledo, Toledo, Ohio. SUPERSONIC CASCADE STUDIES, Part I, PASSAGE STUDIES by Andrew A. Fejer and George L. Heath. December 1961. 90 p. incl. illus. (Project 7063; Task 70151) (Contract AF 33(616)-5737) (ARL 125, Pt. I)
Unclassified Report

An experimental study was made of supersonic flow through various convergent and convergent-divergent passage configurations. The details of the flows were examined by means of total and static pressure surveys and Schlieren photographs and the effects of some changes in passage geometry on the characteristics of the passages were ob-

(over)

UNCLASSIFIED

UNCLASSIFIED

served. Based on the tests, some design criteria were determined for supersonic passages capable of operating at high static pressure ratios. It was concluded that long and narrow convergent-divergent passages are capable of producing a significant pressure rise without extensive separation in the divergent region. However, the values of obtainable pressure rise appears to be substantially lower than anticipated by early designers of supersonic compressor cascades.

UNCLASSIFIED

UNCLASSIFIED

The University of Toledo, Toledo, Ohio. SUPERSONIC CASCADE STUDIES, Part I, PASSAGE STUDIES by Andrew A. Fejer and George L. Heath. December 1961. 90 p. incl. illus. (Project 7063; Task 70151) (Contract AF 33(616)-5737) (ARL 125, Pt. I)
Unclassified Report

An experimental study was made of supersonic flow through various convergent and convergent-divergent passage configurations. The details of the flows were examined by means of total and static pressure surveys and Schlieren photographs and the effects of some changes in passage geometry on the characteristics of the passages were ob-

(over)

UNCLASSIFIED

UNCLASSIFIED

served. Based on the tests, some design criteria were determined for supersonic passages capable of operating at high static pressure ratios. It was concluded that long and narrow convergent-divergent passages are capable of producing a significant pressure rise without extensive separation in the divergent region. However, the values of obtainable pressure rise appears to be substantially lower than anticipated by early designers of supersonic compressor cascades.

UNCLASSIFIED

UNCLASSIFIED

The University of Toledo, Toledo, Ohio.
SUPERSONIC CASCADE STUDIES, Part I,
PASSAGE STUDIES by Andrew A. Fejer and
George L. Heath. December 1961. 90 p.
incl. illus. (Project 7063; Task 70151)
(Contract AF 33(616)-5737) (ARL 125, Pt. I)
Unclassified Report

An experimental study was made of supersonic flow through various convergent and convergent-divergent passage configurations. The details of the flows were examined by means of total and static pressure surveys and Schlieren photographs and the effects of some changes in passage geometry on the characteristics of the passages were ob-

(over)

UNCLASSIFIED

UNCLASSIFIED

served. Based on the tests, some design criteria were determined for supersonic passages capable of operating at high static pressure ratios. It was concluded that long and narrow convergent-divergent passages are capable of producing a significant pressure rise without extensive separation in the divergent region. However, the values of obtainable pressure rise appears to be substantially lower than anticipated by early designers of supersonic compressor cascades.

UNCLASSIFIED

UNCLASSIFIED

The University of Toledo, Toledo, Ohio.
SUPERSONIC CASCADE STUDIES, Part I,
PASSAGE STUDIES by Andrew A. Fejer and
George L. Heath. December 1961. 90 p.
incl. illus. (Project 7063; Task 70151)
(Contract AF 33(616)-5737) (ARL 125, Pt. I)
Unclassified Report

An experimental study was made of supersonic flow through various convergent and convergent-divergent passage configurations. The details of the flows were examined by means of total and static pressure surveys and Schlieren photographs and the effects of some changes in passage geometry on the characteristics of the passages were ob-

(over)

UNCLASSIFIED

UNCLASSIFIED

served. Based on the tests, some design criteria were determined for supersonic passages capable of operating at high static pressure ratios. It was concluded that long and narrow convergent-divergent passages are capable of producing a significant pressure rise without extensive separation in the divergent region. However, the values of obtainable pressure rise appears to be substantially lower than anticipated by early designers of supersonic compressor cascades.

UNCLASSIFIED

UNCLASSIFIED

ARL 125
PART I

SUPERSONIC CASCADE STUDIES

PART I — PASSAGE STUDIES

ANDREW A. FEJER
GEORGE L. HEATH

THE UNIVERSITY OF TOLEDO
TOLEDO, OHIO

DECEMBER 1961

CONTRACT No. AF 33(616)-5737
PROJECT No. 7063
TASK No. 70151

AERONAUTICAL RESEARCH LABORATORY
OFFICE OF AEROSPACE RESEARCH
UNITED STATES AIR FORCE
WRIGHT-PATTERSON AIR FORCE BASE, OHIO

100 - February 1962 - 21-898 & 899

FOREWORD

This final technical report was prepared by the Research Foundation of the University of Toledo, Toledo, Ohio on contract AF 33(616)-5737 for the Aeronautical Research Laboratory, Office of Aerospace Research. The research was carried out under Task 70151, "Investigation of Internal Visco-Compressible Flow Phenomena" of Project 7063, "Mechanics of Flight", under the direct supervision of Dr. Andrew A. Fejer, chief investigator, with the collaboration of George L. Heath and Richard Thomas. Dr. Earl E. Hays and C. S. Hsu also assisted in the work.

ABSTRACT

An experimental study was made of supersonic flow through various convergent and convergent-divergant passage configurations. The details of the flows were examined by means of total and static pressure surveys and Schlieren photographs and the effects of some changes in passage geometry on the characteristics of the passages were observed. Based on the tests, some design criteria were determined for supersonic passages capable of operating at high static pressure ratios. It was concluded that long and narrow convergent-divergent passages are capable of producing a significant pressure rise without extensive separation in the divergent region. However, the values of obtainable pressure rise appears to be substantially lower than anticipated by early designers of supersonic compressor cascades.

Accession For
NTIS GRA&I ☑
DTIC TAB ☐
Unannounced ☐
Justification
By
Distribution/
Availability Codes
Dist | Avail and/or Special
A-1

TABLE OF CONTENTS

SECTION		PAGE
I	INTRODUCTION	1
II	CONVERGENT-DIVERGENT PASSAGE TESTS	2
III	STUDIES OF PASSAGE FLOW DETAILS	6
IV	DISCUSSION OF RESULTS	19
V	CONCLUSIONS	25
	APPENDIX A	31
	REFERENCES	40

LIST OF ILLUSTRATIONS

FIGURE		PAGE
1	Convergent-Divergent Passage Schematic	42
2	Velocity Diagram for Supersonic Inlet and Subsonic Discharge	43
3	Maximum Wedge Angle δ, for Attached Shock vs Inlet Mach Number M_1	44
4	Schematic of Shock System in Convergent-Divergent Passage	45
5	Temperature-Entropy Diagram Depicting Changes of State in the Convergent-Divergent Passage	46
6	Shock Effectiveness, η_s, vs Inlet Mach Number M_1, for Various Wedge Angles, δ	47
7	Increase in Entropy vs M_1 for Optimum δ	48
8	Passage Starting Requirements	49
9	Schematic of Adjustable Convergent Passages	50
10	Typical Schlieren Photographs of Short, Intermediate and Long Passages. M = 2.00, =4°, Maximum Pressure Ratio	51
11	Pressure Ratio vs Passage Convergence	52
12	Short Passage with Single Boundary Layer Trip on Lower Surface	53
13	Short Passage with Single Trips on Upper and Lower Surface	53
14	Schematic of Zero Stagger Passage	54
15	Zero Stagger Passage	54
16	Passages with Curved Entrance Sections	55
17	Passage with Negative Pressure Gradient Along Lower Surface	56
18	Passage with Positive Pressure Gradient Changing to Negative Along Lower Surface	56
19	Pressure Ratio vs Vane Angle - Convex Lower Surface	57

LIST OF ILLUSTRATIONS (cont'd)

FIGURE		PAGE
20	Pressure Ratio vs Vane Angle - Concave Lower Surface	58
21	Comparison of Passages with Sharp and Blunted Lower Leading Edges	59
22	Comparison of Performance of 1.5" Passage with Sharp and Blunted Leading Edges	60
23	Heated Vane Construction	61
24	Comparison of Heated and Unheated Passages	62
25	Schematic of Passage with Removable Blocks for Varying Trailing Edge Location	63
26	Passage with No Extensions Added to Lower Surface	64
27	Passage with One Extension Added to Lower Surface	65
28	Passage with Two Extensions Added to Lower Surface	66
29	Passage with Three Extensions Added to Lower Surface	67
30	Passage with Four Extensions Added to Lower Surface	68
31	Variation of Passage Pressure Ratio with Location of Trailing Edge from Incident Shock	69
32	Passage with Convex Trailing Edge Extension on Lower Surface	70
33	Schematic of Convergent-Divergent Passages	71
34	Pressure Distribution Along Passages with Surface Discontinuities	72
35	Pressure Ratio Along Passages with Surface Discontinuities	73
36	Comparison of Pressures Along Smooth Passage with Pressures Along Passages with Discontinuities	74
37	Convergent-Divergent Passage with No Surface Discontinuities	75

LIST OF ILLUSTRATIONS (Cont'd)

FIGURE		PAGE
38	Convergent-Divergent Passage with .062" Square Groove in Surfaces	76
39	Convergent-Divergent Passage with .062" Square Plus .125" Diameter	77
40	Convergent-Divergent Passage with .375" x .25" Groove in Surfaces	78
41	Schematic of Convergent-Divergent Passage with "Free Jet" Throats	79
42	Pressure Distribution Along Passages with "Free Jet" Throat	80
43	Effect of Back Pressure on Passage with "Free Jet" Throat	81
44	Convergent-Divergent Passage with "Free Jet" Throats	82
A1	Flat Plate Model with Total Head Probe	83
A2	View of Flat Plate with Two-Dimensional trip	84
A3	Typical Schlieren Photograph	85
A4	Schematic Diagram Showing Deduction of Transition Point Location from Change in Boundary Layer	86
A5	Effect of Trip Height on Location of Transition	87
A6	Effect of Trip Height in Terms of Laminar Boundary Layer Displacement Thickness at Trip on Location of Transition	88
A7	Trip Sizes to Cause Transition at Trip Location	89
A8	Effect of Boundary Layer Reynolds Number on Critical Trip Size	90

LIST OF SYMBOLS

A	Area
A_i	Passage inlet area
A_t	Passage throat area
C	Cavity chord length
d	Cavity depth
h	Passage throat height
M	Mach number
P	Static pressure
P_o	Stagnation pressure
T	Static temperature
T_o	Stagnation temperature
T_w	Surface temperature
ΔT	$T_o - T_w$
u	Circumferential velocity
V	Velocity
α	Angle of attack
β_1	Passage inlet angle
β_2	Passage exit angle
δ	Blade wedge angle
ε	Passage diffuser divergence angle
η	Shock wave effectiveness
θ	Inclination angle of shock wave to passage pressure surface

SECTION I
INTRODUCTION

In the past years several investigators have demonstrated the feasibility of compressors with supersonic flow in the blade passages and have shown that one could expect high pressure ratios and good efficiencies from such machines. (Refs. 1, 2, 3, 4). However, experimental studies conducted on supersonic blade passages (Ref. 5) rotors (Refs. 6, 7) and rotor and stator combinations (Ref. 8) have not born out the theoretical predictions. In all cases large discrepancies were noted between the flow patterns on which the passage designs were based and those observed experimentally: the experimentally determined shockwave configurations differed from those forming the basis of the designs and the estimated performance of the subsonic diffuser region of the passages could not be attained. In an effort to throw light on this situation an extensive study was undertaken at the Research Foundation of The University of Toledo under the support of the Aeronautical Research Laboratory, OAR of USAF, that was directed toward an understanding of the fundamental principles governing the flow through supersonic compressor passages of various geometries. The first phase of the study which dealt with passages of convergent-divergent geometries covered the period from 1950 to 1953 and was reported in Ref. 9) in September 1953. The second phase of the work concerned itself primarily with convergent passages; it was completed in 1955 and is contained in Ref. 5. The final phase of the investigations which was conducted from 1955 to 1960 is presented in this report;

various convergent and convergent-divergent passage geometries were considered and the effects of turbulence generators, blunted leading edges, discontinuities in the passage surface in the vicinity of the throat, and alterations in the shape and size of the trailing edge region investigated. In addition, tests were also conducted concerning the nature and magnitude of the energy losses in the mixing region of two supersonic parallel jets; this information is of relevance when supersonic compressors are being considered as the source of motive power for high speed jet pumps.

The material presented in Section II of this report represents a review of results of the first and second phases of the passage studies that have already been reported in detail (Refs. 4, 5) while the third and final phase of the study is covered in Sections III and IV. The study on mixing of the supersonic jets is presented separately as part II of this report.

SECTION II
CONVERGENT-DIVERGENT PASSAGE TESTS

(A) Passage Geometries:

The first phase of the study (Ref. 9) concerned itself with passages of convergent-divergent geometry that were designed for supersonic relative inlet velocities and subsonic discharge flow. Such a passage is shown schematically in Fig. 1. Here, it is assumed that the flow entering the passage will be deflected and decelerated by means of an oblique shock due to the fact that the high pressure surface of the passage profiles includes an angle of attack α with

the incoming flow. The change in direction of the flow equals here the angle of attack α and as shown in Fig. 1 this angle is identical with the wedge angle δ of the profile leading edges. At the passage throat the flow undergoes a further reduction in speed to subsonic values through a normal shock, with subsonic diffusion following in the divergent region of the passage, where the flow is considered to be parallel to the diffusor axis. The velocity diagram representing such a flow is shown in Fig. 2.

In determining the geometry of passages of this type the following considerations were felt to be relevant:

a) at design conditions the wedge angle δ of the leading edge should not exceed the maximum possible value for attached shock corresponding to the relative inlet Mach Number. (The dependence of $\delta_{max.}$ on M_1 is shown in Fig. 3).

b) the pressure ratio across the leading edge oblique shock and through the normal shock in the throat should be limited to values that will not induce separation in the region of interaction between the shockwave and the wall boundary layer; separations of this type can result in a breakdown of the flow in the subsonic diffusor and cause excessive losses. The determination of acceptable limits for the pressure ratio across these shocks was one of the objectives of the present study.

c) the pressure rise through the passage shock system should be apportioned between the oblique and normal shock in a manner which will result in minimum over-all losses. The shock system, as shown in Fig. 4, is

considered to consist of an oblique shock followed by a normal shock; the changes in state corresponding to the shocks are indicated in the T-S diagram in Fig. 5. In view of the fact that in isentropic compression the stagnation pressure remains constant, a change in stagnation pressure is representative of the losses due to the irreversibilities inherent in a shock type compression process. This can be stated in terms of a "shock-effectiveness" which may be defined in the following manner:

$$\eta_s = 1 - \frac{p_{01} - p_{03}}{p_3 - p_1} = 1 - \frac{p_{01}}{p_1}\left[\frac{1 - \frac{p_{03}}{p_{01}}}{\frac{p_3}{p_1} - 1}\right]$$

This effectiveness was evaluated for a series of inlet Mach numbers and leading edge wedge angles. The results of the calculations are presented in Fig. 6. With the aid of the curves shown in the figure one can readily determine for a given value of M_1 the wedge angle δ which will result in maximum shock-effectiveness; the entropy rise corresponding to the optimum combinations of Mach Number and wedge angle is shown in Fig. 7.

d) the ratio of inlet area to throat area A_1/A_t (see Fig. 1) must satisfy the starting requirement; i.e., when at starting a normal shock appears at the passage inlet the Mach Number at the throat M_t must not exceed unity, otherwise the shock cannot pass through the convergent region into the divergent section. If one assumes that the flow is isentropic within the passage this requirement can be obtained from the curve A of Fig. 8. Curve B is representative of test data (Ref. 22) indicating the magnitude of frictional effects.

e) the angle of divergence ϵ of the subsonic portion of the passage should be an optimum selected for maximum efficiency, large angles being the cause of excessive friction losses due to the rapidly thickening boundary layer and small angles resulting in excessive passage length. Available data on low speed diffusers indicate that $\epsilon = 4^{\circ}$ may be considered an appropriate value.

(B) Test Results:

Based on the criteria outlined above three convergent-divergent passages were designed for M = 2.00 and tested. They had identical convergent regions ($A_i/A_t = 1/.78$ and $\delta = 10^{\circ}$), differed, however, in the angle of divergence ϵ of the diffuser region (ϵ was 12° in passage No. 1 and 6° and 0° in passages No. 2 and 3 respectively). The details of these passage geometries and the description of the tests can be found in Ref. 9. The results of these tests show the following: (a) There is a separated region in the diffuser; its extent increases with passage pressure ratio and divergence angle. (b) There appears to be no possibility for the realization of the oblique shock-normal shock configuration that was the basis of the design. The oblique shock at the leading edge materializes in a predictable manner, however, an irregular and complex shock pattern appears in the divergent region instead of the normal shock that was anticipated. This shock pattern extends, at the maximum obtainable pressure ratios, over the greater portion of the divergent section. (c) At M = 2.28 a maximum pressure ratio $P_3/P_1 = 3.8$ is obtained with the passage having 0° divergence angle. This is considerably lower than the pressure ratio of 7.88 expected on the basis of the shock configuration on which the design is based. (d) Supersonic flow could not be established in the

passage, i.e., the passages "did not start," at the design Mach Number of 2.00; only after a slight increase of inlet Mach Number to 2.28 was the shock at the entrance "swallowed" and supersonic flow established within the passage. As this increase in Mach Number is equivalent to an increase by 5% in the minimum throat area required for starting one may conclude that the boundary layer, which is neglected in the calculations of the starting criterion, is in effect reducing the net passage cross section by that amount.

It is evident from the test results that were obtained in the first phase of the study that the flow picture presented in Fig. 1 is over-simplified and that passage design principles based on such a picture are inadequate as demonstrated by the discrepancies between the design flow patterns and the flow patterns observed in the tests. In the subsequent phases of the study, presented in sections III and IV of this report, an effort was made to throw some light on the causes for the discrepancies and to obtain a better understanding of the underlying phenomena. Information of this type is required for the prediction of the flow patterns within convergent-divergent compressor passages of various proportions at various inlet Mach Numbers and for the formulation of recommendations regarding the selection of passage types and the design of the blade contours.

SECTION III
STUDIES OF PASSAGE FLOW DETAILS

(A) The Test Program:

The discrepancies between the desired and observed flow patterns in

the convergent-divergent passages described in the preceding section appeared to have their origins in the boundary layers of the passages. A study of the phenomena responsible for such discrepancies must therefore be focused on the boundary layers and concern itself with aspects of the flow that have an influence on the boundary layer, e.g., pressure gradients along the passage walls, interactions between shock waves and boundary layers, etc. In the following there are listed some of the topics that seem to be pertinent in this connection.

(1) The strength of the shock that will produce separation in a boundary layer.

(2) Criteria for reattachment of a separated boundary to the passage wall.

(3) The effect of the geometry of the region downstream of a shock wave-boundary layer interaction on the nature of the interaction;

(4) The effect of Reynold's Number on the nature of the interaction;

(5) Correlation of the results of two-dimensional cascade tests with the performance of actual compressor stages having comparable geometries.

With these topics in mind a series of tests were conducted on two-dimensional passages of various geometries; some of the passages were equipped with boundary layer trips, on others it was tried to stabilize the shock waves with the aid of concave discontinuities on the surface; on one set of models blunted and serrated leading edges were tried, and in one instance the passage boundary

layers were destabilized by heating. Below is the list of models that were studied experimentally:

(a) three convergent passages with staggered leading edges and having the length to throat ratios of 1.8, 3.5, 5.7 respectively (these passages were tested with and without b. l. trips);

(b) a convergent passage with zero stagger;

(c) passages with curved entrance section (with and without b. l. trips);

(d) a convergent passage with blunted leading edge;

(e) a convergent passage with heated surfaces;

(f) convergent passages with modified trailing edge regions (extensions and cusps);

(g) convergent passages with concave surface discontinuities for shock stabilization;

(h) a convergent-divergent passage with "free jet" throat;

(i) boundary layer trip studies on flat plates (See Appendix A)

It was also intended originally to study, in addition to these passage tests, some rotating cascades and to compare the rotating cascade data with the results of the two-dimensional passage tests. A single stage compressor was actually designed and partially built for this purpose. However, because of scheduling difficulties resulting from extended use of the high speed dynamometers of the Toledo Laboratory by the Continental Motors and Aviation Corporation it was necessary to abandon this phase of the study.

Description of the tunnel of the Toledo Laboratory where the tests were

conducted, details of the test set up and of the construction details of the passage models including the mechanism for changing the pressure ratio of the passages has been presented in an earlier report (Ref. 5) and will not be repeated here.

(B) Test Results:

The test results are discussed with reference to topics 1 through 5 listed in part A above.

(a) Convergent Passages (with stagger)

To simulate the flow conditions in the entrance region of convergent-divergent compressor passages, convergent passage models of the type shown in Fig. 9 were used. The passages have one moveable surface permitting changes in the angle of convergence and terminate in a plenum chamber which is connected with the tunnel proper through a throttle valve; the setting of this valve determines the pressure ratio across the passage. Passages having various leading edge stagger angles and height-to-length ratios were investigated. The length of the shorter passages (1-1/2" upper chord) was sufficient to accomodate one reflection of the leading edge shock from the lower surface while in the longer passages (4-1/2" upper chord) there was room for two reflections. Typical Schlieren photographs of the flow through the short, intermediate, and long passages are given in Fig. 10, for $M = 2.00$; the photographs were taken at 4° convergence and at the maximum pressure ratios at which the passages were capable of operating at that value of the angle of convergence. In these tests the pressure distribution in the passages was determined with the

aid of rows of static pressure orifices on the top and bottom surfaces. The pressure ratio across the shock-boundary layer interaction and the ratio of plenum pressure to inlet pressure resulting from these measurements is shown in Fig. 11 for various degrees of convergence of the long and short passage; for the throttle settings corresponding to the maximum pressure ratios that were obtainable with each configuration. The Reynolds Number per inch at passage inlet conditions was 3.85×10^5 for these tests.

The tests of the convergent passages showed that an abrupt increase in boundary layer thickness occurs across the interaction of the boundary layer with the incident shock; and separation was observed to occur at the interaction whenever the leading edge wedge angle, i.e., the angle of convergence exceeded 4°. For this limiting value of δ the measured pressure ratio across the interaction was found to be 1.71. (The corresponding calculated value for a shock due to a 4° wedge reflected by a flat surface is 1.56).

The transition from laminar to turbulent flow in the boundary layer was observed to occur in some of these tests near the interaction of the incident reflected shock with the boundary layer. As the pressure rise to the separation point may be dependent on the effective Reynold's Number of the boundary layer, tests were also made with artificially induced turbulence. In one group of these tests the boundary layer was tripped by a single two-dimensional disturbance at the leading edge; in a second group of tests a series of disturbances was introduced into the flow in the form of narrow strips of tape placed at equal intervals along the vane surface. A typical Schlieren photograph of the flow in

the short passage equipped with the single boundary layer trip is shown in Fig. 12; the flow in a passage equipped with roughness strips on both the upper and lower surface is shown in Fig. 13.

The maximum pressure ratios obtainable in the passages equipped with roughnesses appears in Table 1. For the sake of comparison the corresponding values for smooth passages are also shown.

(b) Convergent Passage With Zero Stagger:

Whether the distance of the shock-boundary layer interaction from the leading edge of the lower surface has an effect on the performance of convergent passages was investigated using a modification of the basic passage configuration. In this modification the magnitude of the stagger angle was greatly reduced compared to the values used in the earlier tests; this was accomplished with the aid of a combination of upper and lower vanes of appropriate lengths as shown in Fig. 14. The distance of the interaction from the leading edge of the lower surface was 1.25 times the corresponding distance in the short passage shown in Fig. 10a and .73 times that found in the long passage (Fig. 10c). With the angle of the upper vane set at 3° the interaction had the appearance shown in Fig. 15. The ratio of plenum pressure to inlet pressure and the pressure ratio across the interaction in this passage are shown as functions of the vane angle setting in Fig. 11.

(c) Passages With Curved Entrance Sections:

It is well known that pressure gradients along a surface may influence substantially the velocity profiles in the boundary layer when the boundary layer

is laminar (Refs. 10 and 11) or turbulent (Ref. 12) and it is also known that the gradient affects the Reynolds Number at which transition from laminar to turbulent flow takes place (Ref. 13). In replacing the flat lower surface of the convergent passage models by curved contours, as shown in Fig. 16, pressure gradients impressed on the flow in this manner may have an effect on the performance of the passage. In the configuration shown in Fig. 16a this pressure gradient is negative along the entire lower surface while in the configurations shown in Fig. 16b it is positive near the leading edge, changes sign at the inflection point of the contour and is negative over the remaining portion of the surface. The effect of the pressure gradients was investigated for various vane angle settings, i.e., various intensities of the incident shock. Typical Schlieren photographs of the flow in each of the models as shown for maximum pressure ratios in Fig. 17 and 18; the pressure ratio vs. vane angle setting are shown in Figs. 19 and 20.

(d) Passages With Blunted Leading Edges;

One of the parameters known to influence the flow in boundary layers at high speeds is the leading edge thickness. Increasing bluntness of the leading edge has been found to displace the point of transition from laminar to turbulent flow downstream, on flat plates (Ref. 14) and on cones and hollow cylinders (Ref. 15). An effect on the laminar boundary layer development has also been found: an increase in leading edge bluntness being accompanied by an increase in boundary layer thickness (Ref. 16). These effects are apparently manifestations of a shear layer adjacent to the surface produced by the leading edge shock

which becomes increasingly curved near the leading edge as the bluntness of the edge is enlarged. In view of this influence of the leading edge geometry on the boundary layer, tests were undertaken to determine whether blunting of the leading edge would cause changes in the shock boundary layer interaction and maximum pressure ratio of the passage. These tests were conducted on the convergent passage. Fig. 21 shows Schlieren photographs of the flow in the passage with sharp leading edge and with a blunted leading edge of 0.02" thickness. The pressure ratio variations appear for both configurations in Fig. 22. Comparison of the Schlieren photographs with corresponding pictures in passages with sharp leading edge show that, on the lower surface, the distance of the transition point from the leading edge was reduced by 50% by the blunting of the leading edge.

(e) Convergent Passages With Heated Surface:

It is apparent from the boundary-layer equations of motion that the effect of heating of passage walls is analogous to the effect of an adverse pressure gradient, i.e., it causes an increase in the rate of amplification of disturbances. Experimental verification of this conclusion can be found in Ref. 17 where it is demonstrated that heating of a flat plate results in a forward motion of the transition point. This phenomenon is apparently the consequence of changes in the velocity profile in the boundary layer brought about by the heat transfer at the surface and one may expect that heating of the walls of a convergent passage will produce similar effects and result possibly in changes of the performance of the passage.

Several tests of a passage with heated walls were made utilizing the passage of intermediate length. The lower as well as the upper surface of the passage was heated. Stainless steel sheets of .032" thickness were slotted as shown in Fig. 23 and bonded to the altered vanes with epoxy cement. In this manner the surfaces were converted into resistors of sufficient length to provide the heat to the boundary layers at surface temperatures of approximately 150°. The surface temperature was measured by means of thermocouples located in the positions shown in the figure, the average of these thermocouple readings being the value referred to in the data. Representative Schlieren photographs are shown for maximum pressure ratios in Fig. 24a, b, for an upper vane setting of 4°. In the test shown in Fig. 24a, the surface temperature T_w was $75^{\circ}F$ (no heating) while in 24b $T_W = 150^{\circ}F$; the measured stagnation temperature in the tunnel T_o was $101^{\circ}F$ in both instances. A comparison of the transition point location as determined from the photographs shows that the change in temperature differential $T_o - T_w$ from $+26^{\circ}F$ to $-49^{\circ}F$, i.e., a ΔT_w of $75^{\circ}F$ resulted in a decrease in transition point distance from the leading edge of the vane of 20%. The maximum pressure ratio for the heated passage was 2.62 as compared to 2.67 for the unheated passage, both at a vane setting of 4°.

(f) Convergent Passages With Modified Trailing Edge Regions:

When convergent passages operate near their maximum pressure ratio a substantial portion of the rise in pressure occurs usually in the immediate vicinity of the trailing edge. In such cases it was observed in typical Schlieren

photographs (Fig. 26-30) that this pressure rise is connected with a relatively abrupt increase in the thickness of the boundary layer in that region and this thickening of the boundary layer was found to be indicative of an impending separation of the flow from the passage wall at the trailing edge. When separation materialized, it lead in turn, to the complete breakdown of the supersonic flow in the passage. The pressure rise may be caused by one of two types of shock configurations: an incident-reflected shock originating on the leading edge of the upper surface or shock systems located at the trailing edges. As the breakdown of the flow may depend on the manner in which the pressure rise is imposed on the flow and as on the lower surface the two shock systems are usually close to each other and are therefore likely to interact, the distance between the incident-reflected shock and the trailing edge may influence the passage performance. In a series of tests this distance was varied stepwise by means of extensions added to the lower passage surface as shown schematically in Fig. 25; this figure shows five trailing edge configurations made possible with the use of four extensions. Schlieren pictures taken at the maximum pressure ratio for each of these trailing edge locations are shown in Figs. 26-30. In the upper photographs the angle of convergence of the upper vane was set at 2°; in the lower photographs the corresponding pictures for a 4° angle of convergence are shown. The maximum pressure ratios that were obtained in these tests are plotted in Fig. 31, as functions of the trailing edge location. It is apparent from these curves that, at least for the convergent passages tested, the pressure distribution in the region of increasing pressure

is of little or no influence on the magnitude of the attainable pressure rise.

It was also attempted in this series of tests to modify the pressure distribution in the discharge region of the passage by addition of a convex trailing edge extension to the lower surface (cusp); Schlieren pictures of the flow in the passages modified in this manner are shown in Figs. 32a and 32b for angles of convergence of 2° and 4° respectively. The corresponding maximum pressure ratios are shown in Fig. 31 (points A and B).

(g) Convergent-Divergent Passages With Concave Surface Discontinuities

From the data obtained on flows in convergent-divergent passages (Ref. 9) it is apparent that instead of the single normal shock, which forms the basis of the passage design, a series of irregular shocks materialize in the divergent region downstream of the throat; there is also evidence of separation of the flow from the passage walls. On basis of the information gathered from the earlier tests and utilizing the data on shock wave boundary layer interactions obtained with the convergent passage model a convergent-divergent passage geometry was arrived at which was designed for an inlet Mach Number of 1.7. This is a value which can be realized readily with a compressor rotor of 14" tip diameter operating at 30,000 rpm. The contours of this passage are shown schematically in Fig. 33a while a Schlieren photograph of the flow appears in Fig. 37. It is apparent from this figure that the shock system in the convergent section did not give rise to separation; however, separations were present in the divergent region where the static pressure was increased gradually by a multiplicity of shock. The maximum obtainable pressure ratio across the

passage was 2.97; this is slightly less than the pressure ratio which can be achieved by normal shock (3.205). An increase in inlet Mach Number to 1.98 did not result in any improvements in performance.

Surface discontinuities usually have the effect of stabilizing shock formations in supersonic flow and in view of this the convergent-divergent passage was modified to include small cavities of various shapes and sizes. These were of the shapes shown in (Fig. 33b, c & d) and were located in the divergent-section near the passage throat. Tests were conducted to determine whether the cavities would arrest the motion of the shock system from the trailing edge region toward the passage entrance that occurs usually with an increase in the pressure ratio and whether the region occupied by the shock system could be reduced in depth to a point where it would approach in appearance the normal shock configuration.

The results of these tests are presented for flows at the maximum pressure for each configuration in Figs. 34, 35 and 36. In Fig. 34 pressure distributions are presented for the 3 types of cavities shown in Fig. 33. The static pressures along the center line of the upper and lower surface of the passages are plotted in inches Hg absolute in order to permit comparison of the pressures on opposite sides of the channel; in Fig. 35 the same information is presented in the form of dimensionless pressure ratios with the low pressure near the leading edge being used in each case as the reference. It is apparent from these figures that the pressure distributions are on the whole not affected by the presence or shape of the cavities that were used. (In one case - run 5-5 -

where the observed pressure rise was smallest the passage was most likely not operating at its maximum pressure ratio). A comparison of the pressures on a smooth passage with those on one with cavities is shown in Fig. 36. The effect of Mach Number is also demonstrated in this figure; curves at $M_1 = 1.7$ and at $M_1 = 1.92$ are shown. For the tests at the lower Mach Number the passage models were set at a negative angle of attack and this resulted in a shock on the leading edge of the lower surface which caused the desired reduction in inlet Mach Number. The maximum pressure ratio obtainable with the various configurations are summarized in Table II. Typical Schlieren photographs corresponding to the test points shown in the curves appear in Figs. 37-40.

(h) Convergent-Divergent Passages With Free Jet Throat:

The study of the effect of surface discontinuities was extended to cover passages with large rectangular cutouts that simulate, in an approximate manner, free jet conditions in the throat of the passage. As shown in the diagrams in Fig. 41 the cutouts were rectangular in cross section and were positioned in the minimum area portion of the passage. The effect of the cavity on the structure of the boundary layer in the divergent region and on the nature of the interaction with the shock system may of course depend on the depth (d) and the chord length (c) of the cavity, in the slope of the lip contours and on the exact location in the passage. However, the study of the possible effect of these parameters was considered outside of the scope of these investigations. It was merely attempted to establish whether a significant effect on passage performance could be detected. In view of this the depth of the cavities was

made as large as the passage models could accomodate (0.25") and only two chord lengths were used. In the case of the shorter cavity, shown in Fig. 41a, the chord is equal to the height of the passage throat (c = h = 0.6") while in the larger cavity shown in Fig. 41b the chord exceeds this value by 0.38'. The ratio of depth to chord length d/c was 0.42 and 0.26 respectively; it was felt that this parameter must be kept sufficiently large in order to prevent the main flow from turning into the cavity. Recently published data on flows in rectangular cavities (Ref. 18) indicate that a value of d/c of 0.16 would probably have sufficed.

The results of these tests are summarized in Figures 42 and 43. Fig. 42 shows the pressure distribution on the walls of the passages with the cavities of 0.6" and 0.98" chord length; the pressure distribution on the original passage without cavities is also included. Fig. 43 shows for the case of the 0.6" cavity the effect of back pressure (throttle position) on the pressure distribution from minimum (wide open throttle) to the maximum that can be maintained across the passage. The values of the maximum pressure ratios appear also in Table II. Typical Schlieren photographs for these passages are shown in Fig. 44.

SECTION IV
DISCUSSION OF RESULTS

(A) Convergent Passage Tests:

In the tests of the convergent passage models it was found that the

supersonic flow through the passage will break down if the ratio of the static pressure at the discharge to that at the inlet of the passage exceeds a certain maximum. At that point a drastic change occurs in the flow pattern which causes blockage of a portion of the area at the discharge choking thereby the passage and forcing a detached shock wave to appear at the passage entrance.

From Schlieren observations of the flow by means of high speed motion pictures it was determined that the change in flow pattern was triggered by a rapid thickening of the boundary layer which was followed in some instances by separation of the flow from one of the passage walls. At small angles of convergence this disturbance occurred at the trailing edges due to the fact that the shock wave at the leading edge of the upper surface was relatively weak and the major portion of the pressure rise took place through oblique shock originating at the passage exit. With an increase in the angle of convergence the shock at the leading edge of the upper surface became stronger and an increasingly larger portion of the total pressure rise occurred at the point of incidence of the leading edge shock on the lower surfaces. This is apparent from the lower curves in Fig. 11 which shows the manner in which, at that point, the pressure ratio across the shock boundary layer interaction increases with increasing values of the angle of convergence. The pressure ratio across the passage is also shown in the upper curves of the figure. And while the curve representing the interaction pressure ratio approaches with increasing angle of convergence the upper curve the interaction pressure ratio is always less than the passage pressure ratio. This is due to the fact that the

angle of convergence of the passage is limited by the ratio of the discharge area to the inlet area which is inversely proportional to the degree of convergence. Thus there is for each of the passage configurations a limiting degree of convergence; it is approximately 4°, 6° and 10° respectively for the large, intermediate and short passage configurations.

It is also apparent from Fig. 11 that the total pressure rise on the passage is independent of the angle of convergence, i.e., it is immaterial whether the major portion of the pressure rise takes place at the trailing edge, whether it is distributed equally between the interaction and the trailing edge or whether most of it occurs at the interaction. This finding agrees with the general conclusions reached by Kuehn (Ref. 19) on the basis of a study of the pressure rise required for incipient separation of a turbulent boundary layer in two dimensional supersonic flow. It is reported in that study that for low supersonic Mach Numbers (from about 1.7 to 3.6) the incipient separation pressure ratios are approximately the same for an incident shock and a compression corner and that in the low Mach Number range incipient separation conditions for various model shapes may be described at a given value of the Mach Number and Reynold's Number in terms of a single pressure ratio; at $M = 2.00$ this pressure ratio was found to be approximately 2.25 (Fig. 20 of Ref. 19) and the Reynold's Number at the interaction was given there as $R = 4.5 \times 10^4$ which compares favorably with the Reynold's Number of 3.85×10^5 per inch in the convergent passages used in the present studies. Furthermore, it appears from Kuehn's study (Fig. 24 of Ref. 19) that for model geometries

for which the size of the separated region is a continuous function of M and R incipient separation may occur at pressure ratios as high as 2.8.

In the present study the maximum pressure ratio of convergent passages was observed to be in general between 2.5 and 2.7. The data presented in Fig. 11 indicate however that small but noticeable differences exist between the various passage configurations and that the longer passages are able to withstand the higher pressure ratios. As the pressure rise occurs in the longer passages through a larger number of weaker shock waves and the interactions of these waves with the boundary layer are distributed over a greater distance this result is not unexpected.

Changes in the interaction Reynold's Number were effected by changes in the angle of stagger of the leading edges; an increase in stagger angle being inversely proportional to the distance of the interaction on the lower surface from the leading edge. It is apparent from Fig. 11 which includes the data on a passage with zero stagger that a change in stagger angle did not influence the passage performance. One may therefore conclude that at M = 2.00 and for free stream Reynold's Number in the vicinity of 5×10^5 per inch the effect of Reynold's Number is negligible. This finding is also born out by the results of the tests published by Kuehn (Ref. 19) who is pointing out that for compression corners, curved surfaces and incident shock waves the pressure rise required for separation decreases substantially in the range of Mach Numbers from 3 to 4 when the Reynold's Number R_δ is increased from 2×10^4 to 10^5 while at Mach Numbers near 2.0 the effect of Reynold's Number is small and seems to

approach zero at the higher values of R_δ .

The results of the tests on the passages with curved lower surfaces, with blunt leading edges and with heated surfaces described in the previous section also point to the absence of significant Reynold's Number effects for $1.7 < M < 2.3$ and $R = 4 \times 10^5$ per inch. These passage geometries represented changes in basic passage configurations that were made with the intention of altering the boundary layer flow in the critical regions of the passage. The observed passages were however found to be relatively insensitive to the changes affecting the boundary layer structure. It was also found that the maximum pressure ratio was not affected by changes in the distance of the point of incidence of the leading edge shock from the trailing edge. Variations of that distance were realized by means of extensions that were attached to the lower surface as described in the preceeding section.

(B) Convergent-Divergent Passage Tests:

The information that was obtained from the studies described in the preceeding sections of this report were applied to a convergent-divergent passage design for an inlet Mach Number of 1.7. Tests of this passage revealed that the maximum pressure ratio of the passage is slightly below the value associated with a normal shock; the pressure rise through the passage was found to be gradual and while separation was apparent in the divergent-section the extent of the separated region appeared to be quite small. This is felt to be of some significance when a cascade utilizing blades of this geometry is to be used in conjunction with other rows of blades.

While it has been known that the static pressure rise obtainable in passages of constant or nearly constant area corresponds that across a normal shock at inlet Mach Number (Ref. 20) it does not follow necessarily that a pressure ratio of this magnitude can always be obtained. This is apparent from the fact that a change in the inlet Mach Number of the convergent-divergent passage from 1.7 to 1.98 did not result in a significant increase in pressure ratio (see Table II). This represents essentially a deterioration of the passage performance as compared to the normal shock pressure rise. The cause of this may be a mismatch between inlet geometry and inlet Mach Number: at $M_1 = 1.98$ the leading edge shock impinges on the lower surface at a point downstream of the throat, i.e., in the divergent section and a large separation may occur at the point of incidence. In support of this interpretation attention should be called to the convergent-divergent passage with free jet throat (Fig. 41) in which a maximum pressure ratio of 3.45 was obtained.

SECTION V
CONCLUSIONS

The following conclusions were drawn from the investigations on convergent and convergent-divergent passages with reference to supersonic compressor cascade applications:

(1) Convergent-divergent passage contours are suitable for supersonic stator and rotor applications provided that the solidity ratio of profile length to profile spacing is sufficiently high to prevent extensive separation in the divergent sections.

(2) The angle of convergence at the inlet (leading edge wedge angle) must be kept small so that separation is minimized at the point of incidence of the leading edge shock on the lower surface. The pressure ratio for incipient separation of a turbulent boundary layer due to an incident shock (Ref. 19) appears to be a satisfactory criterion for the choice of an appropriate leading edge shock strength. Care must be taken, however, that the boundary layer be actually turbulent at the location of the interaction.

(3) The ratio of throat area to inlet area is limited by passage starting considerations. The usual impirical starting criteria for supersonic diffusors appears to be applicable to convergent-divergent passages.

(4) In order to prevent large flow separations in the divergent region a constant area section of sufficient length should be provided in the passage throat between the convergent and divergent region.

(5) The optimum passage performance that should be anticipated corresponds to the pressure recovery across a normal shock at the inlet Mach Number. Consequently reasonably efficient supersonic cascades are most likely to be realized with relatively low supersonic Mach Numbers.

(6) By further experimentation with convergent-divergent passages it should be possible to obtain pressure recoveries in excess of the normal shock values. In this connection attention should be called to the significant improvement in the performance of a divergent passage that was obtained by Weise many years ago by means of boundary layer control (Ref. 21).

List of References

1. Kantrovitz, A., "The Supersonic Axial-Flow Compressor," NACA T.R. 974, 1950.

2. Wright, C.C., Klapproth, J.F., "Performance of Supersonic Axial Flow Compressors Based on One-Dimensional Analysis," NACA RM E8L10, 1949.

3. Schnell, E., "Problems des Ueberschall Axialverdichters," M.T.Z. vol. 16, No. 2, February 1955, 42-46.

4. Fejer, A., Wenzlau, W.D., Report AE1, University of Toledo Research Foundation, USAF Contract AF33(038)11377, June, 1951.

5. Fejer, A.A., "Supersonic Cascade Studies," WADC T.R. 55-396, June, 1955.

6. Ritter, W.K., Johnsen, I.A., "Performance of 24" Supersonic Axial Flow Compressor in Air," NACA RM E8G01. 1949.

7. Lown, H., Hartmann, M.J., "Investigation of a 24" Shock-in-Rotor Type Supersonic Compressor Designed For Simple Radial Equilibrium Behind Normal Shock," NACA RM E51H08, 1951.

8. Goldstein, A.W., Schacht, R.L., "Performance of a Supersonic Compressor With Swept and Tilted Diffuser Blades," NACA RM E54L29, 1955.

9. Fejer, A.A., "Supersonic Cascade Studies," Report AE2, Research Foundation of The University of Toledo, USAF Contract 33(616)-12, September, 1953.

10. Low, G.M., "Simplified Method For Calculation of Compressible Laminar Boundary Layer With Arbitrary Free Stream Pressure Gradient," NACA TN 2531, October 1951.

11. Low, G.M., "The Compressible Laminar Boundary Layer With Heat Transfer And Small Pressure Gradient," NACA TN 3028, October, 1953.

12. Reshotko, E., and Tucker, M., "Approximate Calculation of The Compressible Turbulent Boundary Layer With Heat Transfer And Arbitrary Pressure Gradient," NACA TN 4156, December, 1957.

13. Tani, T., "On The Design of Airfoils in Which The Transition of The Boundary Layer is Delayed," Aeronautical Research Institute Tokyo

Imperial University, Rept. 250, Vol. 19, No. 1, January, 1949 (Translation NACA TM 1351, 1952).

14. Moeckel, W.E., "Some Effects of Bluntness on Boundary Layer Transition And Heat Transfer at Supersonic Speeds," NACA T.R. 1312, 1957.

15. Monta, W.O., Howard, P.W., and Czarnecki, K.R., "Effect of Nose Bluntness on Transition For a Cone and a Hollow Cylinder at Mach Numbers 1.41 and 2.01," NASA TN D-717, April, 1961.

16. Bradfield, W.S., DeCoursin, D.G., and Blumer, C.B., "The Effect of Leading Edge Bluntness on a Laminar Supersonic Boundary Layer," Journal of the Aeronautical Sciences, Vol. 21, No. 6, June, 1954, pp. 373-382.

17. Liepmann, H.W., and Fila, G., "Investigations of The Effect of Surface Temperature And Single Roughness Elements on Boundary Layer Transition," NACA T.R. 890, 1947.

18. McDearman, R.W., "Investigation of The Flow in a Rectangular Cavity on a Flat Plate at M = 3.55 NASA T.N. D523, September, 1960.

19. Kuehn, D.M., "Experimental Investigation of The Pressure Rise Required For The Incipient Separation of Turbulent Boundary Layers in Two Dimensional Supersonic Flow," NASA Memo 1-21-59A, February, 1959.

20. Neumann, E.P., and Lustwerk, F., "High Efficiency Supersonic Diffusers," Journal Inst. of Aero Sciences, Vol. 18, No. 6, p. 369.

21. Weise, A., "Ueber die Stroemungsabloesung durch Verdichtungs - Stoesse," Technische Berichte, Vol. 10, 1943, pp. 59-61.

22. Goldbaum, G. C., "Aerodynamic Characteristics of Nozzles and Diffusers for Supersonic Windtunnels"; Defense Research Laboratory, University of Texas, August, 1954.

TABLE I

Comparison of maximum pressure ratios of 1.5 inch passage of 6° convergence with various types of roughness.

Description of Roughness	Maximum Pressure Ratio
Series of strips .047" wide x .0026" high .0625 inches apart along upper vane	2.33
Series of strips .047" wide x .0026" high .0625 inches apart along upper and lower vanes	2.25
Single strip .047" wide x .0208" high on lower vane	2.32
Single strip .047" wide x .0208" high on lower vane / single strip .047" wide x .0203" high on upper vane	2.44
No roughness	2.5

TABLE II

Effect of concave surface discontinuities on flow in convergent-divergent passage.

Description of Discontinuity	$M_1 = 1.7$		$M_1 = 1.92$	
	Run	Max. Pr. Ratio	Run	Max. Pr. Ratio
None - Smooth Surface	1-5	2.97	1-8	3.06
.062" Square Groove	5-3	3.02	5-5	2.93
.062" Sq. Plus .125" Dia. Groove	7-5	2.8	7-2	2.96
.375" x .25" Groove	8-5	2.84	8-2	3.06
.6" Chord "Free Jet" Throat			9-3	3.45
.98" Chord "Free Jet" Throat			10-2	3.18

APPENDIX A

Boundary Layer Trip Study

I. Introduction:

From the experimental studies of shock-boundary layer interactions (Ref. A1) it is readily apparent that the nature of the interaction is governed by conditions in the main stream (Mach number, pressure gradient, etc.) and the nature of the flow in the boundary layer. It is, of course, well known that these influences are interrelated because the main stream is coupled to the boundary layer flow and consequently the nature of an interaction of a shock with a laminar boundary layer is quite different from a turbulent boundary layer interaction.

In the study of supersonic passages described in the main body of the report, it seemed appropriate to select model passage dimensions that would insure that the boundary layer was always turbulent in the regions where it interacted with shockwaves; however, the Reynolds number of the boundary layer at the interaction closest to the leading edge was considered marginal (2×10^5) and while it appeared from Schlieren photographs that the interaction was a turbulent one it was decided to equip several of the models with tripping devices in order to increase, in this manner, the effective Reynolds number of the boundary layer. A tripping device may of course have undesirable side effects as far as passage performance is concerned, e.g. increased frictional losses, and it is therefore important to use the smallest possible trips capable

of causing boundary layer transition.

A survey of the information on boundary layer tripping devices available in the literature indicated that data on artificially induced turbulence in supersonic flow is extremely meager and limited in scope (Refs. A2, A3, A4, A5). It was decided for this reason to undertake an investigation of the characteristics of boundary layer trips on a flat plate at M = 2. It should be pointed out, however, that the results of this study were primarily intended for use in connection with the tests conducted in the supersonic wind tunnel of the Toledo Laboratory and care has to be exercised in applying them to flows in other environments where the scale and intensity of free stream turbulence, stagnation pressure, rate of heat transfer to model walls and other details of the flow may be sufficiently different to influence significantly the performance of the trips. The details of the study and the results derived from it are presented in the following.

II. Description of Experimental Set-up and Techniques:

A flat plate 3-3/4 inches wide and 6 inches long was utilized in the study. It was equipped with a wedge shaped leading edge (18° wedge angle); the upper side of the wedge was in line with the plate surface. The model is shown in Figs. A1 and A2. The surface of the plate was smooth (the average roughness was about 16 micro inches) and it was carefully aligned with the direction of flow in the constant pressure portion of the test section of the 5-1/2" x 6-3/4" wind tunnel. In order to assure two-dimensional flow over the plate it was at first equipped with glass side plates, but later in the program the side plates

were omitted when it was found that they had little effect on the magnitude and direction of the flow velocity along the center line of the plate.

Three techniques were used to locate the transition point along the center line of the plate: skin temperature distributions, total head surveys and Schlieren photographs. On the model devised for the temperature distribution method, a thin plate (.031") was used; it was thermally insulated from the supporting structure and it was equipped with a row of thermocouples located on .25 inch centers. The thermocouple readings along the plate revealed an increase in local temperature recovery factor in the transition region; however, the rate of change of temperature along the plate was found to be too gradual to permit pinpointing of the transition point location with sufficient accuracy. On the other hand the transition point locations determined from the Schlieren photographs and total head surveys agreed with each other in most instances very well; in the few instances when discrepancies did appear they did not exceed 6% of the distance from the leading edge. A typical Schlieren photograph is presented in Fig. A3 which also shows the type of total head probe that was used for the pressure surveys. The probe was supported from the back and could be moved along the axis of the plate and along the normal to the plate surface.

The majority of the boundary layer trips that were used were two-dimensional; a few three-dimensional trips were also studied. The two-dimensional trips were rectangular ridges of .094 inches in width and were made up of individual layers of cellophane tape; the ridges varied in height from 0.0026

inches to 0.0234 inches depending on the number of layers used. The three-dimensional trips consisted of single rows of glass beads of 0.015 inches diameter glued to the surface. The trips were arranged to cover the entire width of the plate and were located at various distances from the leading edge of the plate; the range of distances covered was .078" to 1".

The tests were conducted at a fixed Mach number (M = 2.00) with stagnation pressure and stagnation temperature held also constant.

III. Test Data and Results:

a) Two-dimensional trips:

In the first troup of tests conducted on the two dimensional trips a thin plate was used; it was mounted between parallel side plates of glass and equipped with thermocouples indicating the temperature gradient along the center line of the plate. The results obtained by means of the temperature distribution method were however inconclusive, as mentioned before, and therefore detailed description of this phase of the studies is not given. In all subsequent tests a thicker plate was used, the side plates were omitted and the model was equipped with a total pressure survey probe.

The information recorded during each of the tests included the pressures and temperatures required to determine the tunnel operating point, static pressures at several stations on the plate and a series of total pressures obtained with the traversing probe along a vertical line normal to the surface of the flat plate, at various distances from the leading edge of the plate. Traverses were made starting with the center of the probe .010" from the surface

and ending with the probe in the free stream with the distance between the individual points of the traverse being .005". The distance between the survey stations on the center line of the plate was .5 inches. During each of the vertical traverses several Schlieren photographs were taken.

From the total pressure distributions that were obtained in the manner described above, data were deduced regarding the thickness of the boundary layer and the location of the transition point in a simple manner indicated schematically in Fig. A4. This figure also serves to define the terms "boundary layer thickness "y" and transition point location "x_t" as used here.

A summary of the results of the tests is given in Table AI. The symbols used in this table are summarized in the following:

List of Symbols

x_d Distance of upstream edge of trip from leading edge of plate.

x_{to} Distance of transition point from leading edge on smooth plate.

x_t " " " " " " " " " " " " plate with trip.

d Height of trip.

P_o Free stream stagnation pressure.

T_o Free stream stagnation temperature.

$R_e = \frac{U}{\nu}$ Reynolds number, per inch of length at free stream P, T.

$R_t = \frac{Ux_t}{\nu}$

$R_{x_d} = \frac{Ux_d}{\nu}$

$R_d = \frac{ud}{\nu}$

$R_o = \frac{ux_{to}}{\nu}$

δ^* Displacement thickness of compressible laminar boundary layer at a distance x, from leading edge of plate. (calculated according to Ref. A5).

δ_d^* Displacement thickness at trip location (in absence of trip).

d_{crit} Critical trip height, causing transition at trip location ($x_t = x_d$)

It is evident that the location of the transition point (x_t) will depend on the Reynolds number of the flow, shape and size of the trip, trip location x_d, scale and intensity of free stream turbulence, static pressure of the free stream, Mach number and temperature of the free stream and the temperature of the wall. For a given trip shape and fixed values of free stream pressure, temperature, and turbulence, and neglecting changes in the wall temperature one may write the functional relationship between the dependent and independent variables in the following dimensionless form

$$x_t / x_{t_o} = f(R_{x_d}, d/_{x_{to}}) \quad \ldots . \quad (1)$$

If the data of Table AI are presented in a graphical form based on such a relation, Fig. A5 results. In Fig. A5 each of the curves labeled $R_{xd} = C$ corresponds to a fixed trip location, characterized by the value of R_{xd}, with the trip size ($d/_{x_{to}}$) increasing along the abscissa. The solidly drawn portions of the curves indicate the range of trip sizes for which $x_t > x_d$; x_t decreases from the maximum value of x_{to} on the smooth plate (i.e., $d = 0$) with increas-

ing trip height d, to the minimum where $x_t = x_d$. The trip height corresponding to this minimum is referred to here as the critical trip height causing transition at the trip location. From the critical point on, the curves in Fig. A5 are horizontal as a trip height exceeding d_{crit} can have no further effect on x_t. A critical analysis by Dryden of various published low speed trip studies (Ref. A8) shows acceptable correlations between the results of these studies when the trip size is expressed in terms of the laminar boundary layer displacement thickness δ^* at the trip location. In this manner one includes the Reynolds number of the flow implicitely in δ^* as $\delta^* = f(Re, x)$ and consequently Eqn. 1 can be restated in this case in the following form:

$$x_t / x_{t_o} = f(d/\delta^*_d, x_d / x_{t_o}) \quad \ldots\ldots\ldots\ldots\ldots (2)$$

In Fig. A6 the data from Table I are presented in the form corresponding to Eqn. 2. The ordinate in this figure is again x_t / x_{t_o} but the abscissa is now d/δ^*_d; here the displacement thickness δ^* has been calculated with the aid of the relations given by Chapman and Rubesin in Ref. A5.

It is apparent from Fig. A6 that when transition occurs downstream of the trip, i.e., when $x_d < x_t$ the data obtained with various trip locations fall all on a single curve. This result is in agreement with the findings of Tani, Hama and Mitsisi (Ref. A6) and Tani and Hama (Ref. A7) obtained in incompressible flow with cylindrical trips. It should be noted however, that as far as sizes of the trips is concerned, the values of d/δ^* required to trip the boundary layer in the present study are considerably larger than the corresponding values used in incompressible flow in Refs. A6, A7, A8 and in the recent

results of Smith and Clutter (Ref. A9).

The minimum trip sizes that are necessary to move the transition point to the trip location (i. e. for $x_t = x_d$) referred to here as critical trip sizes are denoted by $(d/\delta^*)_{crit}$ and these are presented for the various trip locations and boundary layer Reynolds numbers in Figs. A7 and A8. It is apparent from these figures that near the leading edge of the plate, where R_{x_d} and R_{δ^*} are small, the height of the required tripping device is a larger multiple of the local boundary layer thickness than at locations that are further downstream; at $x_d = 0.078$ inches, $(d/\delta^*)_{crit}$ is 7.25, while at the 1 inch location it is only 3.4.

b) Three Dimensional Trips:

The results discussed so far refer to two-dimensional, rectangular-ridge types of tripping devices. While the disturbances produced by a two-dimensional ridge, are larger than those present in the wake of three-dimensional trips of equal height, it would seem that the latter should be more effective: two-dimensional disturbances must first break up into three-dimensional vorticity before they can produce turbulence type perturbations in the boundary layer. Consequently the effect of three-dimensional trips on x_t/x_{to} ought to be less pronounced than that of a two-dimensional trip of equal height. However, as shown by point A in Figs. A5 and A6 tests made with three-dimensional trips consisting of a row of spherical glass beads do not support this hypothesis. In these tests the beads were 0.015 inches in diameter, located at $x_d = 0.5''$ and arranged on 0.031" centers. It appears that the test point A falls within the

range of the data obtained with two-dimensional trips. A possible explanation of this may be that the spacing between the beads was too small (2 diameters between centers) to permit three-dimensional wakes to develop.

List of References

A1 Chapman, D. R., Kuehn, D. M. and Larson, H. K. "Investigation of separated Flows in Supersonic and Subsonic Streams With Emphasis on The Effect of Transition" NACA TN 3869, March 1957.

A2 Brinich, P. F., "Boundary Layer Transition at M = 3.12 With and Without Single Roughness Elements" NACA TN 3267, Dec. 1959.

A3 VanDriest, E. R., and Boison, J. C., "Experiments on Boundary Layer Transition at Supersonic Speeds" Journal of Aero. Sciences, Vol. 24, No. 12, pp. 885, Dec. 1957.

A4 Braslow, A. L., "Effect of Distributed Granular Type Roughness on Boundary Layer Transition at Supersonic Speeds With and Without Surface Cooling". NACA RML 58 A17, March 1958.

A5 Chapman, D. R. and Rubesin, M. W., "Temperature and Velocity Profiles in The Compressible Laminar Boundary Layer With Arbitrary Distribution of Surface Temperature" Journal of the Aero Sci., Vol. 16, No. 9, pp. 547, Sept. 1949.

A6 Tani, I., Hama, R., and Mituisi, S. "On The Permissible Roughness in the Laminar Boundary Layer" Aeronautical Research Institute of Tokyo, Rep. 199, 1940.

A7 Tani, I., and Hama, R., "Some Experiments on the Effect of a Single Roughness Element on Boundary Layer Transition" Journal of the Aero. Sci., Vol. 20, No. 4, pp. 289, April 1953.

A8 Dryden, H. L., "Review of Published Data on The Effect of Roughness on Transition From Laminar to Turbulent Flow". Journal of the Aero. Sci., Vol. 20, No. 7, pp. 477, July 1953.

A9 Smith, A.M.O. and Clutter, D. W., "The Smallest Height of Roughness Capable of Affecting Boundary-Layer Transition". Journal of the Aero/Space Sciences, Vol. 26, No. 4, pp. 229, April 1959.

TABLE A1

Test No.	x_d''	$d'' \times 10^3$	Po lbs/ft.	To °F	Re/inch $\times 10^{-5}$	x_t Graph	x_t Schl.	$R_t \times 10^{-5}$	$R_d \times 10^{-2}$	x_t/x_{t_o}	$d/x_t \times 10^{-3}$	d/d_*
26, 28	0.50	0	2574	105	3.636	2.40		8.73	0	1.000	0	0
30	"	2.6	2531	120	3.448	2.00	1.980	6.86	8.95	.832	1.085	0.68
32, 33	"	5.2	2588	120	3.526		1.575	5.55	18.30	.655	2.17	1.37
27	"	7.8	2545	105	3.595	1.40	1.350	4.95	27.80	.572	3.25	2.05
31	"	10.4	2559	120	3.487	1.10	0.940	3.60	36.40	..480	4.33	2.73
34	"	13.0	2559	115	3.529	1.00	0.935	3.53	45.90	.404	5.41	3.42
28	"	15.6	2581	105	3.646	0.80	0.790	2.92	57.00	.332	6.50	4.10
--	"	18.2									7.57	4.79
29	"	20.8	2620	105	3.701	0.50	0.500	1.85	77.00	.208	8.66	5.47
35	0.078	2.6	2538	115	3.500	1.50	1.500	5.25	9.10	.624	1.08	2.00
36	"	5.2	2612	110	3.646	1.00	0.850	3.10	19.0	.354	2.17	4.00
37	"	7.8	2531	110	3.533	0.50	0.450	1.59	27.5	.187	3.25	6.00
38	1.000	7.8	2578	115	3.555		1.650	5.87	27.7	.686	3.25	1.50
41	"	15.6	2623	110	3.660	1.20	1.100	4.03	57.2	.458	6.50	3.00
39	"	23.4	2570	110	3.587		1.000	3.59	84.0	.416	9.75	4.50
40	0.50	15.0	2637	112	3.660	0.75	0.720	2.64	54.9	.300	6.24	4.55

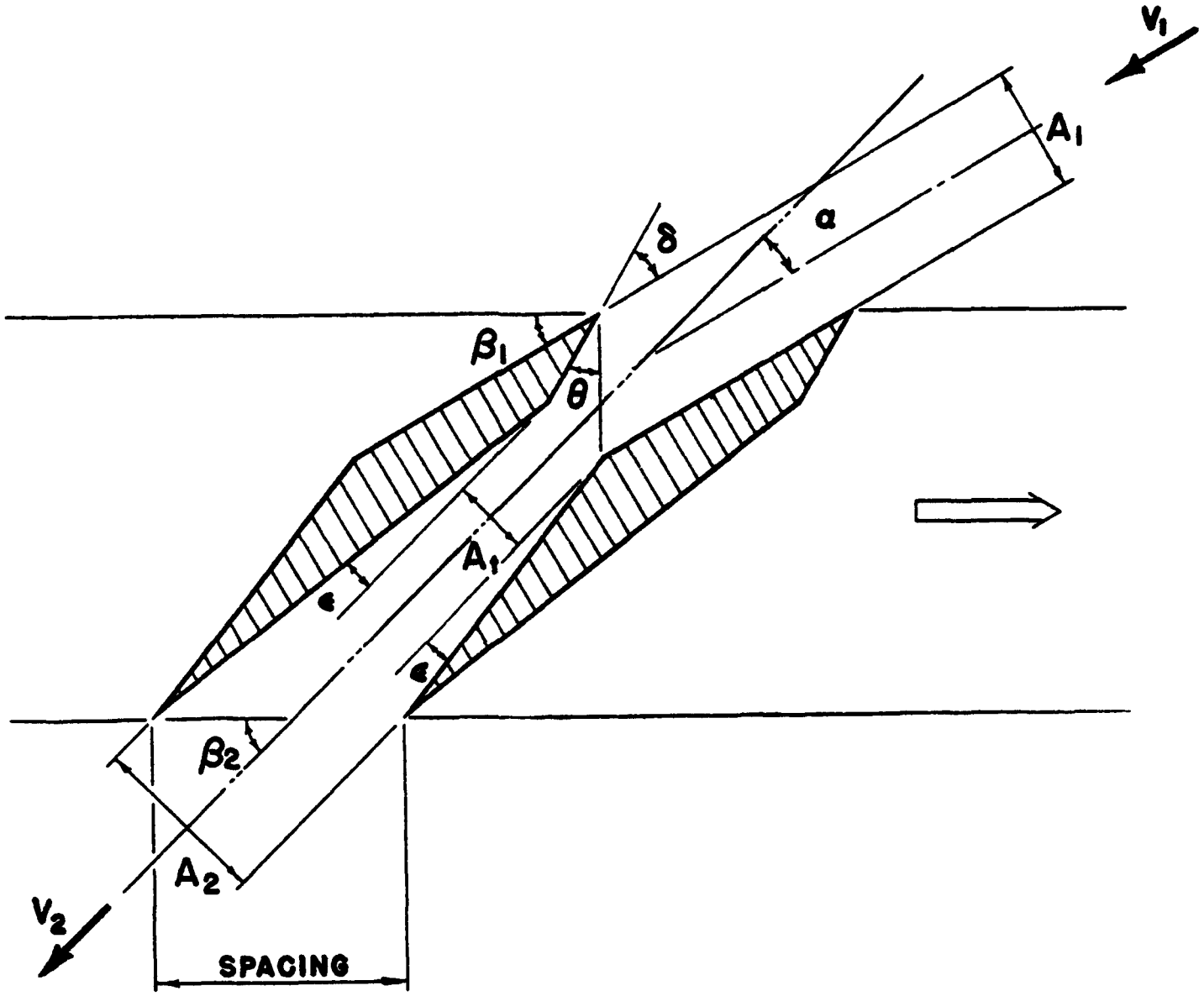

Figure 1. Convergent-Divergent Passage Schematic

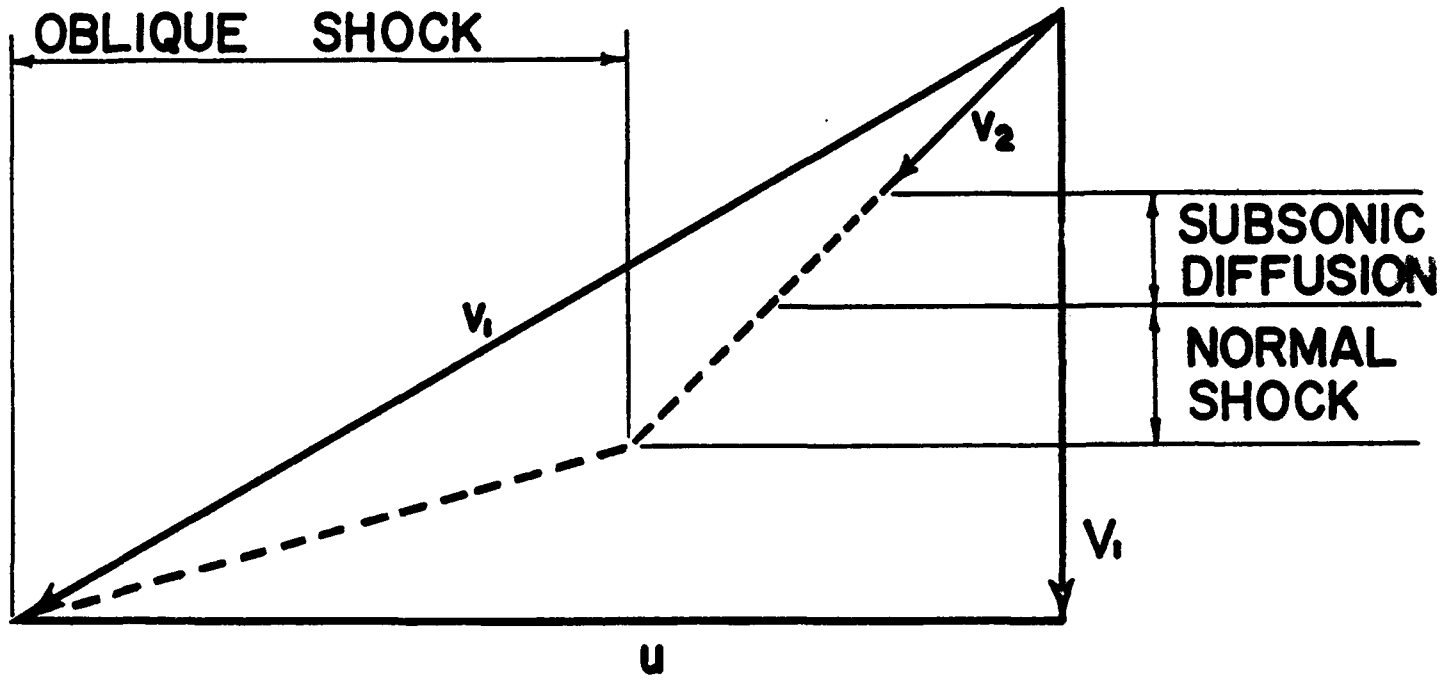

Figure 2. Velocity Diagram for Supersonic Inlet and Subsonic Discharge

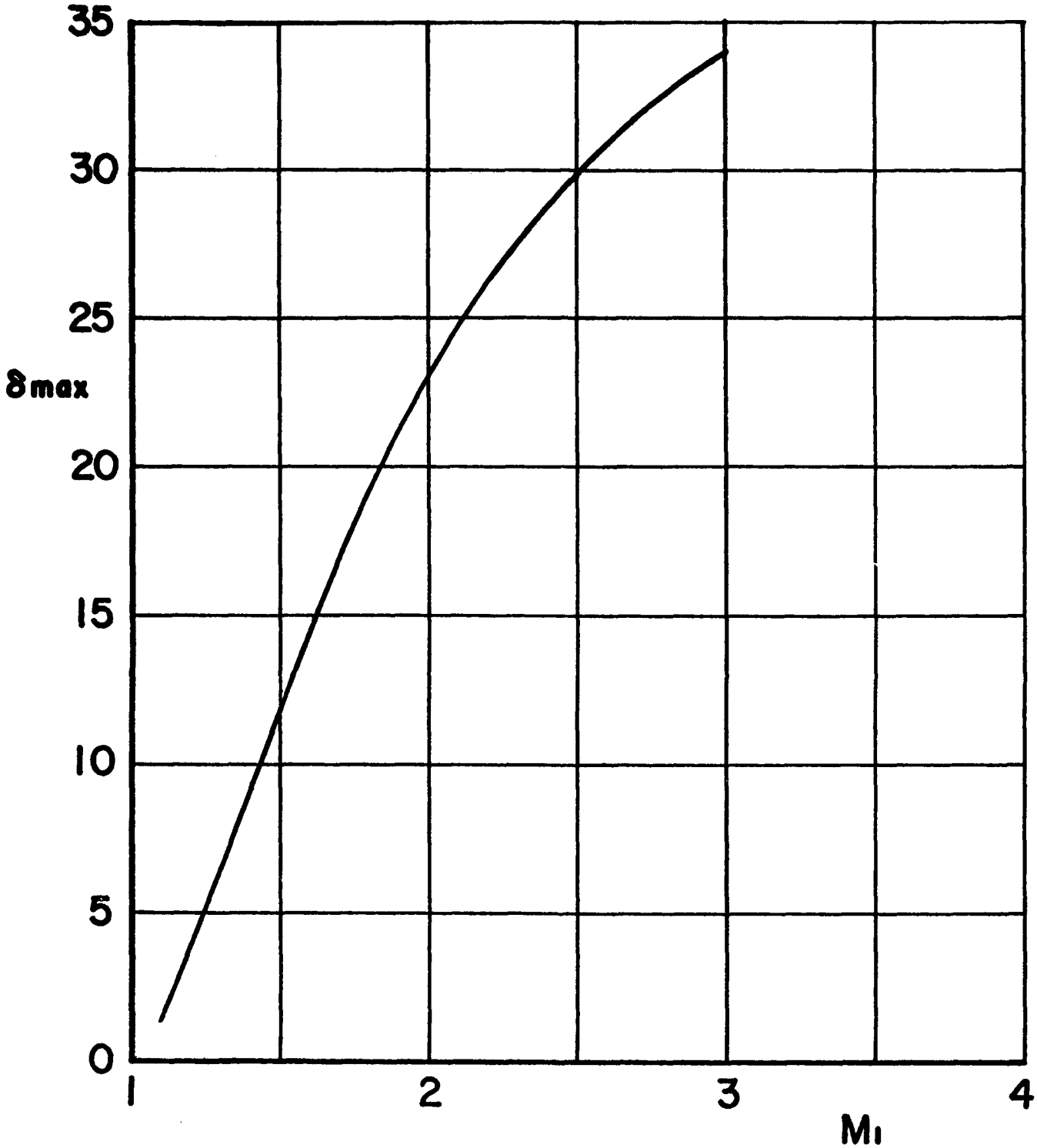

Figure 3. Maximum Wedge Angle δ , for Attached Shock vs Inlet Mach Number M_1

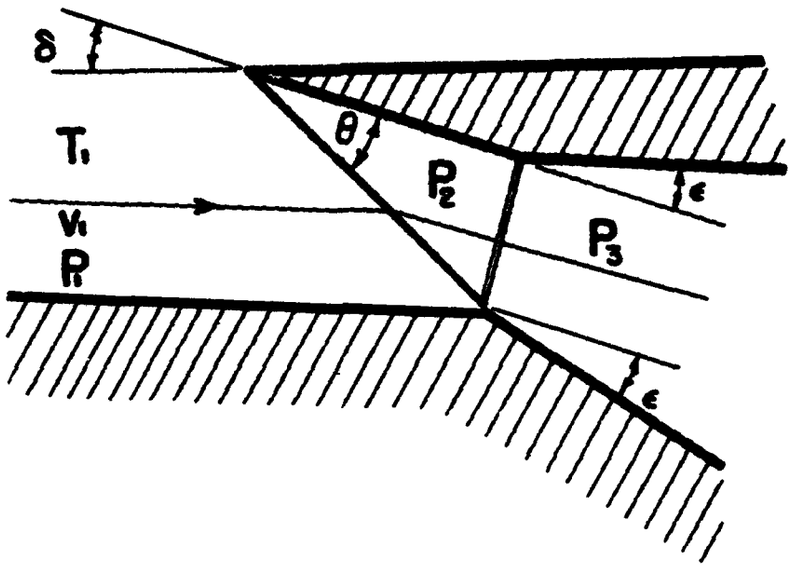

Figure 4. Schematic of Shock System in Convergent-Divergent Passage

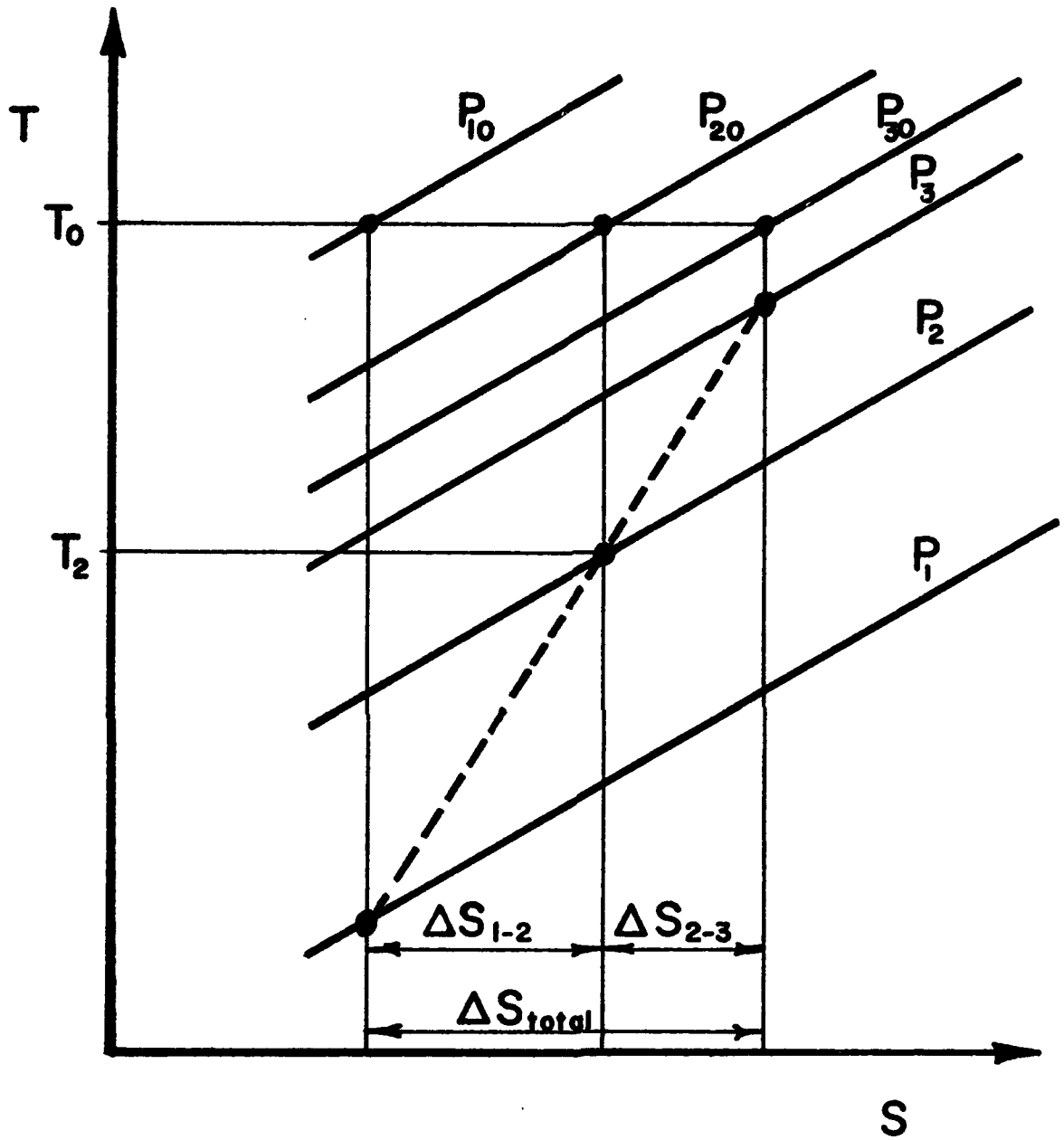

Figure 5. Temperature-Entropy Diagram Depicting Changes of State in the Convergent-Divergent Passage

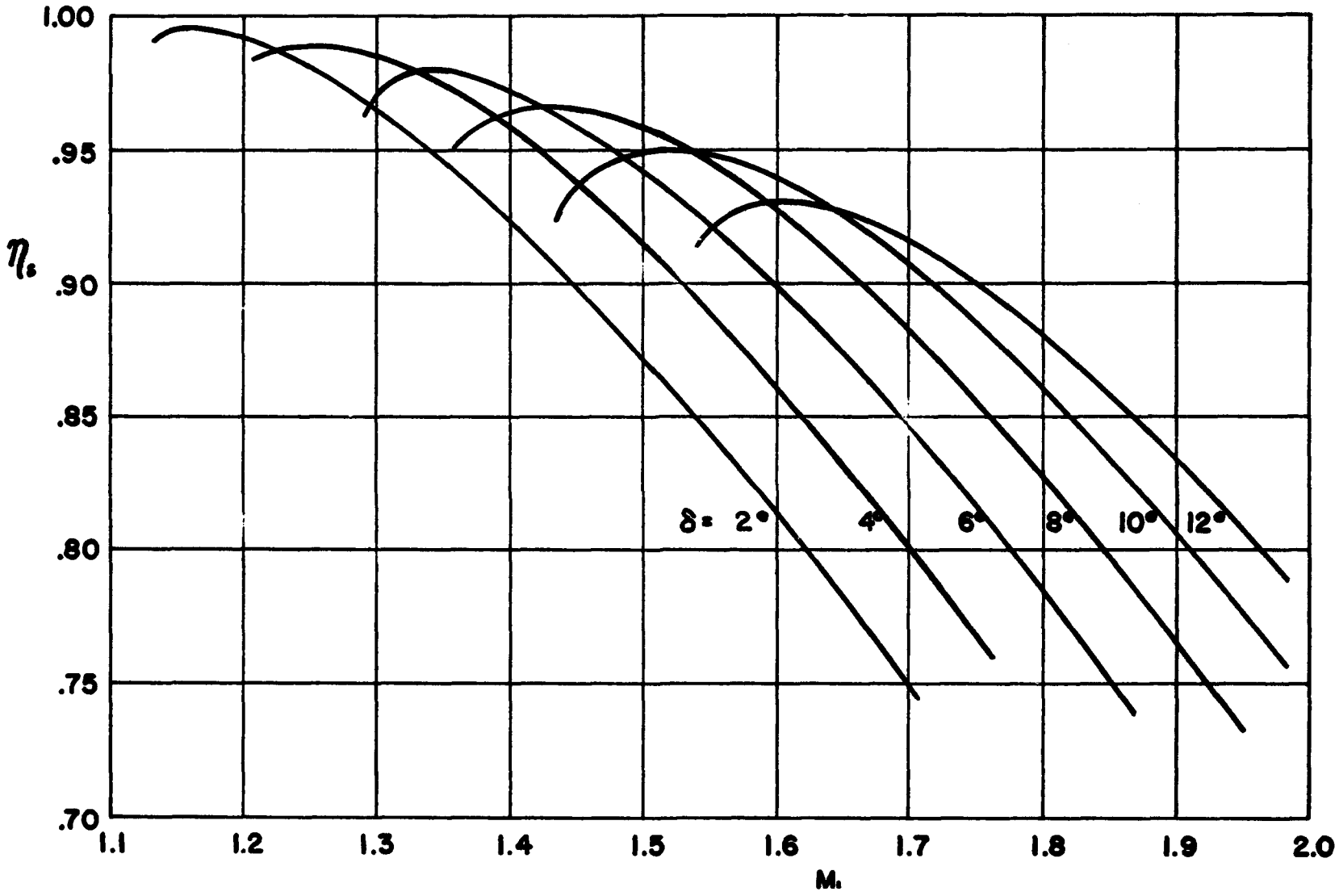

Figure 6. Shock Effectiveness η_s, vs Inlet Mach Number, M_1, For Various Wedge Angles δ

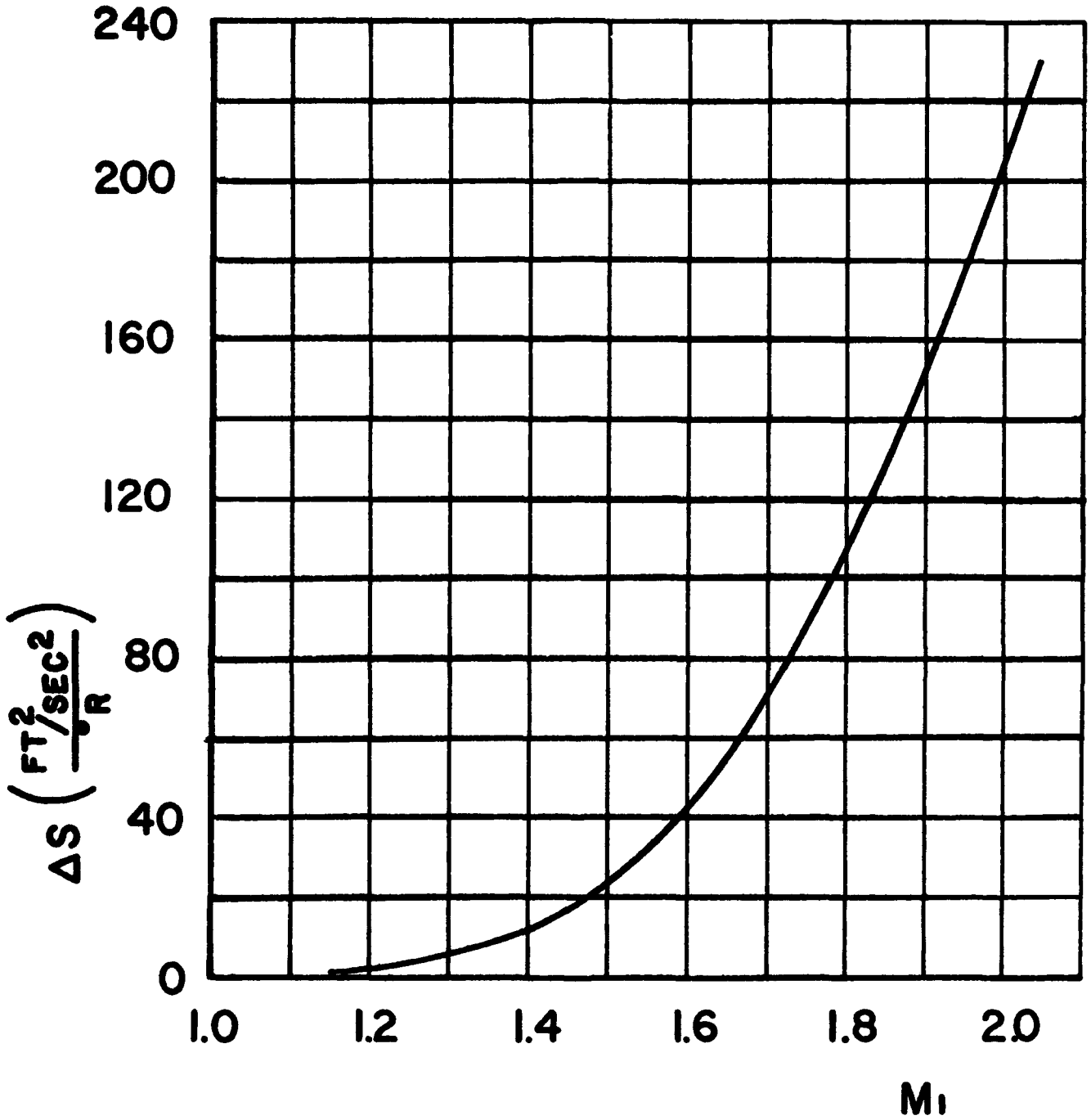

Figure 7. Increase in Entropy vs M_1, for Optimum δ

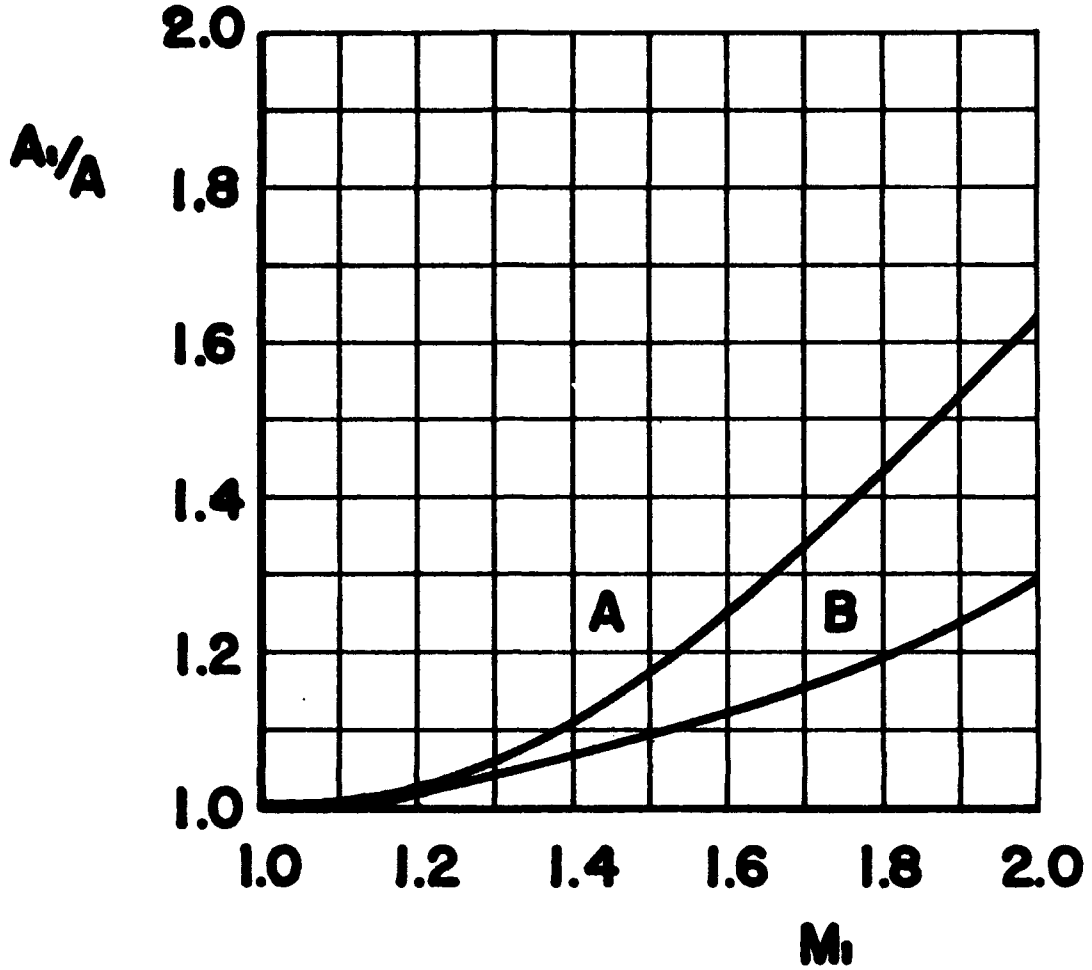

Figure 8. Passage Starting Requirements

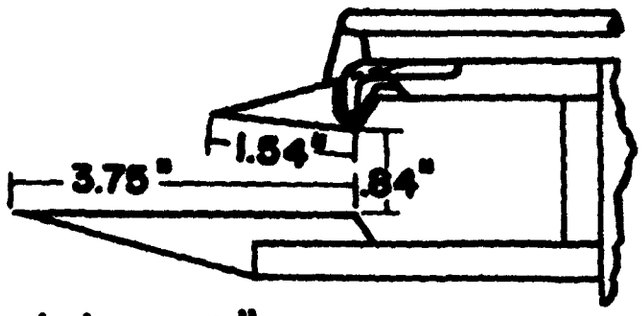

(a) 1.5" PASSAGE

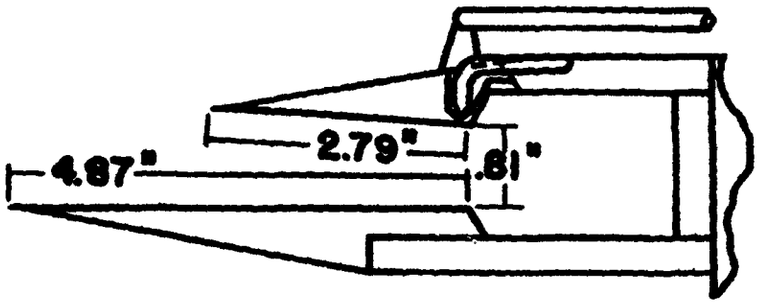

(b) 2.75" PASSAGE

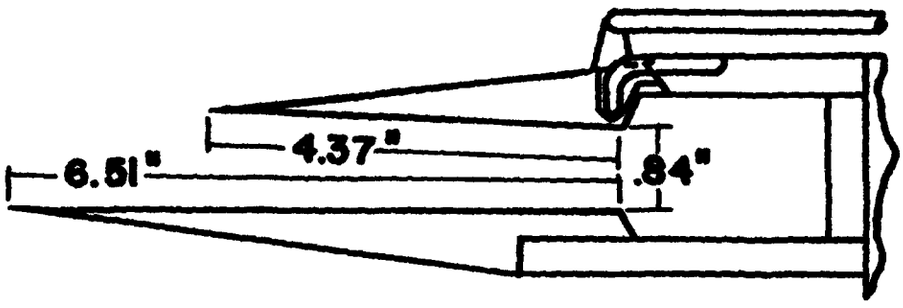

(c) 4.5" PASSAGE

Figure 9. Schematic of Adjustable Convergent Passages

Figure 10. Typical Schlieren Photographs of Short, Intermediate and Long Passages M = 2.00, =4°, Maximum Pressure Ratio

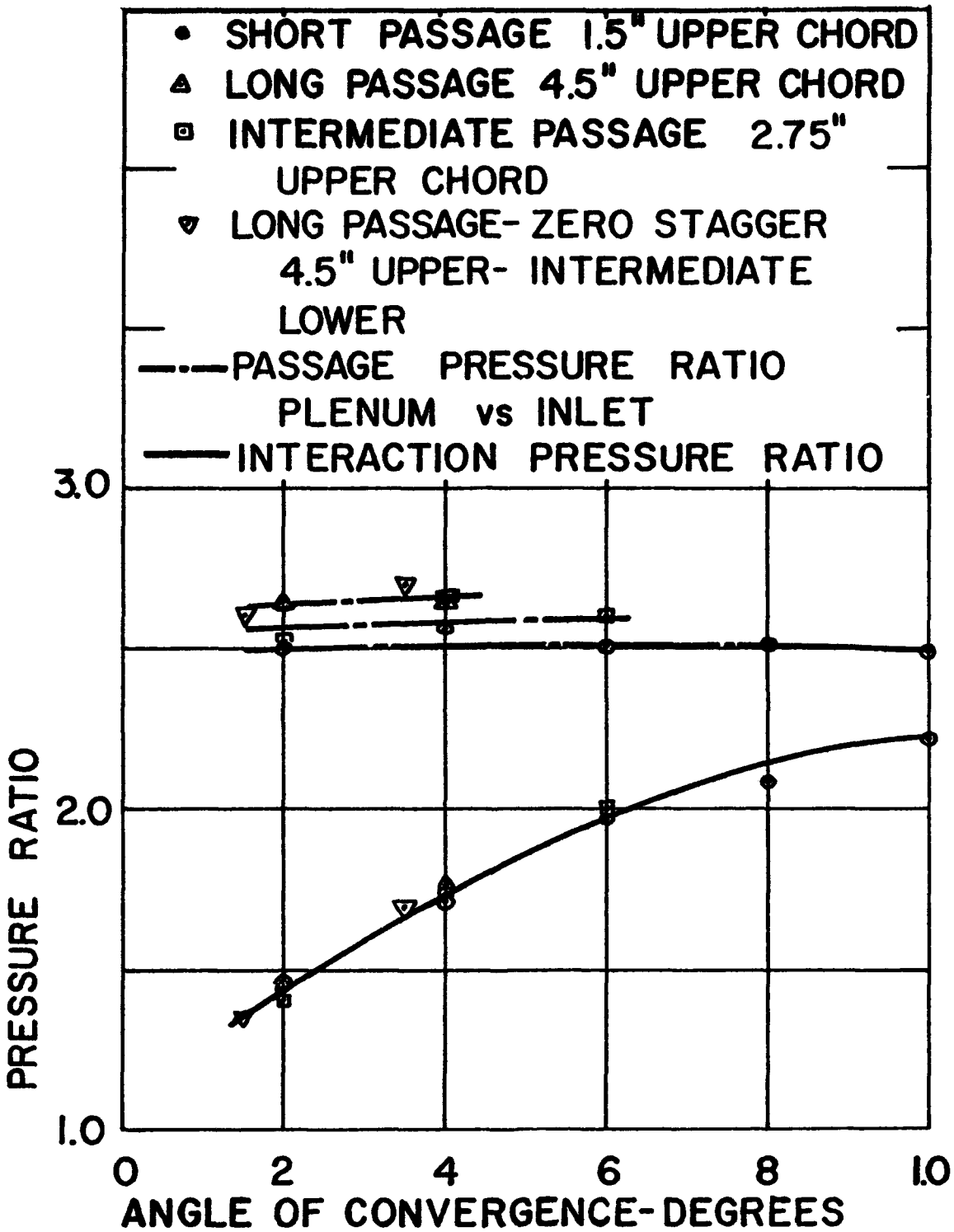

Figure 11. Pressure Ratio vs Passage Convergence

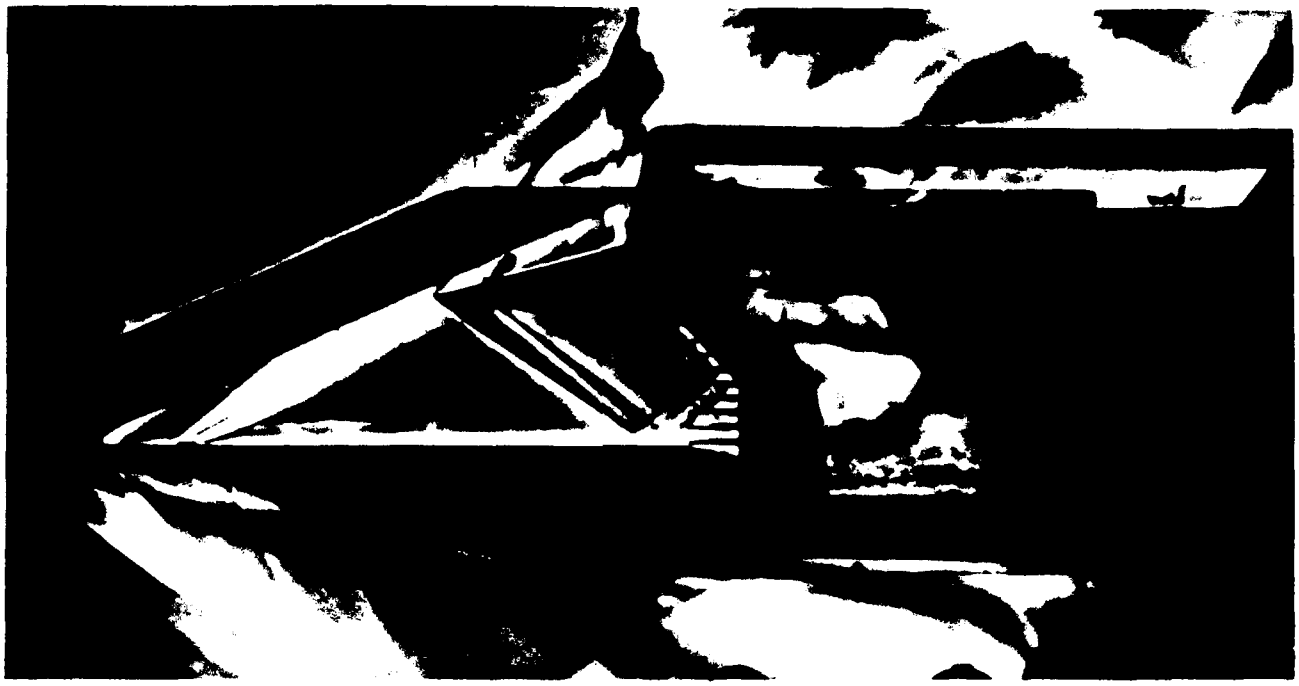

Figure 12. Short Passage with Single Boundary Layer Trip on Lower Surface

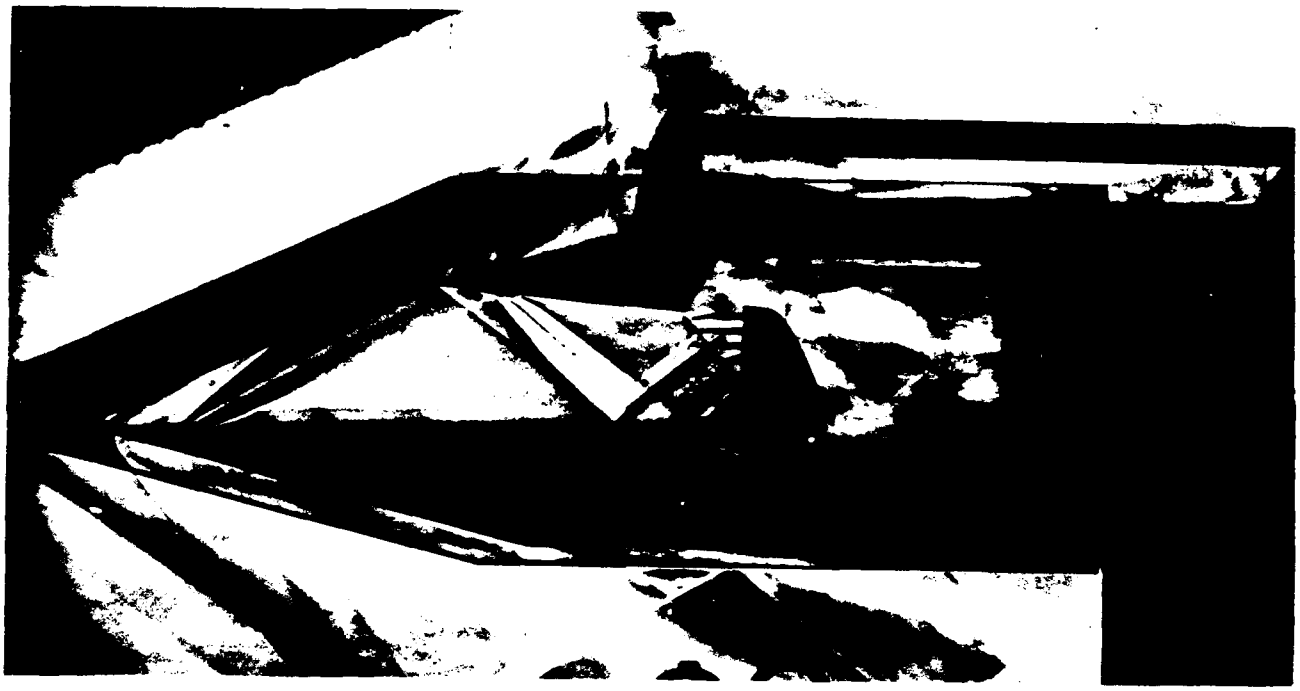

Figure 13. Short Passage with Single Trips on Upper and Lower Surfaces

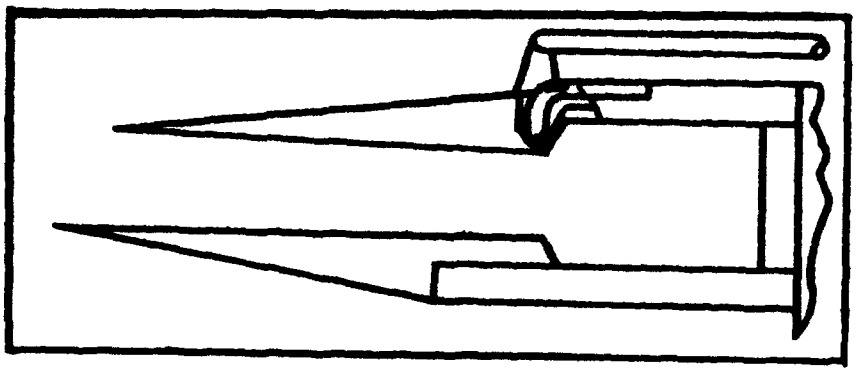

Figure 14. Schematic of Zero Stagger Passage

Figure 15. Zero Stagger Passage

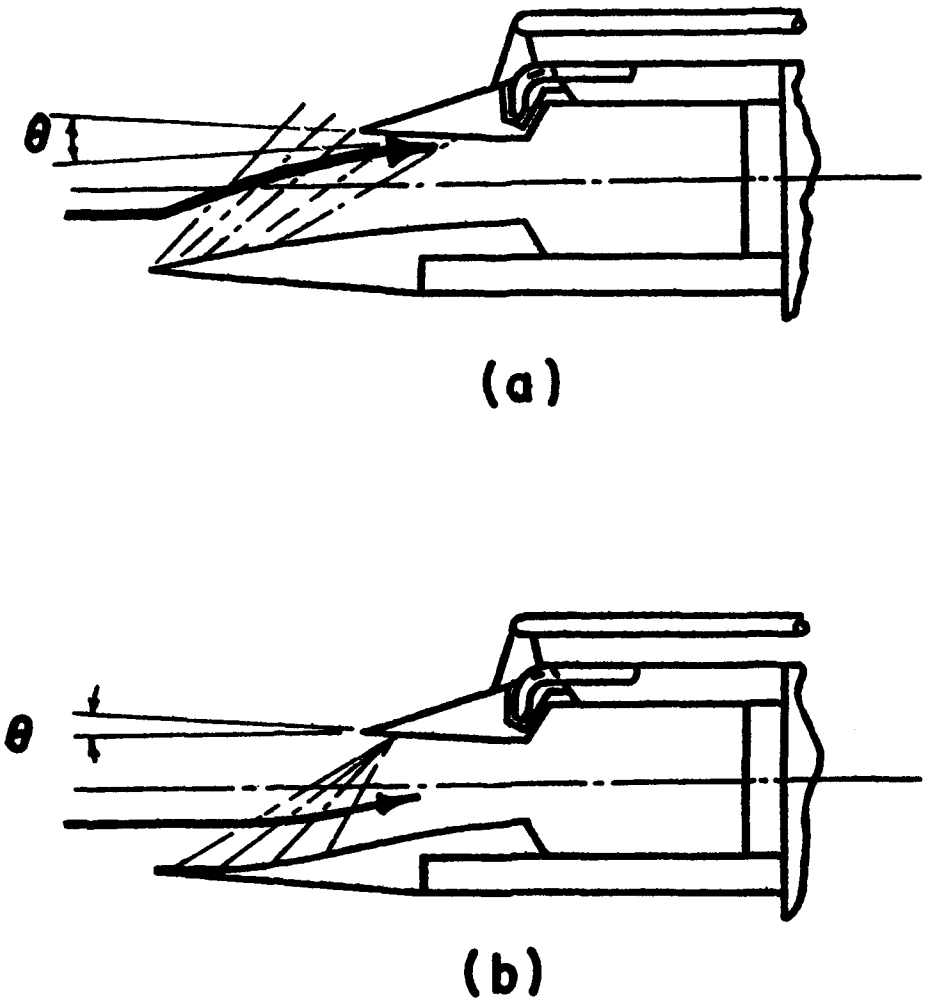

Figure 16. Passages with Curved Entrance Sections

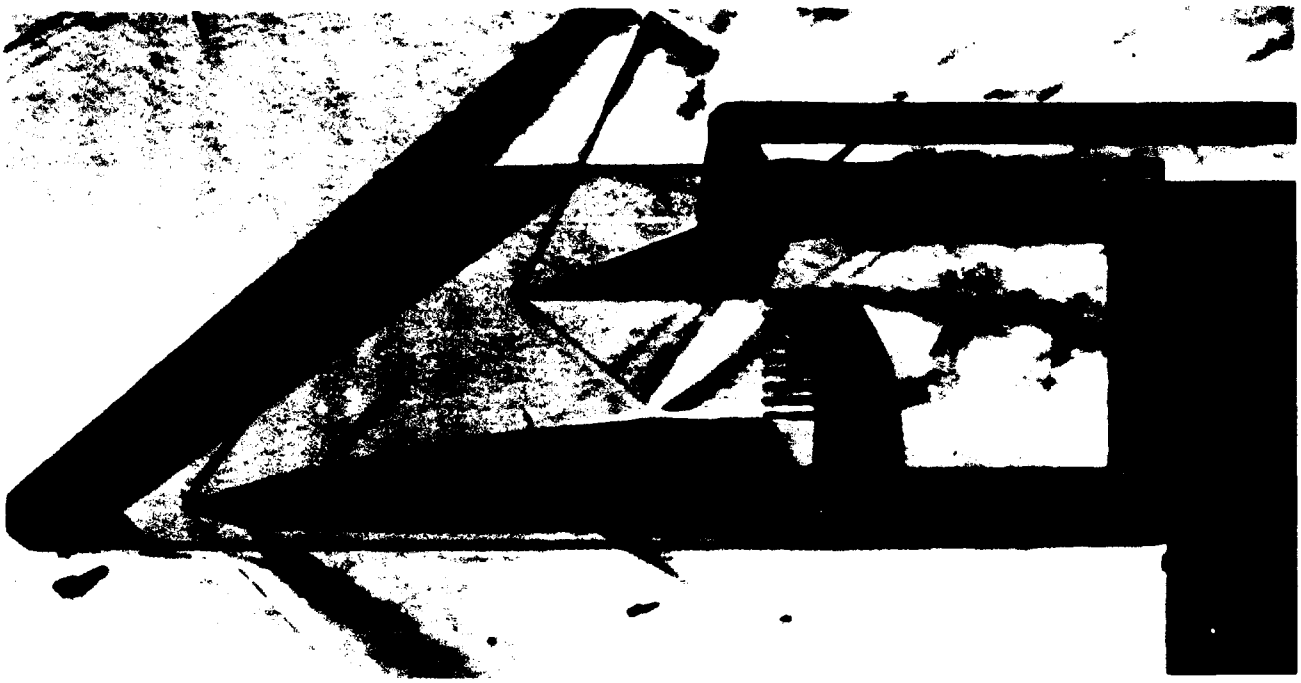

Figure 17. Passage with Negative Pressure Gradient Along Lower Surface

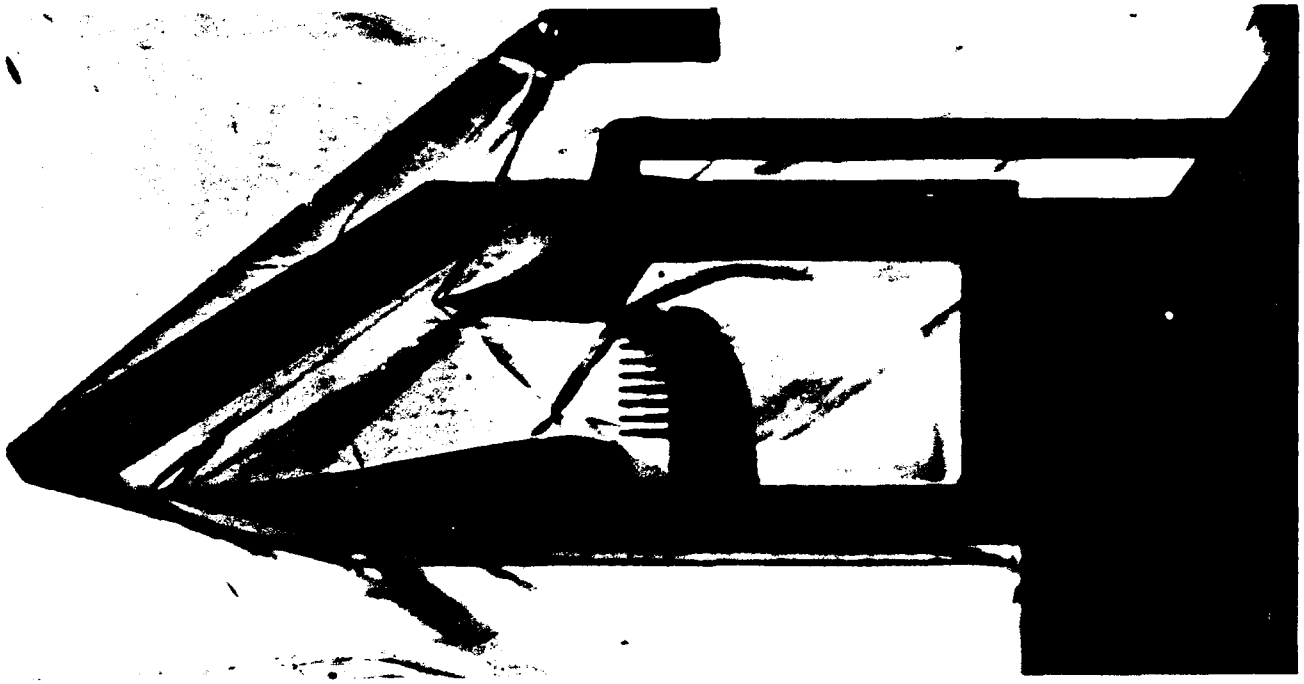

Figure 18. Passage with Positive Pressure Gradient Changing to Negative Along Lower Surface

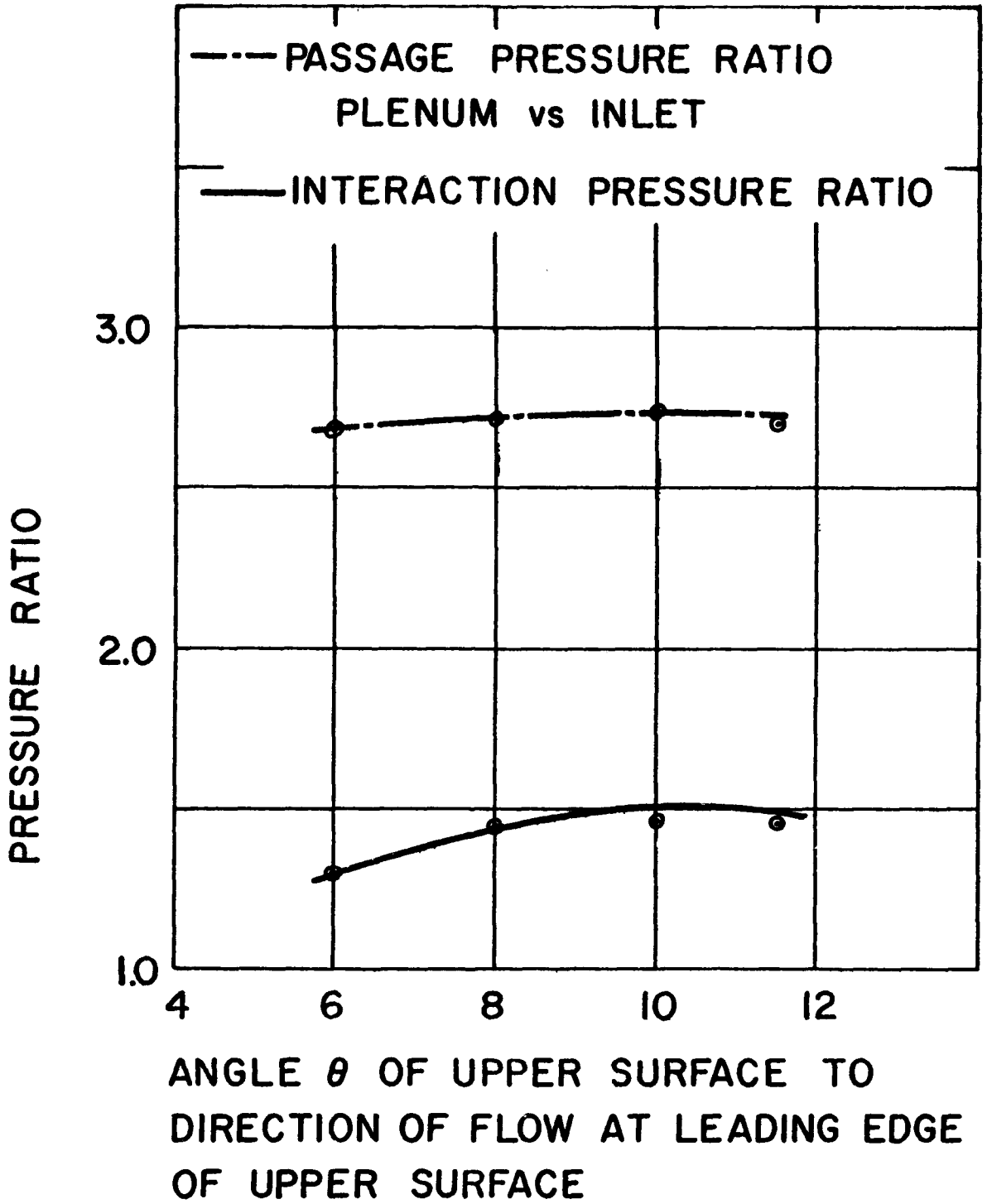

Figure 19. Pressure Ratio vs Vane Angle - Convex Lower Surface

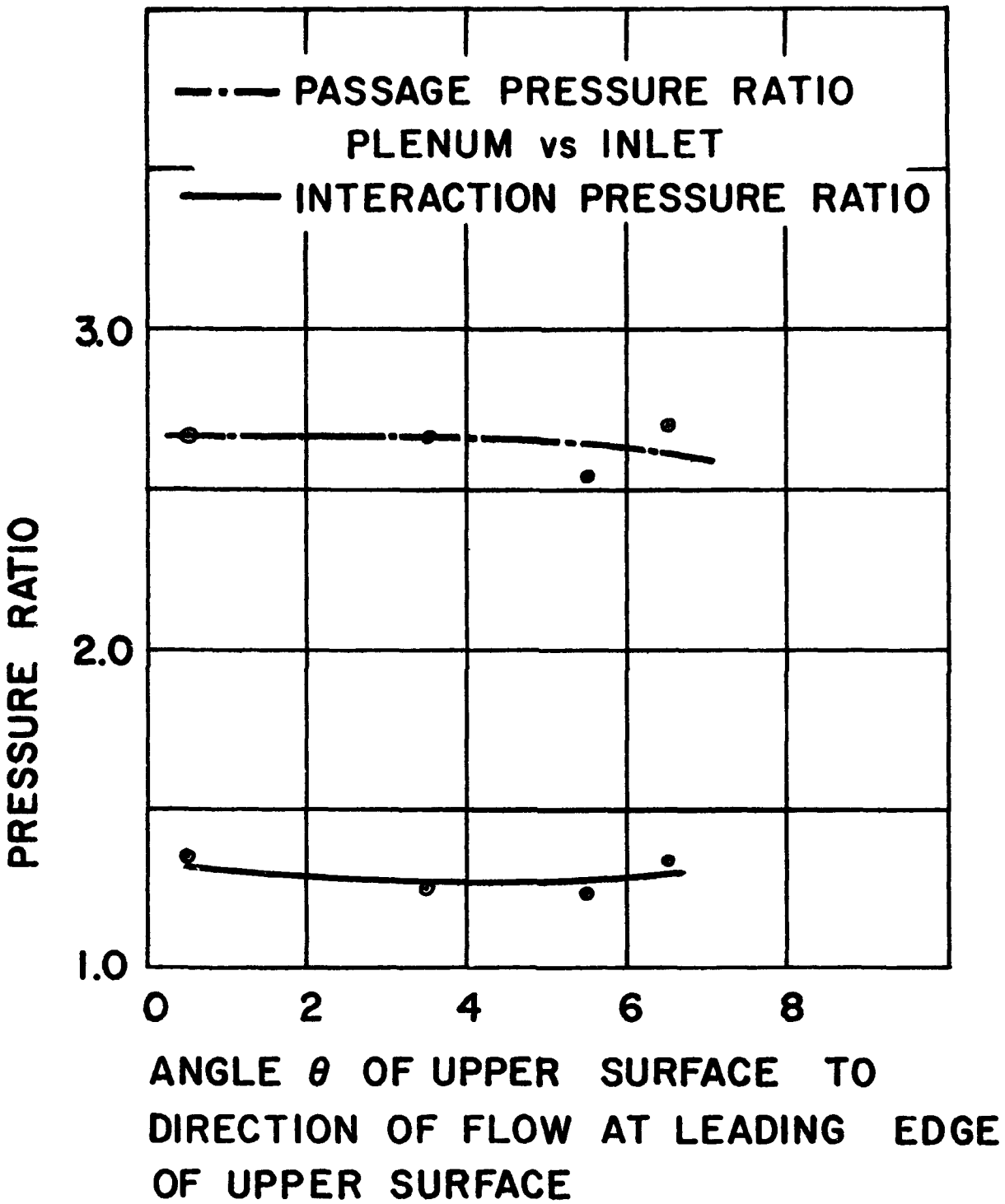

Figure 20. Pressure Ratio vs Vane Angle - Concave Lower Surface

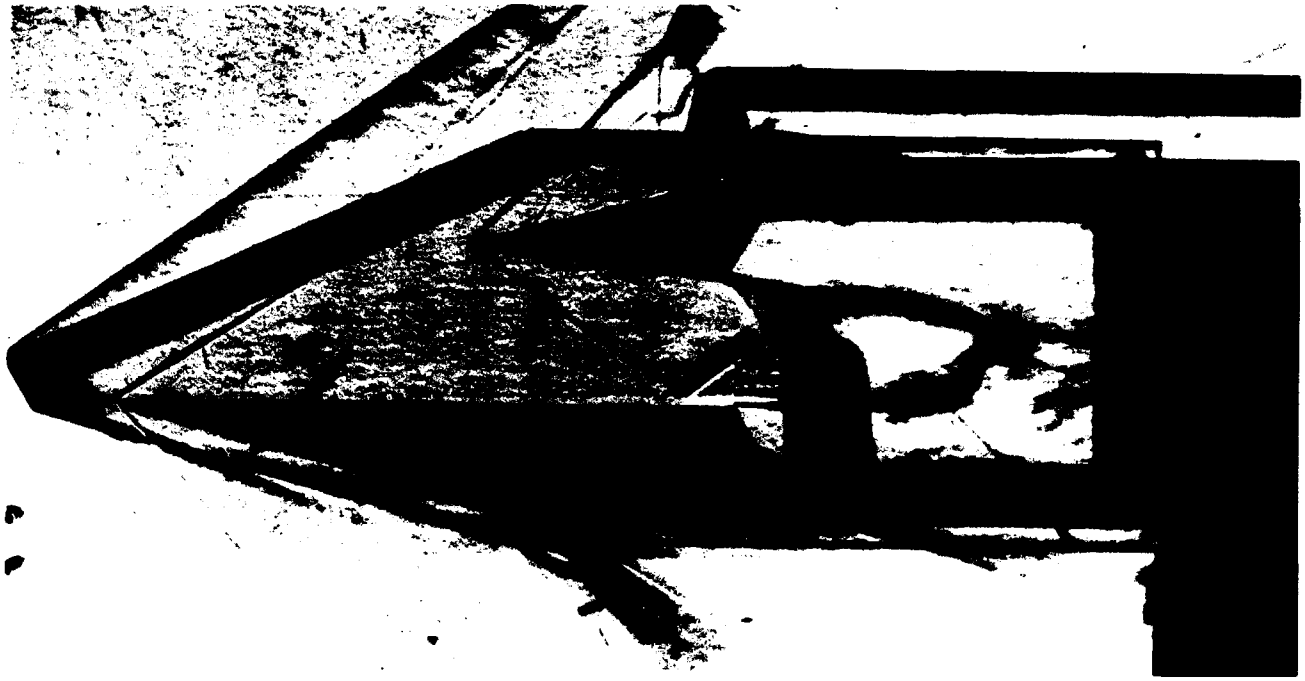

(a) Sharp lower leading edges

(b) Blunted (.02") lower leading edge

Figure 21. Comparison of Passages with Sharp and Blunted Lower Leading Edges

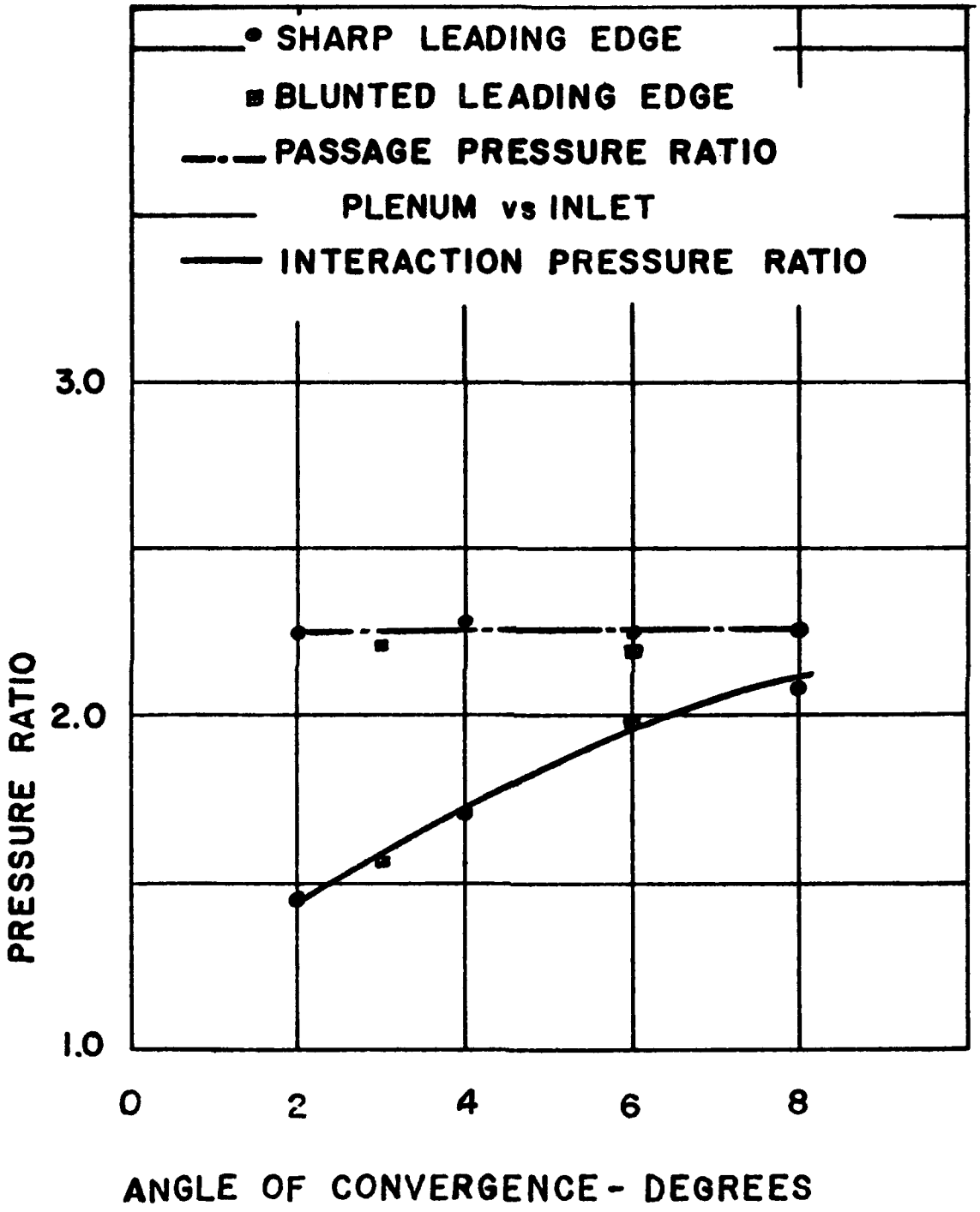

Figure 22. Comparison of Performance of 1.5" Passage with Sharp and Blunted Leading Edges

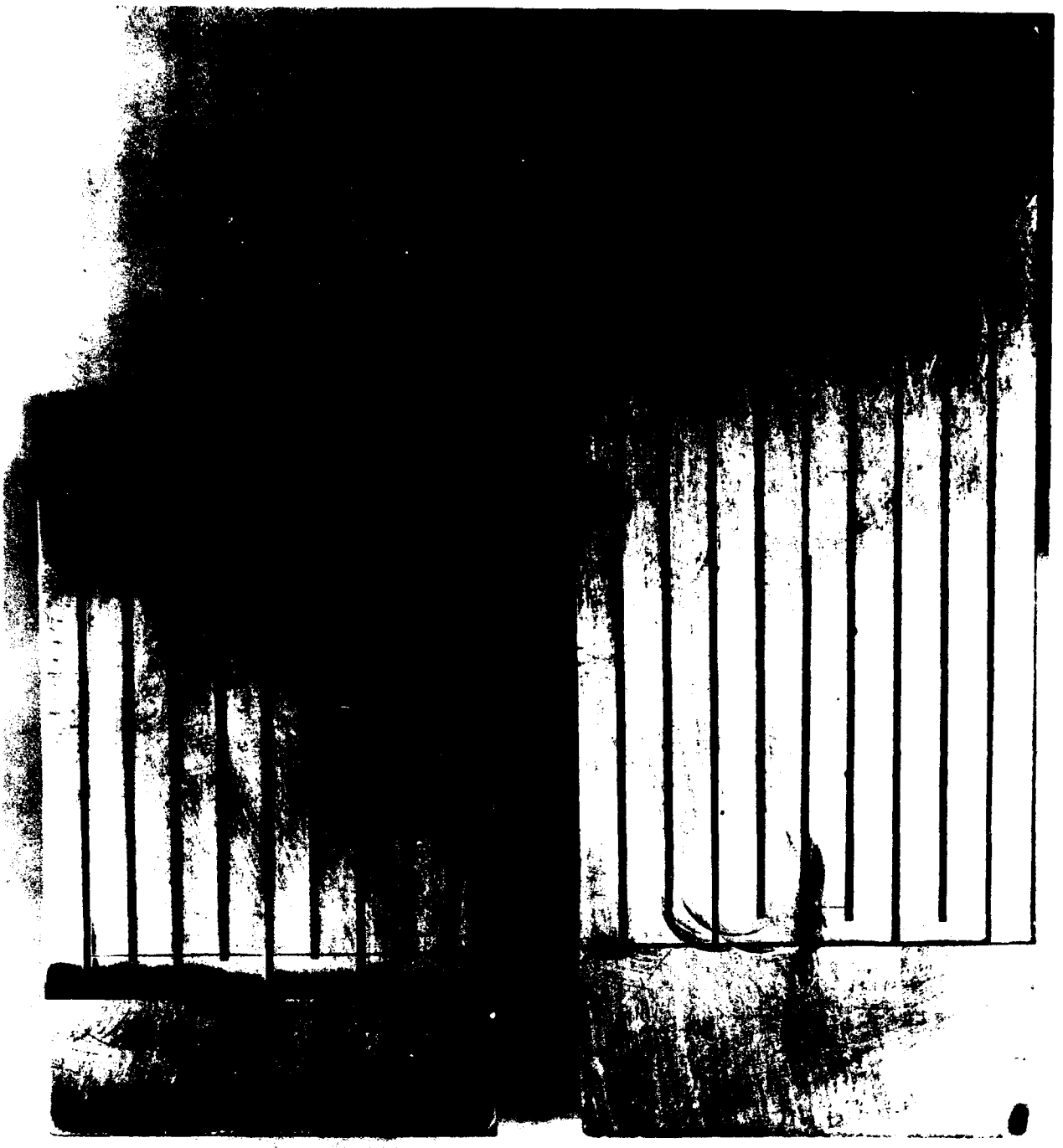

Figure 23. Heated Vane Construction

(a) No heating. $T_w = 75\,^{o}F$

(b) Heated. $T_w = 150^{o}F$

Figure 24. Comparison of Heated and Unheated Passages

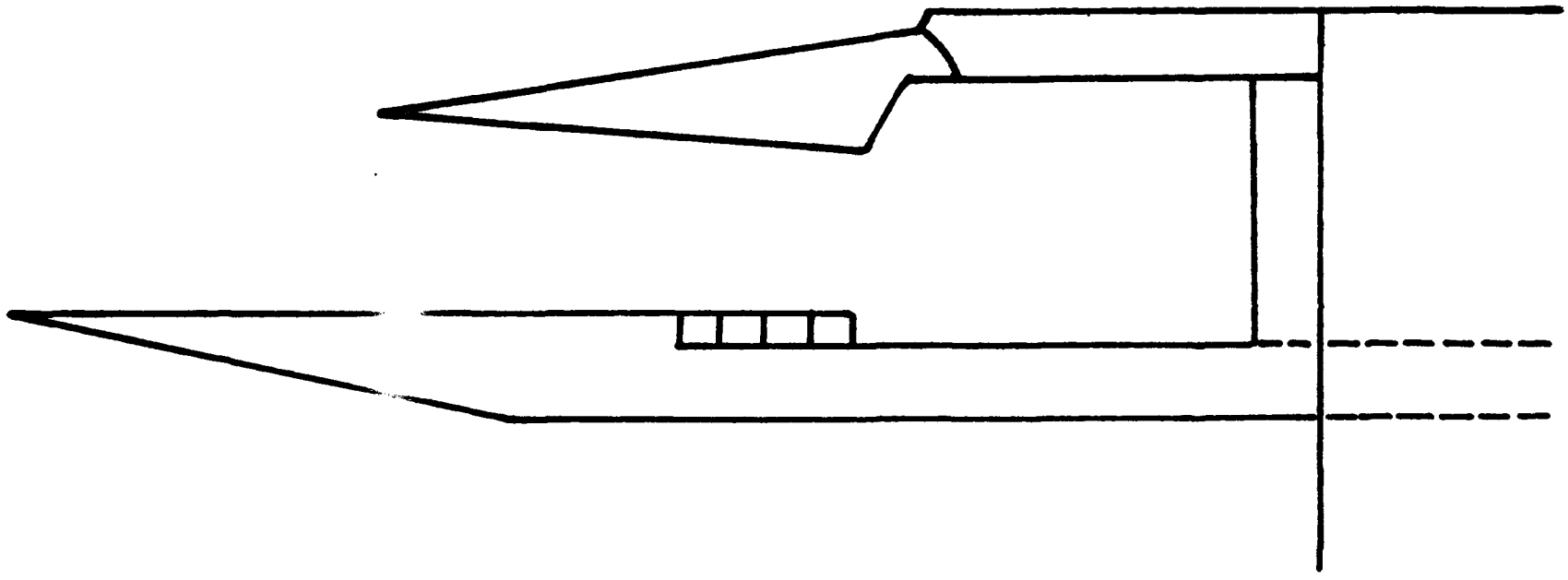

Figure 25. Schematic of Passage with Removable Blocks for Varying Trailing Edge Location

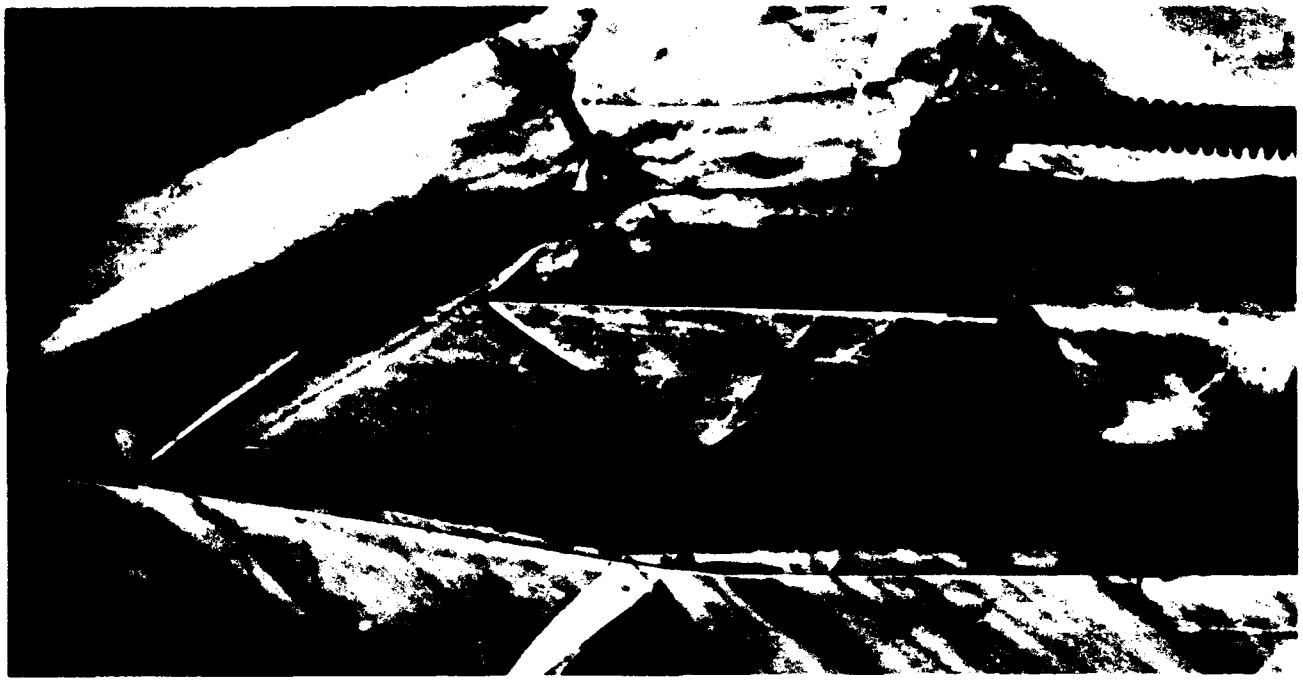

(a) $\delta = 2^{\circ}$

(b) $\delta = 4^{\circ}$

Figure 26. Passage with No Extensions Added to Lower Surface

(a) $\delta = 2^{o}$

(b) $\delta = 4^{o}$

Figure 27. Passage with One Extension Added to Lower Surface

(a) $\delta = 2^{o}$

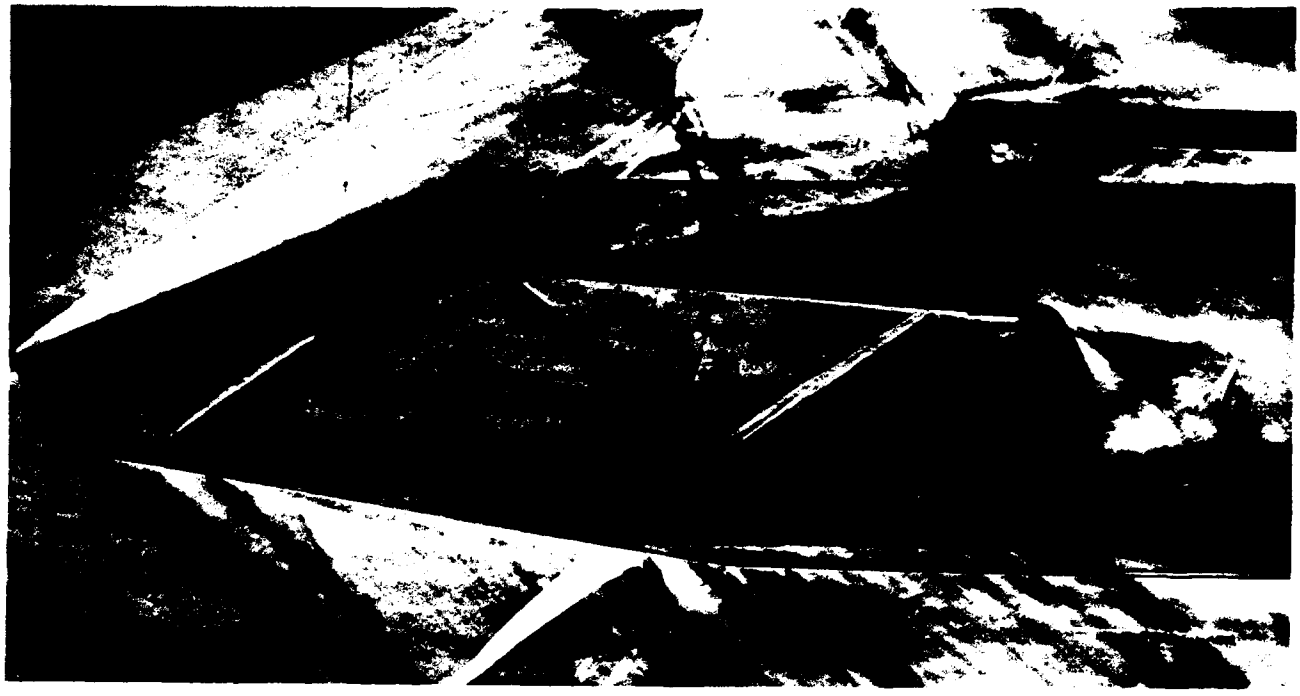

(b) $\delta = 4^{o}$

Figure 28. Passage with Two Extensions Added to Lower Surface

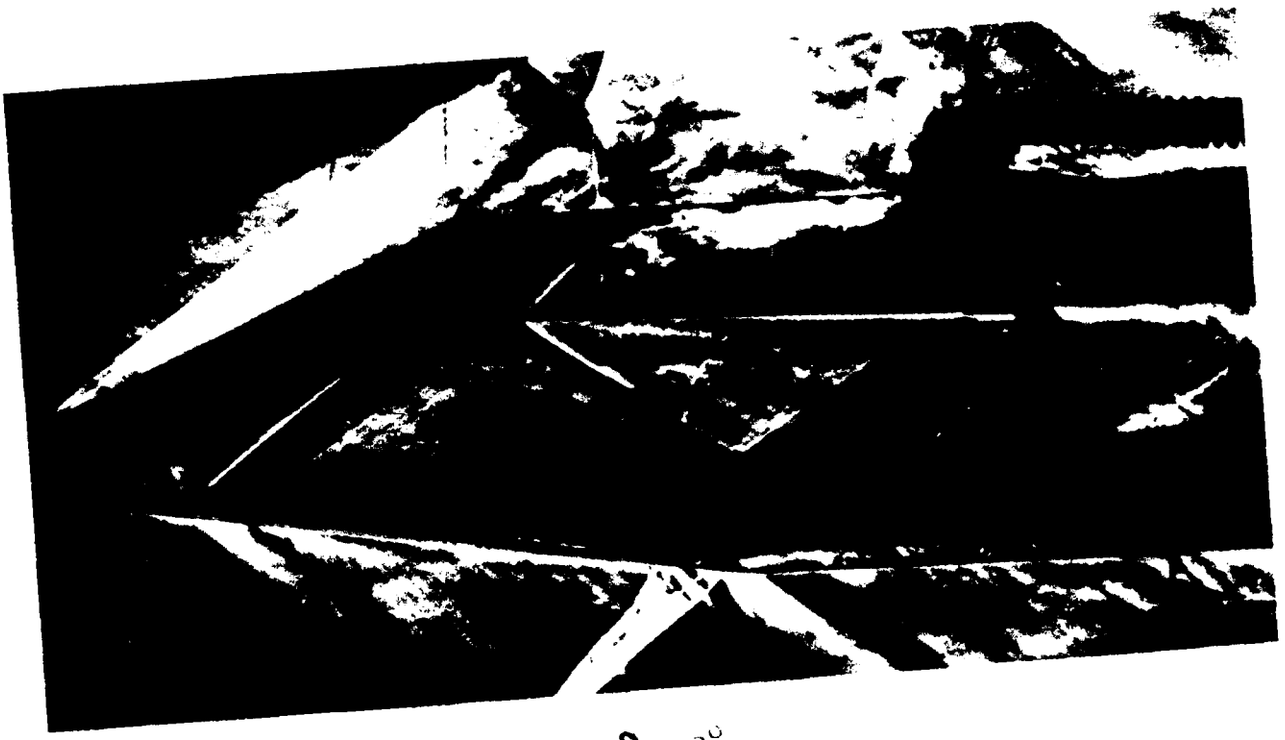

(a) $\delta = 2^{\circ}$

(b) $\delta = 4^{\circ}$

Figure 29. Passage with Three Extensions Added to Lower Surface

(a) $\delta = 2^{o}$

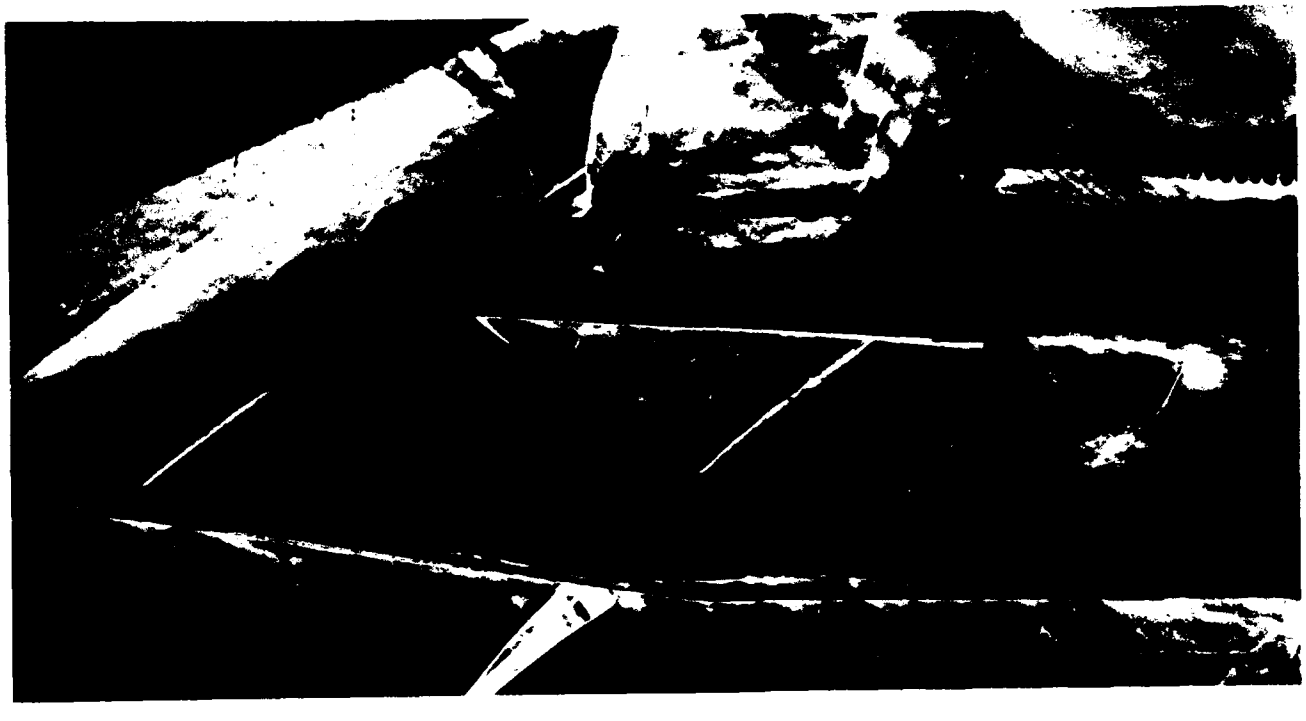

(b) $\delta = 4^{o}$

Figure 30. Passage with Four Extensions Added to Lower Surface

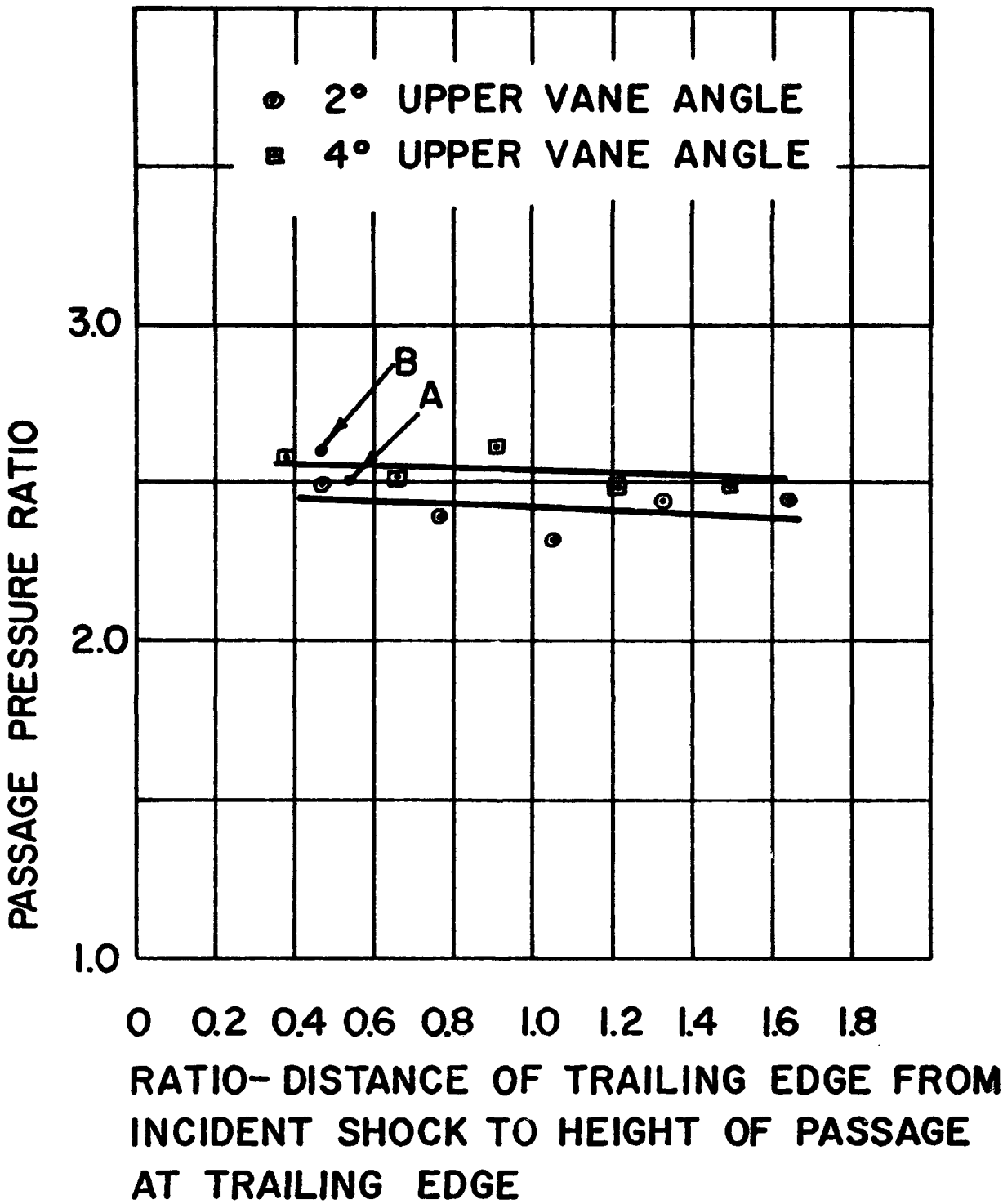

Figure 31. Variation of Passage Pressure Ratio with Location of Trailing Edge from Incident Shock

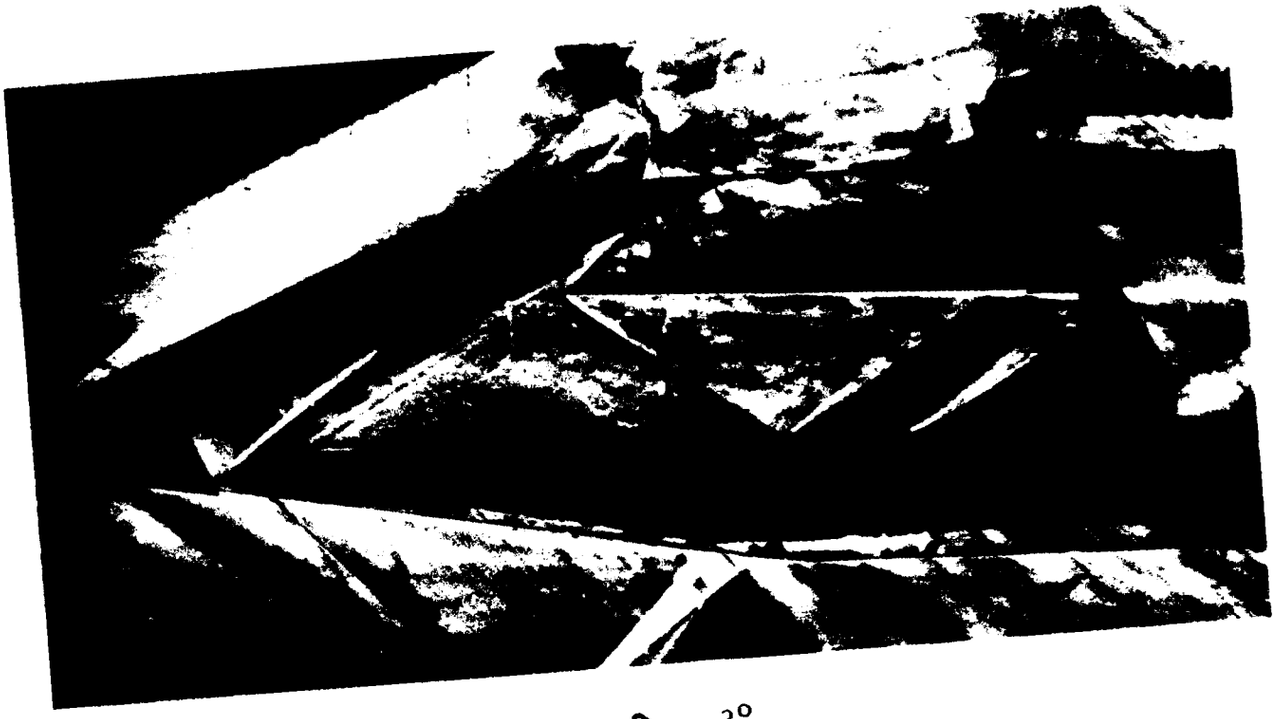

(a) $\delta = 2^{\circ}$

(b) $\delta = 4^{\circ}$

Figure 32. Passage with Convex Trailing Edge Extension on Lower Surface

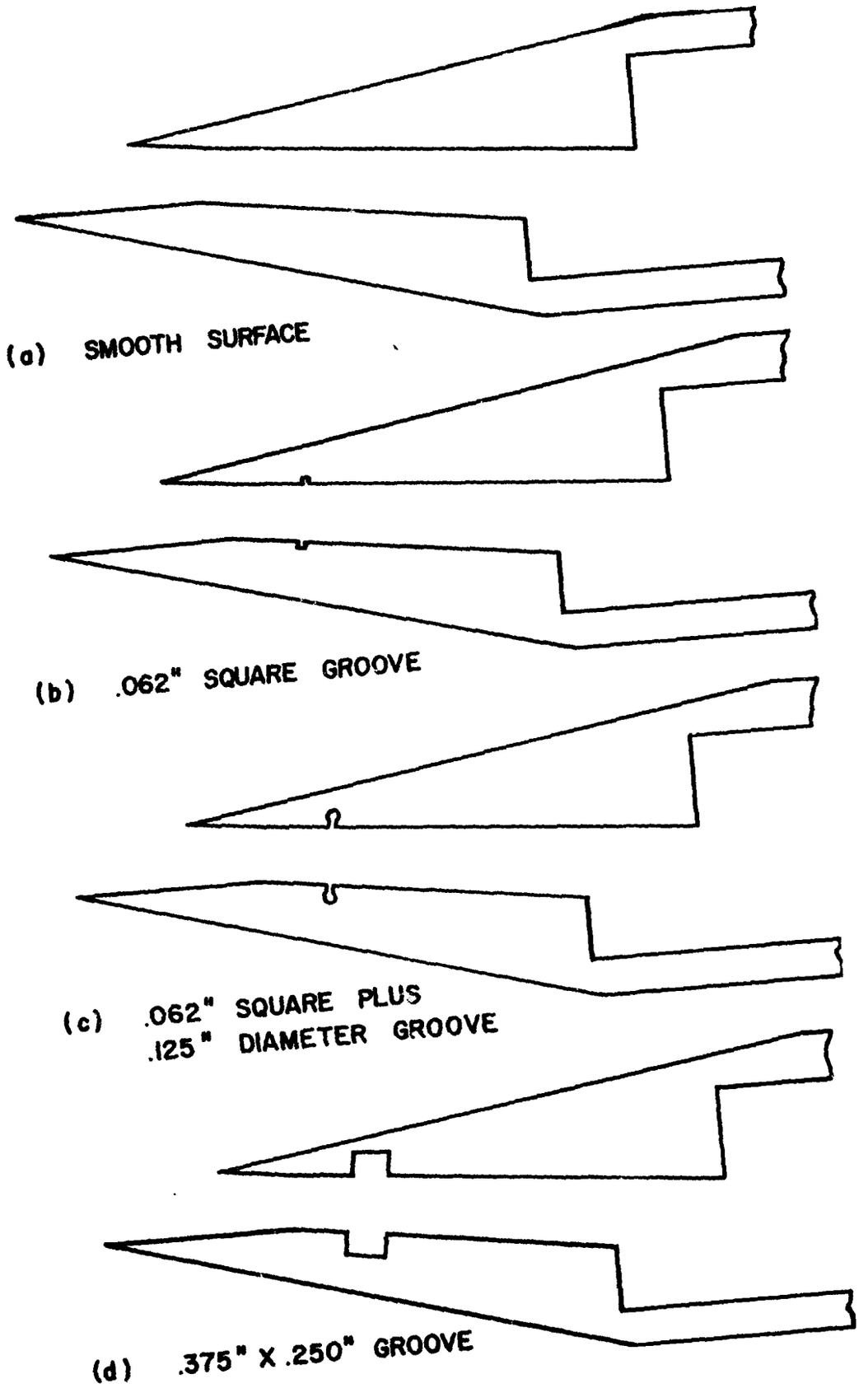

Figure 33. Schematic of Convergent-Divergent Passages

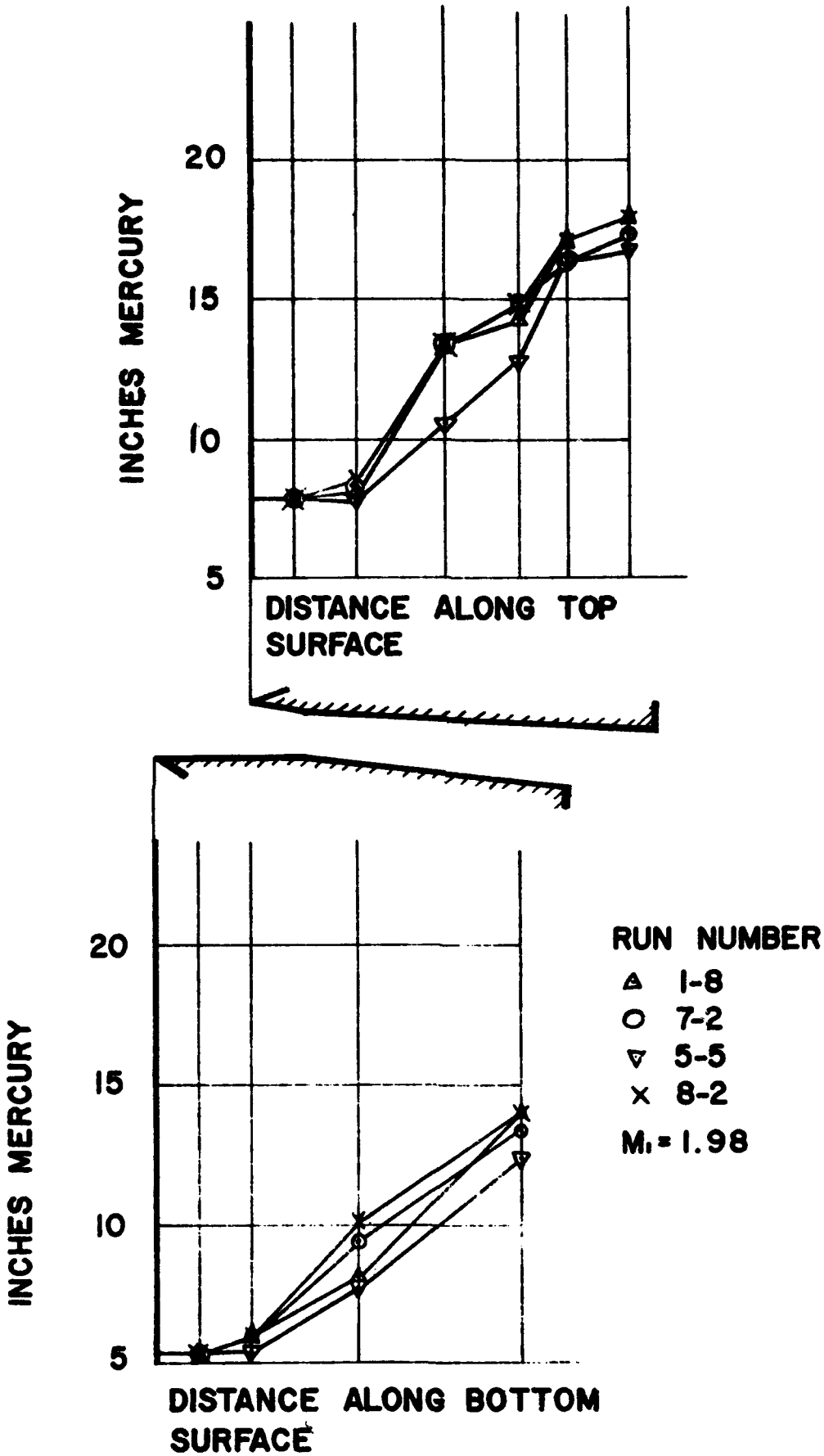

Figure 34. Pressure Distribution Along Passages with Surface Discontinuities

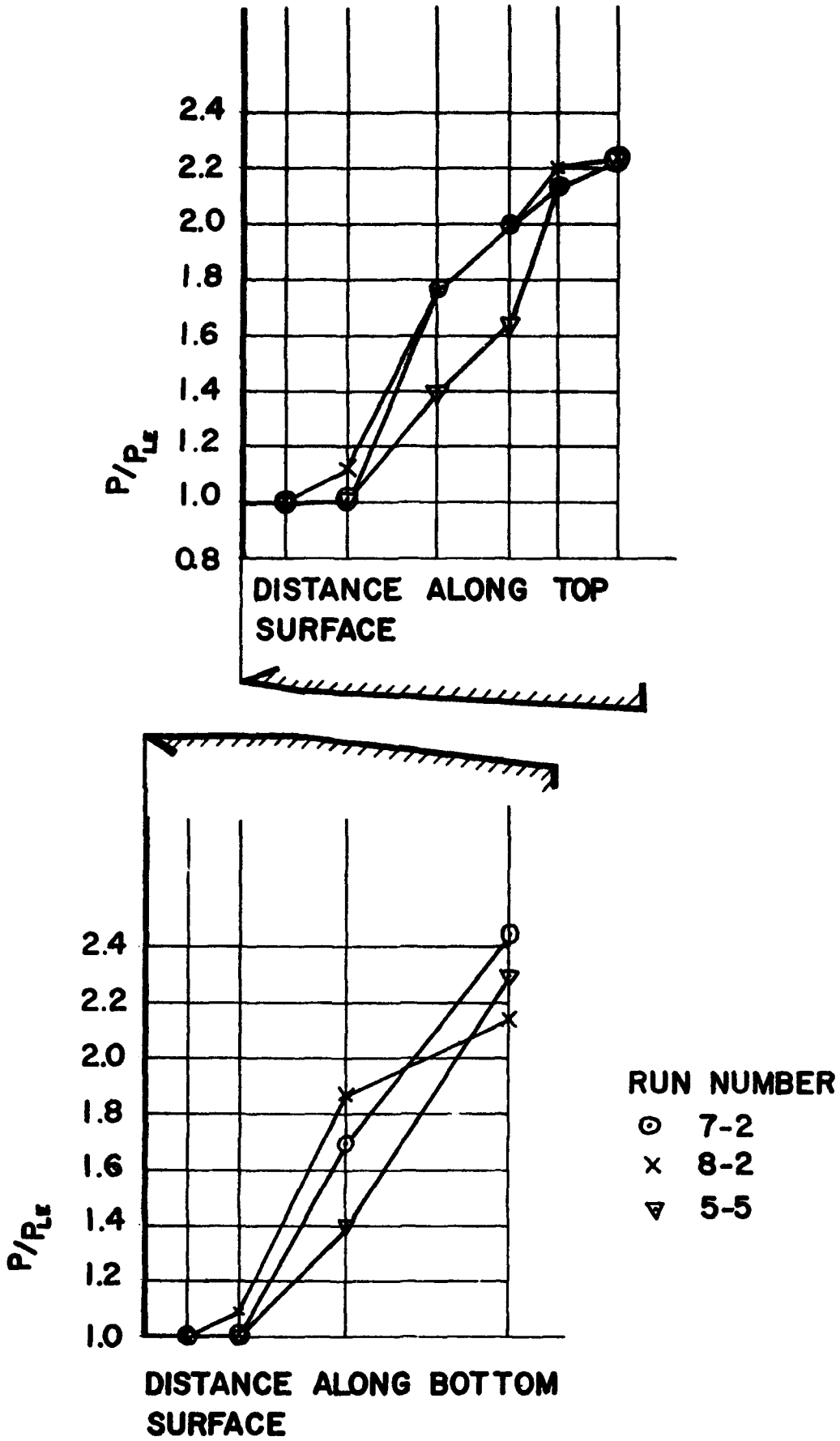

Figure 35. Pressure Ratio Along Passages with Surface Discontinuities

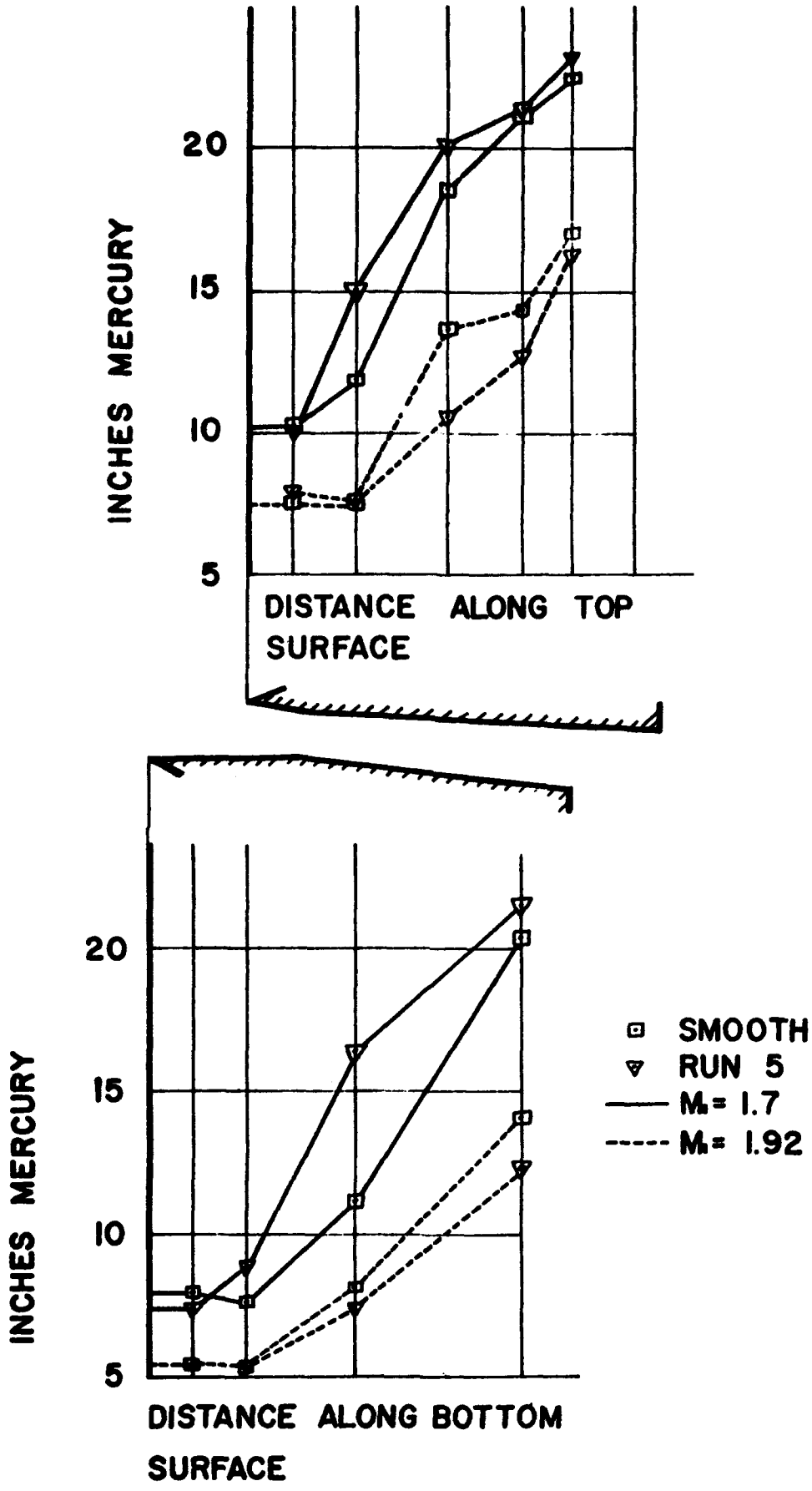

Figure 36. Comparison of Pressures Along Smooth Passage with Pressures Along Passages with Discontinuities

(a) $M_1 = 1.7$

(b) $M_1 = 1.92$

Figure 37. Convergent-Divergent Passage with No Surface Discontinuities

(a) $M_1 = 1.7$

(b) $M_1 = 1.92$

Figure 38. Convergent-Divergent Passage with .062" Square Groove in Surfaces

a) $M_1 = 1.7$

b) $M_1 = 1.92$

Figure 39. Convergent-Divergent Passage with .062" Square Plus .125" Diameter Groove in Surface

(a) $M_1 = 1.7$

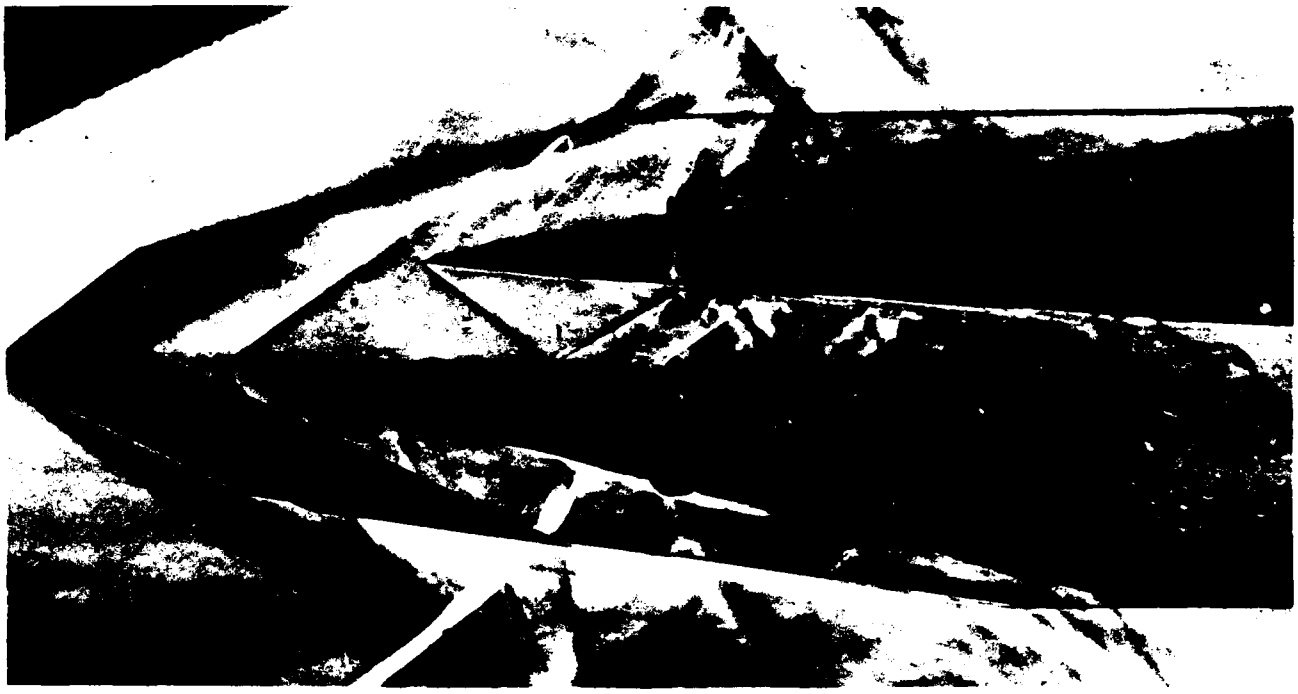

(b) $M_1 = 1.92$

Figure 40. Convergent-Divergent Passage with .375" x .25" Groove in Surfaces.

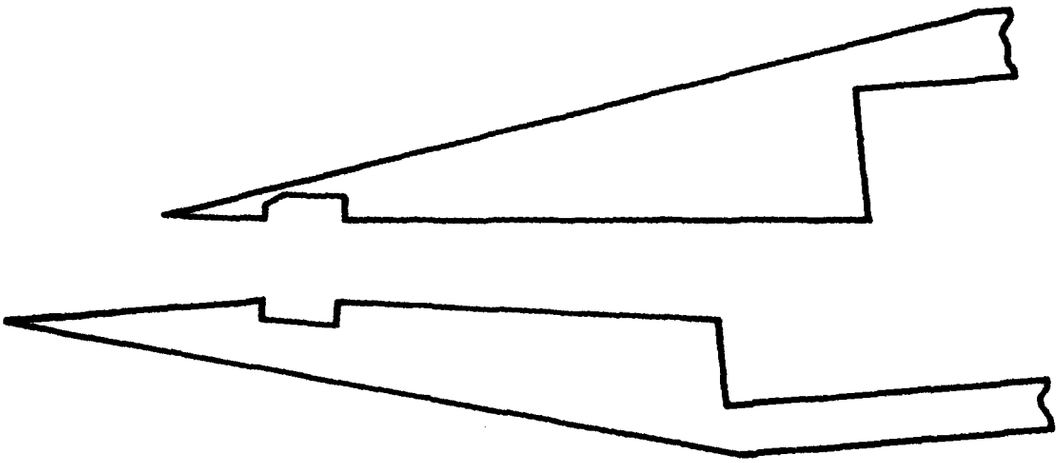

(a) .6" CHORD CAVITY

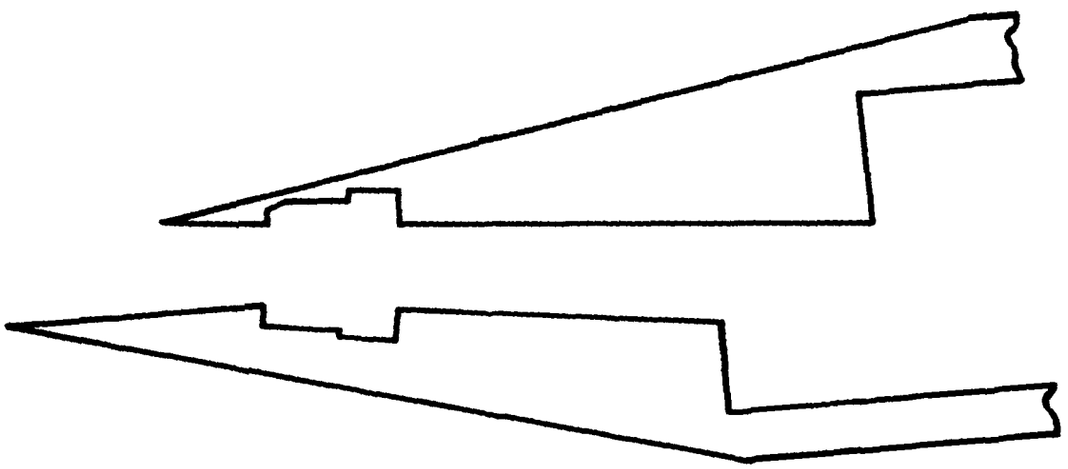

(b) .98" CHORD CAVITY

Figure 41. Schematic of Convergent-Divergent Passage with "Free Jet" Throats

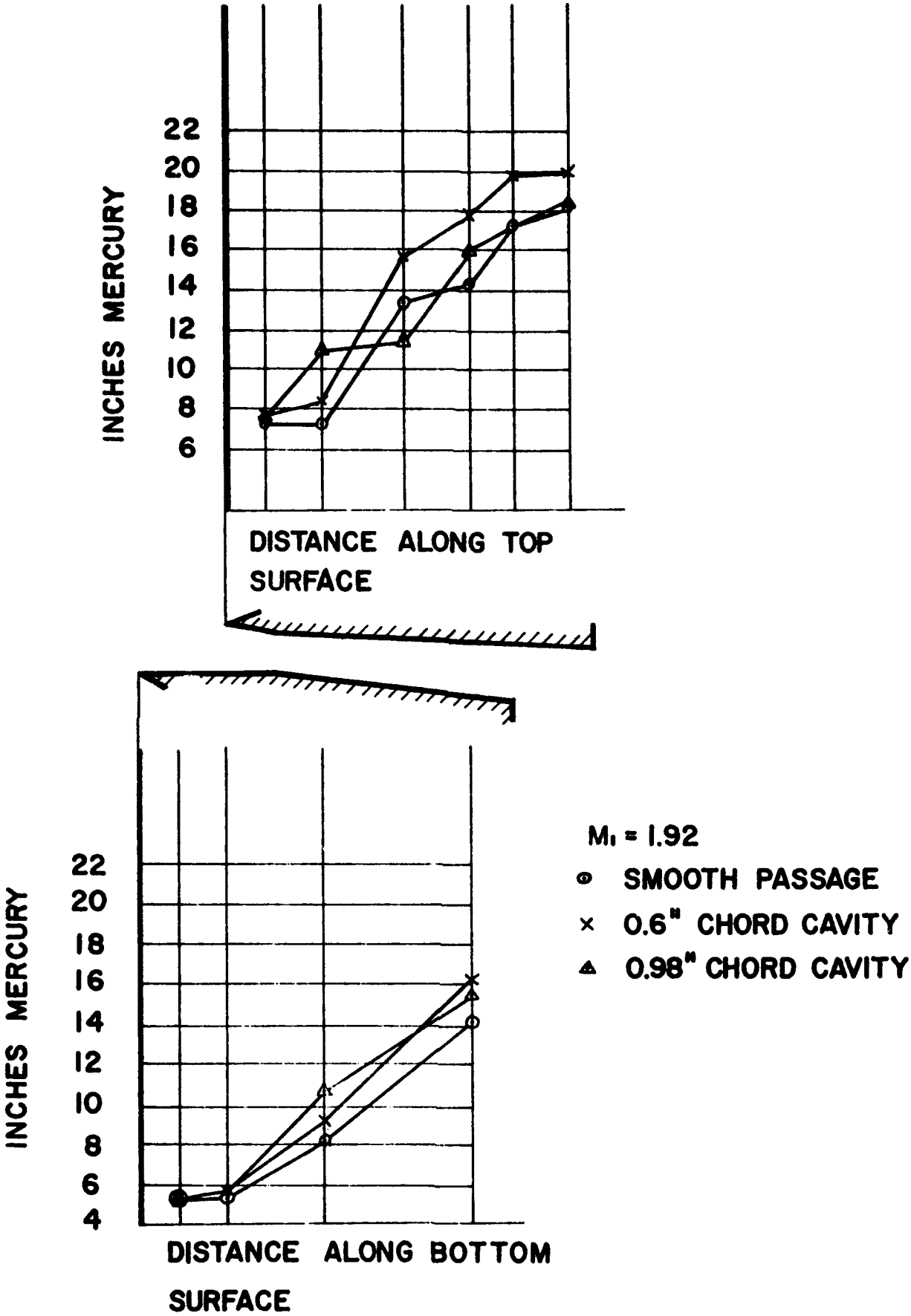

Figure 42. Pressure Distribution Along Passages with "Free Jet" Throat

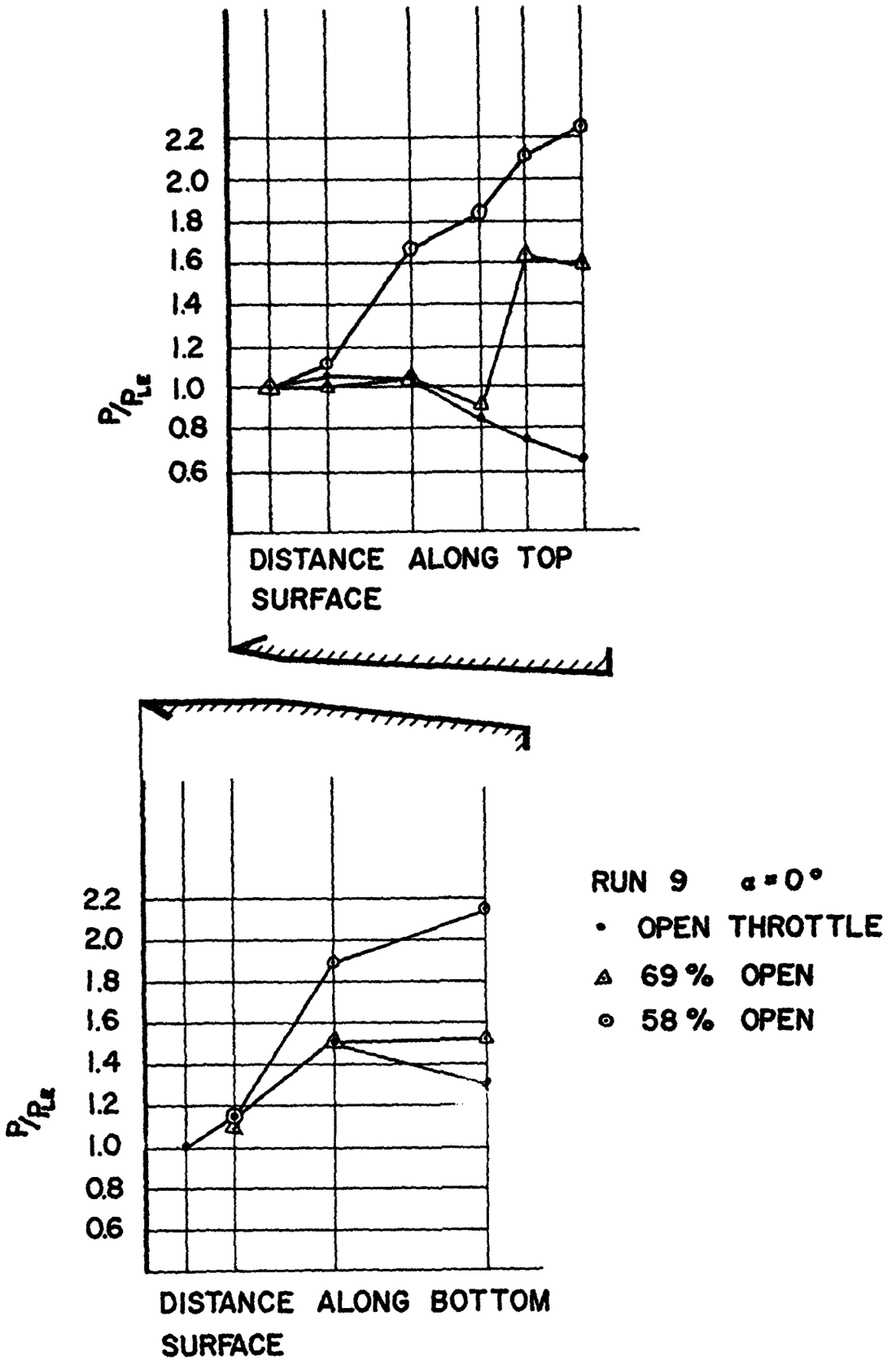

Figure 43. Effect of Back Pressure on Passage with "Free Jet" Throat

(a) .6" chord cavity

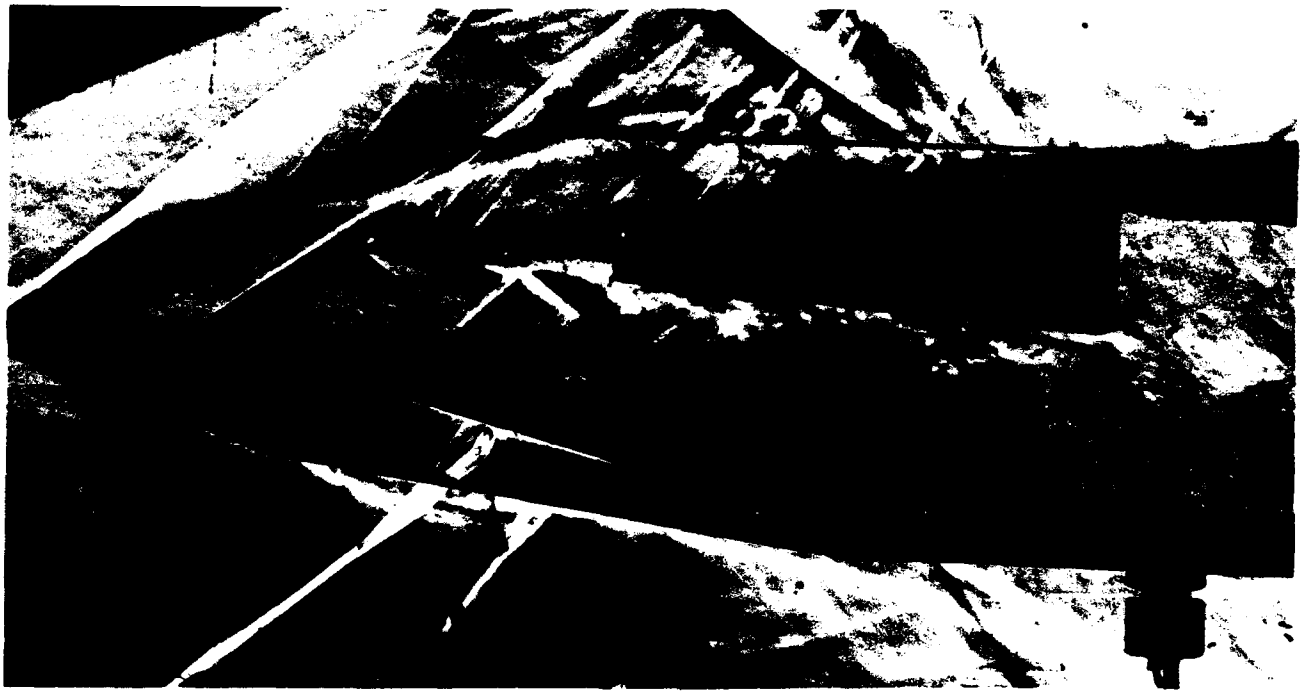

(b) .98" chord cavity

Figure 44. Convergent-Divergent Passage with "Free Jet Throats"

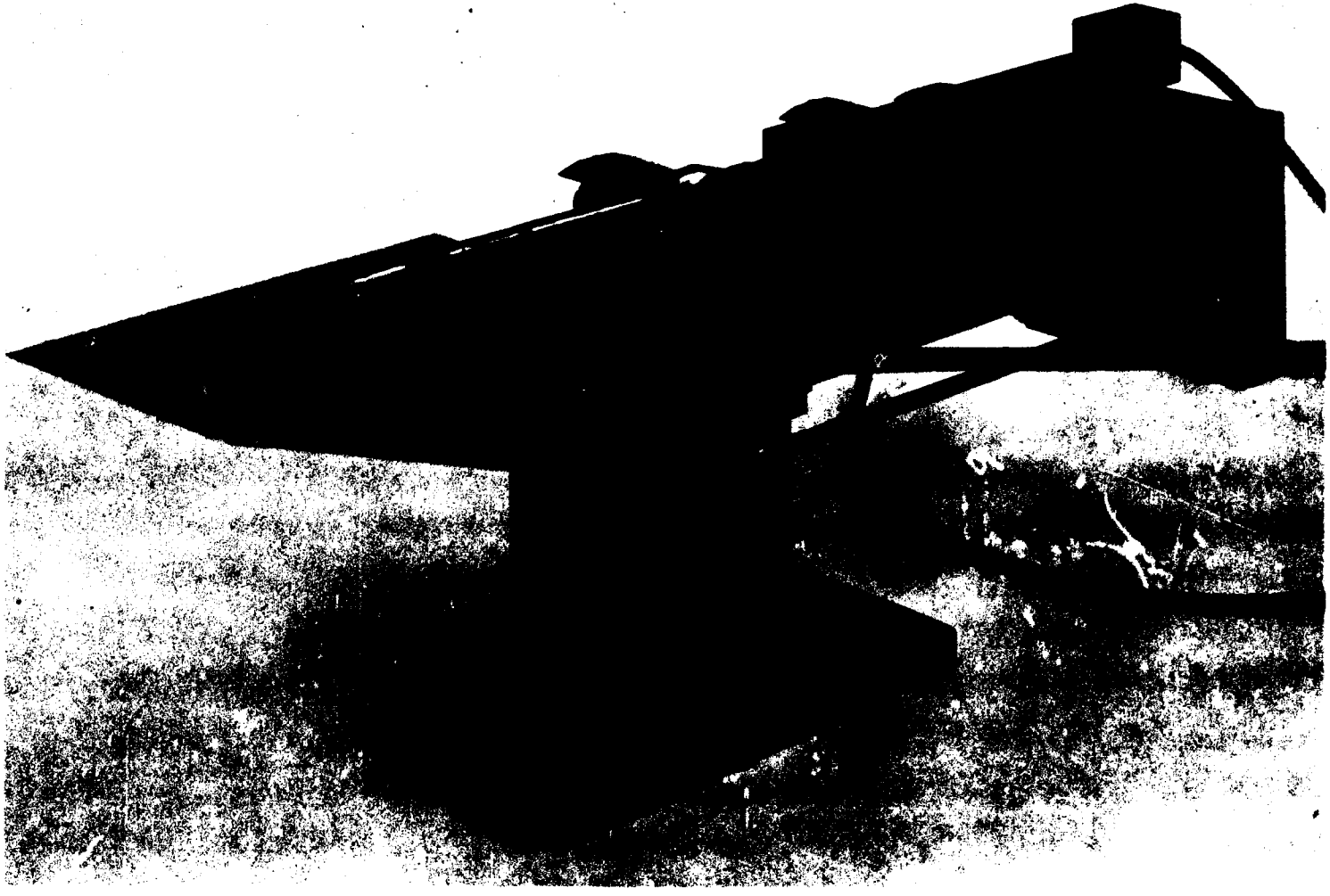

Figure A1. Flate Plate Model with Total Head Probe

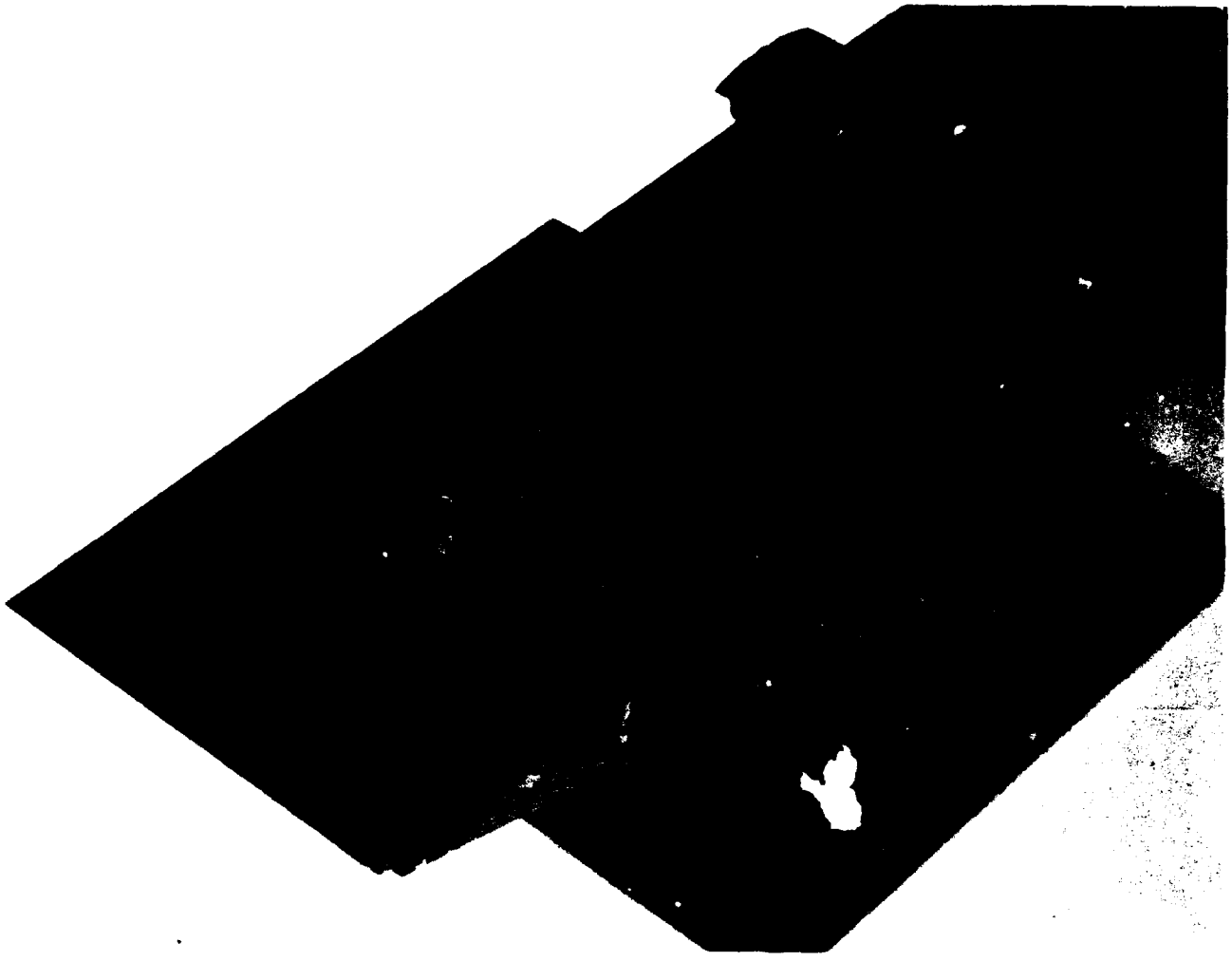

Figure A2. View of Flat Plate with Two-Dimensional Trip

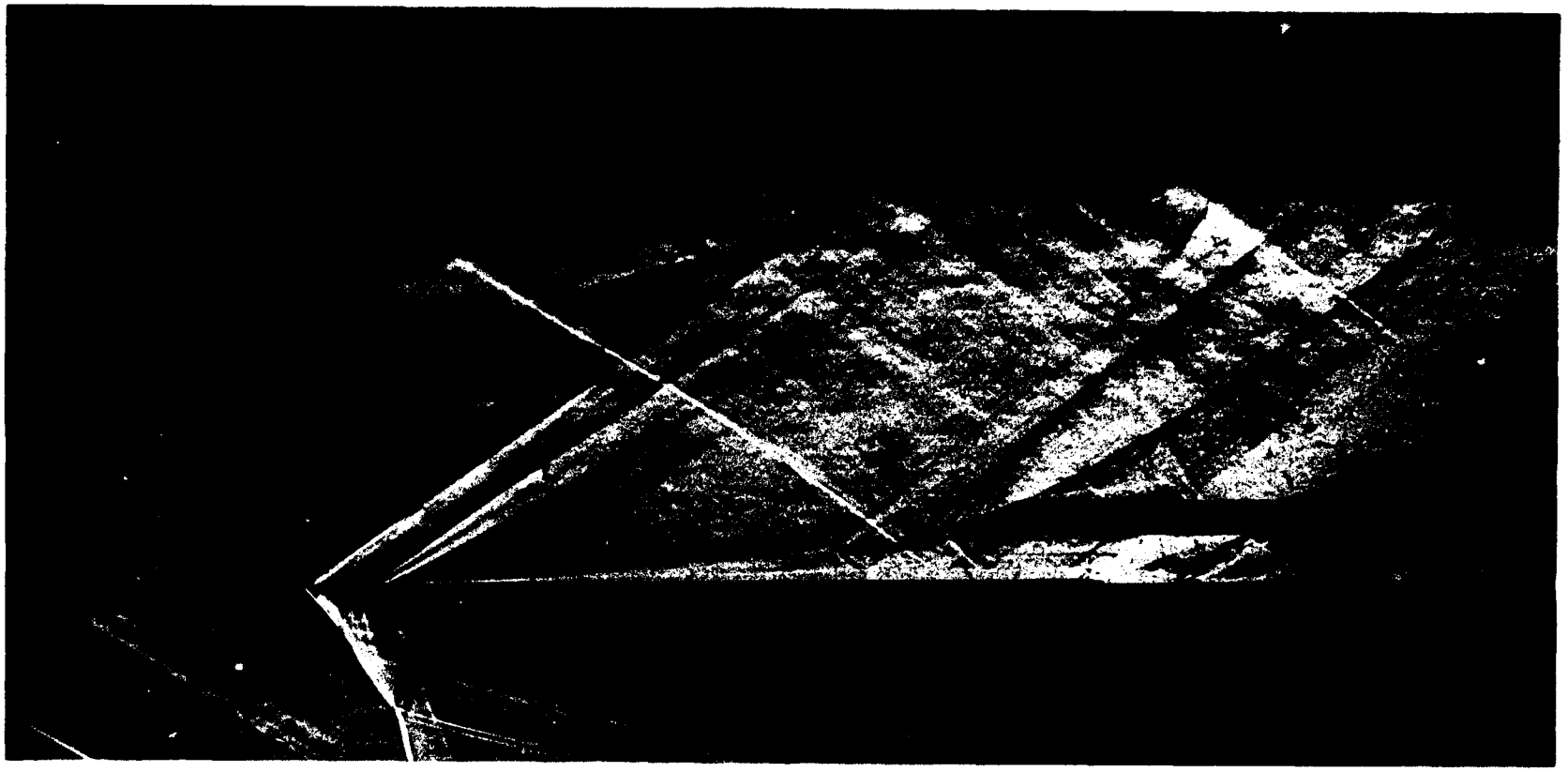

Figure A3. Typical Schlieren Photograph

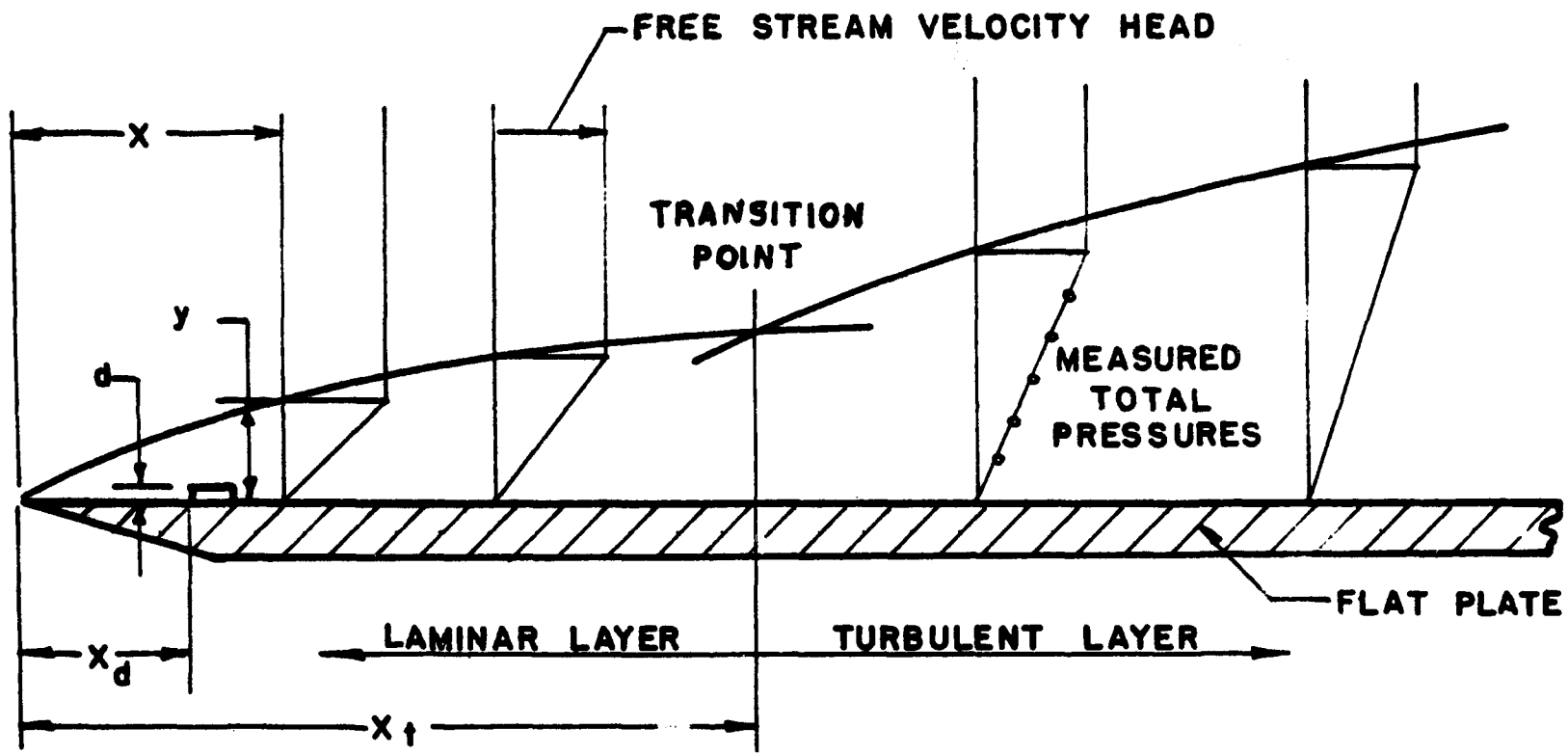

Figure A4. Schematic Diagram Showing Deduction of Transition Point Location from Change in Boundary Layer

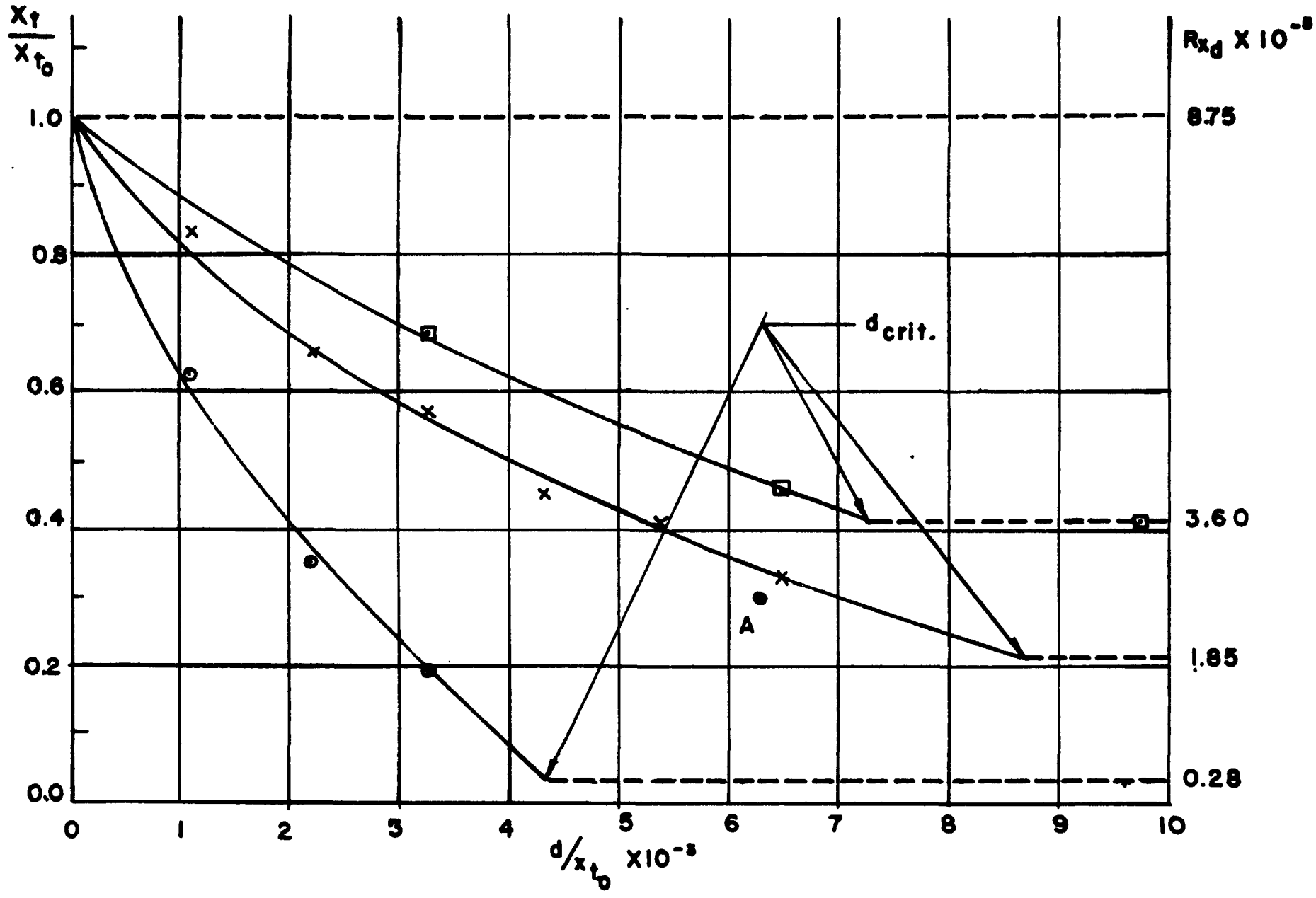

Figure A5. Effect of Trip Height on Location of Transition

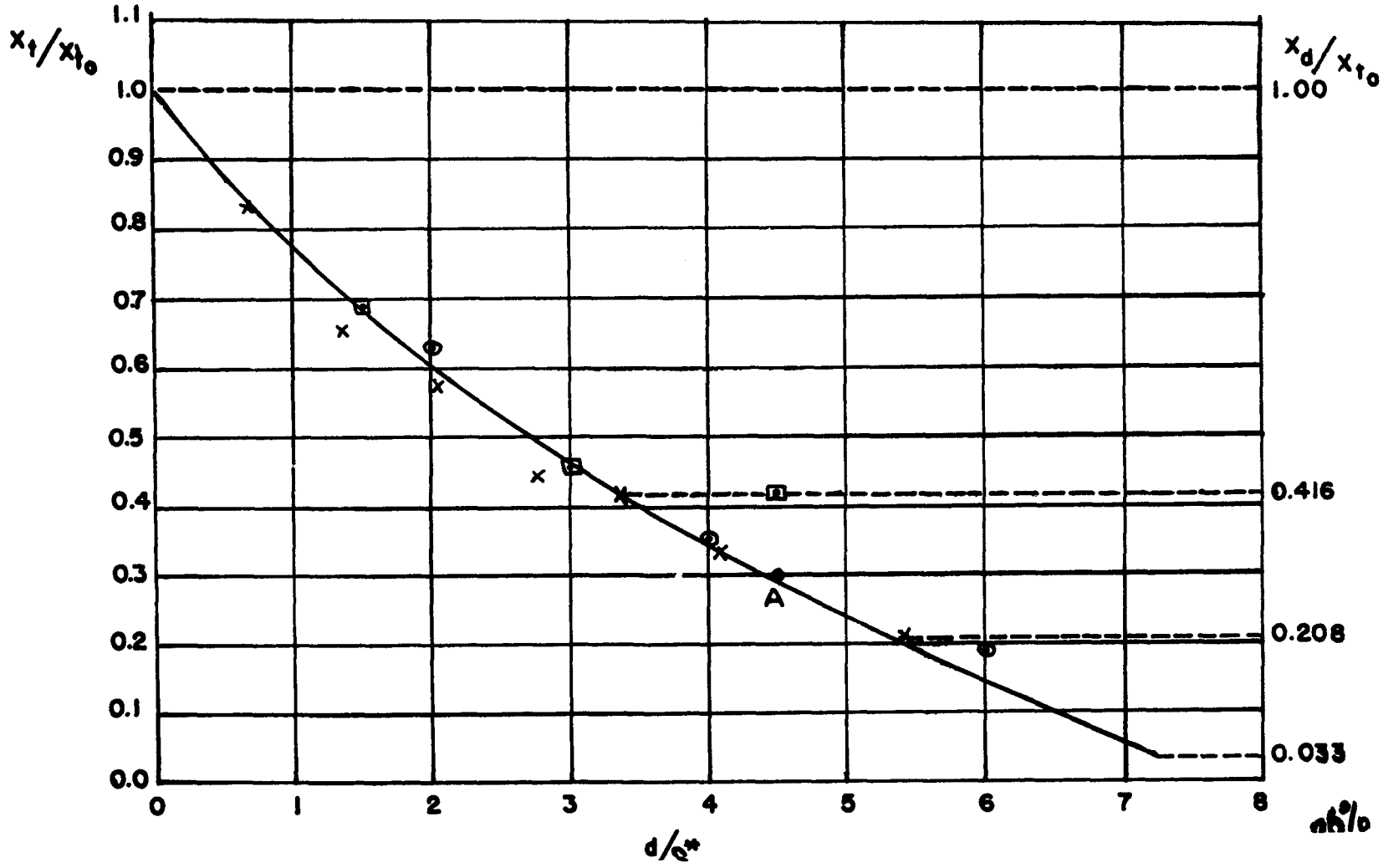

Figure A6. Effect of Trip Height in Terms of Laminar Boundary Layer Displacement Thickness at Trip on Location of Transition

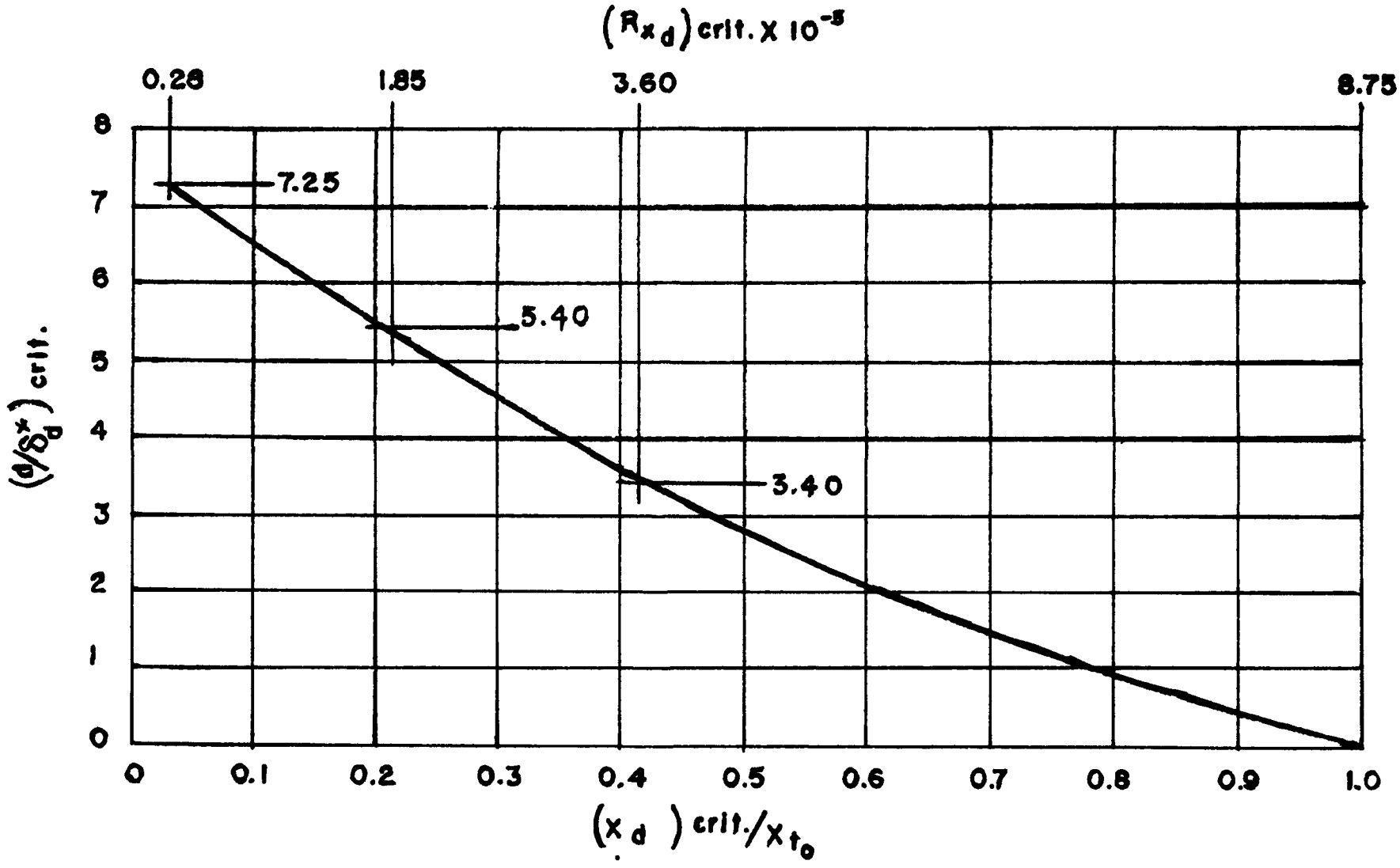

Figure A7. Trip Sizes to Cause Transition at Trip Location

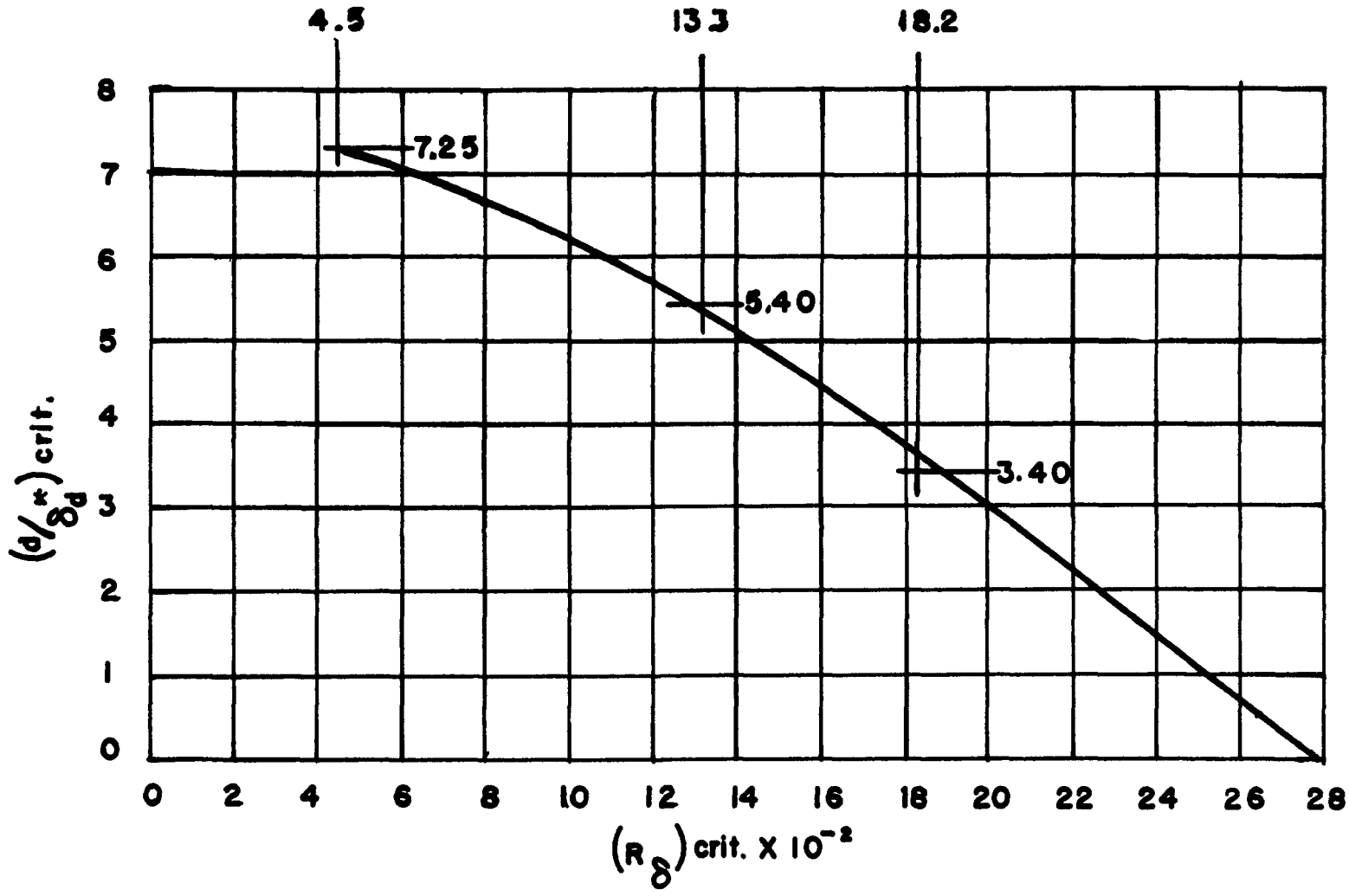

Figure A8. Effect of Boundary Layer Reynolds Number on Critical Trip Size

UNCLASSIFIED

The University of Toledo, Toledo, Ohio. SUPERSONIC CASCADE STUDIES, Part I, PASSAGE STUDIES by Andrew A. Fejer and George L. Heath. December 1961. 90 p. incl. illus. (Project 7063; Task 70151) (Contract AF 33(616)-5737) (ARL 125, Pt. I)
Unclassified Report

An experimental study was made of supersonic flow through various convergent and convergent-divergent passage configurations. The details of the flows were examined by means of total and static pressure surveys and Schlieren photographs and the effects of some changes in passage geometry on the characteristics of the passages were ob-

(over)

UNCLASSIFIED

UNCLASSIFIED

served. Based on the tests, some design criteria were determined for supersonic passages capable of operating at high static pressure ratios. It was concluded that long and narrow convergent-divergent passages are capable of producing a significant pressure rise without extensive separation in the divergent region. However, the values of obtainable pressure rise appears to be substantially lower than anticipated by early designers of supersonic compressor cascades.

UNCLASSIFIED

UNCLASSIFIED

The University of Toledo, Toledo, Ohio. SUPERSONIC CASCADE STUDIES, Part I, PASSAGE STUDIES by Andrew A. Fejer and George L. Heath. December 1961. 90 p. incl. illus. (Project 7063; Task 70151) (Contract AF 33(616)-5737) (ARL 125, Pt. I)
Unclassified Report

An experimental study was made of supersonic flow through various convergent and convergent-divergent passage configurations. The details of the flows were examined by means of total and static pressure surveys and Schlieren photographs and the effects of some changes in passage geometry on the characteristics of the passages were ob-

(over)

UNCLASSIFIED

UNCLASSIFIED

served. Based on the tests, some design criteria were determined for supersonic passages capable of operating at high static pressure ratios. It was concluded that long and narrow convergent-divergent passages are capable of producing a significant pressure rise without extensive separation in the divergent region. However, the values of obtainable pressure rise appears to be substantially lower than anticipated by early designers of supersonic compressor cascades.

UNCLASSIFIED

The University of Toledo, Toledo, Ohio. SUPERSONIC CASCADE STUDIES, Part I, PASSAGE STUDIES by Andrew A. Fejer and George L. Heath. December 1961. 90 p. incl. illus. (Project 7063; Task 70151) (Contract AF 33(616)-5737) (ARL 125, Pt. I)
Unclassified Report

An experimental study was made of supersonic flow through various convergent and convergent-divergent passage configurations. The details of the flows were examined by means of total and static pressure surveys and Schlieren photographs and the effects of some changes in passage geometry on the characteristics of the passages were ob-

(over)

UNCLASSIFIED

UNCLASSIFIED

served. Based on the tests, some design criteria were determined for supersonic passages capable of operating at high static pressure ratios. It was concluded that long and narrow convergent-divergent passages are capable of producing a significant pressure rise without extensive separation in the divergent region. However, the values of obtainable pressure rise appears to be substantially lower than anticipated by early designers of supersonic compressor cascades.

UNCLASSIFIED

UNCLASSIFIED

The University of Toledo, Toledo, Ohio. SUPERSONIC CASCADE STUDIES, Part I, PASSAGE STUDIES by Andrew A. Fejer and George L. Heath. December 1961. 90 p. incl. illus. (Project 7063; Task 70151) (Contract AF 33(616)-5737) (ARL 125, Pt. I)
Unclassified Report

An experimental study was made of supersonic flow through various convergent and convergent-divergent passage configurations. The details of the flows were examined by means of total and static pressure surveys and Schlieren photographs and the effects of some changes in passage geometry on the characteristics of the passages were ob-

(over)

UNCLASSIFIED

UNCLASSIFIED

served. Based on the tests, some design criteria were determined for supersonic passages capable of operating at high static pressure ratios. It was concluded that long and narrow convergent-divergent passages are capable of producing a significant pressure rise without extensive separation in the divergent region. However, the values of obtainable pressure rise appears to be substantially lower than anticipated by early designers of supersonic compressor cascades.

UNCLASSIFIED

UNCLASSIFIED